

学位論文  
**Doctoral Thesis**

**Study of draxin and Tsukushi function in brain development and injury**

( 脳発生と障害における draxin と Tsukushi の果たす機能解析 )

マームド ホセイン

**Mahmud Hossain**

熊本大学大学院医学教育部博士課程医学専攻神経分化学

指導教員

田中 英明 教授

熊本大学大学院医学教育部博士課程医学専攻神経分化学

2012年9月

# 学 位 論 文

## Doctoral Thesis

### Study of draxin and Tsukushi function in brain development and injury

( 脳発生と障害における draxin と Tsukushi の果たす機能解析 )

著 者 名 : マームド ホセイン  
(単名) Mahmud Hossain

指導教員名 : 熊本大学大学院医学教育部博士課程医学専攻神経分化学 田中 英明 教授

審査委員名 : 生体機能病態学担当教授 福田 孝一  
脳回路構造学学担当教授 玉巻 伸章  
知覚生理学学担当教授 宋 文杰  
脳発生学担当教授 嶋村 健児

2012年9月

# Contents

|  |     |
|--|-----|
| <b>Abstract</b>  | IV  |
| <b>List of Abbreviations</b>                               | V   |
| <b>List of Publications</b>                                | VI  |
| <b>Acknowledgements</b>                                    | VII |
| <br>   |     |
| <b>1. Introduction</b>                                     |     |
| 1-1. Literature review                                     | 1   |
| 1-1-1. Axon guidance molecules and their receptors         | 1   |
| 1-1-2. Overview of proteomics approach                     | 10  |
| 1-1-3. Overview of ischemic stroke and neuronal cell death | 14  |
| 1-2. Background and Specific aims                          | 19  |
| <br>   |     |
| <b>2. Materials and Methods</b>                            |     |
| 2-1. Mice  | 21  |
| 2-2. $\beta$ -gal staining and histological analyses       | 21  |
| 2-3. DiI labeling  | 21  |
| 2-4. Hematoxylin and Kluver–Barrera (KB) staining          | 22  |
| 2-5. Preparation of conditioned medium                     | 22  |
| 2-6. Brain lysate preparation                              | 22  |
| 2-7. Immunoprecipitation (IP) assay                        | 23  |
| 2-8. In situ hybridization                                 | 23  |
| 2-9. Explant cultures                                      | 24  |
| 2-10. Growth cone collapse and neurite outgrowth assays    | 25  |

|  |    |
|--|----|
| 2-11. AP binding assay   | 26 |
| 2-12. Mouse draxin monoclonal antibody productions   | 27 |
| 2-13. Transient global cerebral ischemia   | 28 |
| 2-14. Focal cerebral ischemia (Middle cerebral artery occlusion)                                       | 29 |
| <br>   |    |
| <b>3. Results</b>  |    |
| <br>   |    |
| <b>3-1. Part A</b>   |    |
| 3-1-1. CC and AC formation in draxin/TSK doubly heterozygous mice is severely affected                 | 31 |
| 3-1-2. Draxin and TSK proteins do not interact biochemically   | 36 |
| 3-1-3. Expression of <i>draxin</i> and TSK mRNA is observed in the strategic region of AC and CC axons | 36 |
| 3-1-4. TSK inhibits neurite outgrowth  | 40 |
| 3-1-5. TSK protein directly binds to both AON and cortical axons                                       | 45 |
| 3-1-6. Growth cone collapse is induced by TSK protein  | 45 |
| 3-1-7. The effects of TSK and draxin on neurite outgrowth inhibition are additive                      | 48 |
| <br>   |    |
| <b>3-2. Part B</b>   |    |
| 3-2-1. Mouse draxin monoclonal antibody productions  | 51 |
| 3-2-2. Immunoprecipitation assay followed by mass spectrometry   | 53 |
| <br>   |    |
| <b>3-3. Part C</b>   |    |
| 3-3-1. Establishment of transient global ischemia  | 55 |
| 3-3-2. <i>draxin</i> expressions is up regulated after transient global ischemia                       | 60 |
| 3-3-3. Establishment of Focal cerebral ischemia  | 61 |

|                               |    |
|-------------------------------|----|
| <b>4. Discussion</b>          |    |
| <b>4-1. Part A</b>            | 64 |
| <b>4-2. Part B</b>            | 69 |
| <b>4-3. Part C</b>            | 70 |
| <b>5. Conclusion</b>          | 72 |
| <b>6. Future perspectives</b> |    |
| <b>6-1. Part A</b>            | 73 |
| <b>6-2. Part B</b>            | 73 |
| <b>6-3. Part C</b>            | 74 |
| <b>7. References</b>          | 75 |

## **Abstract**

**Background and Purpose:** Previously we reported the identification of two secreted proteins: draxin and Tsukushi (TSK). *Draxin* knockout mice showed agenesis of all forebrain commissures: corpus callosum (CC), hippocampal commissure (HC), and anterior commissure (AC). Moreover, genetic deletion of *TSK* in mice also results in the agenesis of AC and CC, also suggesting the importance of TSK function in forebrain commissure formation. As both *draxin* and *TSK* single mutant mice converge into common phenotypes, there is a possibility that the combined function of these two proteins is essential for the formation of forebrain commissures. Furthermore, we documented that draxin exerts its chemorepulsive function through netrin's chemoattractive receptor, DCC. As different ligands interacted with the same receptor, DCC and shows opposite functions of axon guidance, there might be some other molecule(s) that also interact with DCC to perform the opposite signaling pathway. Additionally, we also tried to explore the function of draxin after brain injury.

**Methods:** To analyze the forebrain commissures, we generated *draxin/TSK* doubly homozygous and heterozygous mice; and histological, biochemical and *in vitro* culture was performed. Antibody production, co-immunoprecipitation and mass spectrometry analysis were performed to identify the receptor-associated molecule(s) by proteomics approach. To explore the new function of draxin global cerebral ischemia and middle cerebral artery occlusion were performed in adult mice.

**Results:** Higher prevalence of CC malformation and agenesis of the AC in the *draxin/TSK* doubly homozygous and heterozygous mice implies the genetic interaction between draxin and TSK. Importantly, in this study, we established TSK as a new chemorepulsive axon guidance molecule that function to guide anterior olfactory neuronal (AON) and cortical axons. We also observed that TSK and draxin had additive effects in inhibiting cortical and AON neurite outgrowth. Besides, we found some probable candidates as the DCC receptor associated molecules. Furthermore, we found that draxin is re-expressed and/or up regulated in the dentate gyrus and olfactory bulb after ischemia.

**Conclusion:** Combined guidance activities of draxin and TSK regulate forebrain commissure formation. DCC might have some partner molecules to exert its opposite signal transduction and there is a high possibility that draxin has some new roles along with axon guidance.

## List of Abbreviations

|        |   |
|--------|---|
| µg:    | Microgram                               |
| µm:    | Micrometer                              |
| mm:    | Millimeter                              |
| nM:    | Nanomolar                               |
| mM:    | Milimolar                               |
| FCS:   | Fetal calf serum                        |
| DMEM:  | Dulbecco's Modified Eagles Medium       |
| CNS:   | Central nervous system                  |
| DCC:   | Deleted in Colorectal cancer            |
| BMP:   | Bone Morphogenetic Protein              |
| Eph:   | Erythropoietin producing hepatocellular |
| β-gal: | Beta-galactosidase                      |
| AP:    | Alkaline phosphatase                    |
| DIG:   | Digoxigenin                             |
| MCAO   | Middle Cerebral Artery Occlusion        |
| TTC    | 2,3,5-triphenyltetrazolium chloride     |
| CCA    | Common Carotid Artery                   |
| ICA    | Internal carotid artery                 |
| ECA    | External Carotid Artery                 |
| HAT    | Hypoxanthine-Aminopterin-Thymidine      |

## List of Publications

1. **Mahmud Hossain**, Giasuddin Ahmed, Iftekhar Bin Naser, Yohei Shinmyo, Ayako Ito, M. Asrafuzzaman Riyadh, Athary Felemban, Xiaohong Song, Kunimasa Ohta, Hideaki Tanaka. The combinatorial guidance activities of draxin and Tsukushi are essential for forebrain commissure formation. **Dev. Biol.** (In press)
2. Song X, Sato Y, Felemban A, Ito A, **Hossain M**, Ochiai H, Yamamoto T, Sekiguchi K, Tanaka H, Ohta K. Equarin is involved as an FGF signaling modulator in chick lens differentiation. **Dev. Biol.** 368(1):109-17, Aug, 2012
3. Ahmed G, Shinmyo Y, Ohta K, Islam SM, **Hossain M**, Naser IB, Riyadh MA, Su Y, Zhang S, Tessier-Lavigne M, Tanaka H. Draxin inhibits axonal outgrowth through the netrin receptor DCC. **J Neurosci.** 31(39):14018-23, Sep, 2011.
4. Ahmed G, Shinmyo Y, Naser IB, **Hossain M**, Song X, Tanaka H. Olfactory bulb axonal outgrowth is inhibited by draxin. **Biochem. Biophys. Res. Commun.** 398(4):730-4, Aug, 2010.

## **Acknowledgements**

All praises to Almighty Allah whose mercy and kindness enabled me to successfully finish this work.

I wish to express my sincere gratefulness to my supervisor and mentor Professor Hideaki Tanaka for accepting me as a Doctor course student and his constructive criticism of my research work and critical reading of my thesis and manuscript. My heartfelt aspiration to Allah for his sound health.

I would like to express my gratitude to our Associate Professor Dr. Kunimasa Ohta for his unconditional support regarding my experiments as well as for his advice and inspiring notes that smoothen my daily life in Japan.

I am very much indebted to our Assistant Professor Dr. Yohei Shinmyo who really works as a catalyst for me to sustain in Japan. His incredible cooperation, support, and advice helped me a lot not only in my research, but also in the daily life.

I would like to appreciate all of my fellow lab members for their support, guidance, and encouragement to successfully finish this work. Especially, I am very much grateful to Ms. Mihoko Ilmori, Ms. Ai Hamashima, Mr. Hirohisa Yamada and our lab secretary Ms. Mitsue Kumamaru for their boundless technical supports.

I would also like to have the pleasure to acknowledge my gratitude to my Japanese friend Mr. Hiroyuki Yoneda and his wife Ms. Eri Yoneda for their amiable affection and moral support during my stay in Japan.

I am thankful to Ministry of Education, Science, Sports and Culture of Japan (MEXT), the Global COE program (Cell Fate Regulation Research and Education Unit), Japan and Kumamoto University for financial support.

I am deeply obliged to my parents, brothers, sisters, friends and my teachers in the department of Biochemistry and Molecular Biology, University of Dhaka for their uninterrupted support and encouragement during this study. Finally, I am glad to dedicate this work to my family members especially to my parents for their wisdom, patience and blessings.

# **Introduction**

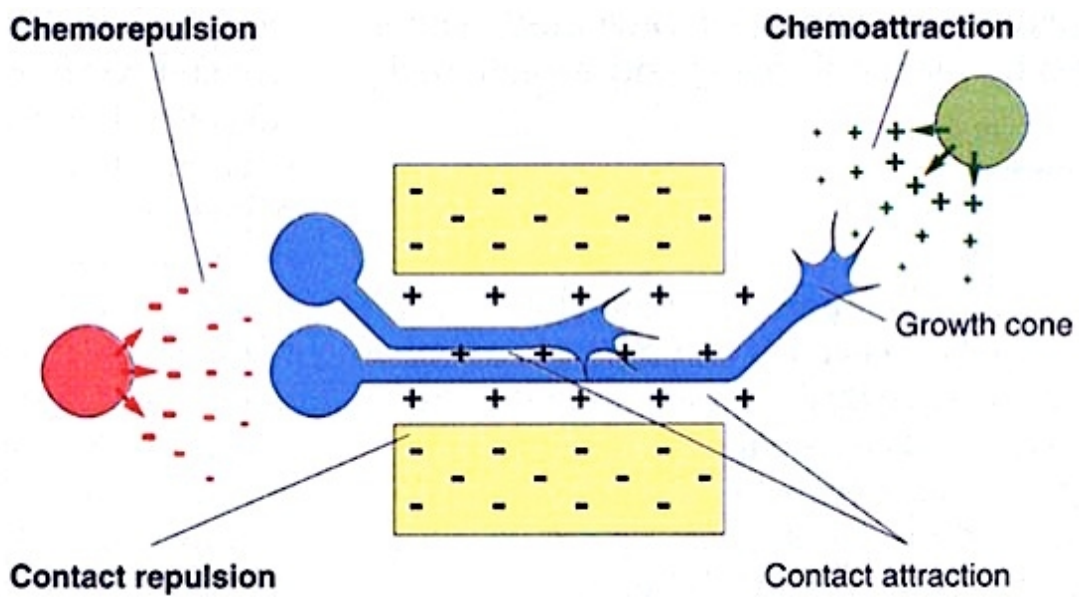
## **1-1. Literature review**

### **1-1-1. Axon guidance molecules and their receptors**

The function of the mammalian central nervous system critically depends on the correct wiring of neural circuits and the exquisite complexity of the nervous system reflects the remarkable ability of neurons to form precise circuits. During development, neurons project axons over long distances to reach their specific synaptic targets. Axonal growth is steered by a motile and intricately sensitive structure called growth cone tipped at its leading edge, that allow to serve as a sensor to explore the presence of a myriad guidance molecules in the surrounding extracellular matrix and the surfaces of other cells. The guidance molecules are classified into two groups—attractants and repellents and they guide the growing axons by four types of mechanisms: chemoattraction, chemorepulsion, contact attraction and contact repulsion. Usually secreted (act on long range) guidance cues mediate their action through chemoattraction and/or chemorepulsion; and non diffusible or membrane bound cues (act on short range) mediate by contact attraction and/or repulsion (Fig. 1). However, a particular guidance cue can function as attractant for some neurons while repellent for others, depending on the type of receptor(s) that express at the growth cone. To date several axon guidance proteins and their receptor have been identified and so far four conserved families of axon guidance cues, the netrin, semaphorin, ephrin and Slit proteins (Fig. 2) mediate their guidance effects via receptors of the DCC or UNC5, Neuropilin/Plexin, Eph, and Robo families, respectively (Tessier-Lavigne and Goodman, 1996; Dickson, 2002).

## Axon guidance cue, netrin and its receptors

The netrins are a small family of phylogenetically conserved secreted proteins with amino acid sequence similarity to proteins of the laminin family (Huber et al., 2003). Netrin was first identified as an outgrowth-promoting factor homologous to *C. elegans* UNC-6 for neurites from rodent dorsal spinal cord explants (Serafini et al., 1994) and



### Known guidance cues

Netrins  
Semaphorins  
Slits  
Ephrins  
Draxin

### Morphogens

Shh  
Wnts  
BMPs

**Fig. 1.** Basic mechanisms of growth cone guidance (Modified from Tessier-Lavigne and Goodman, 1996)

a chemoattractant for spinal commissural axons (Kenedy et al., 1994). Genetic study showed that netrin is required for ventral projection of spinal commissural axons toward the floor plate and for the formation of forebrain commissures: the corpus callosum, hippocampal commissures and anterior commissures *in vivo* (Serafini et al., 1996).

Netrin was also reported as chemorepellent for trochlear motor axons (Colamarino and Tessier-lavigne, 1995a). Furthermore, netrin is involved in other kinds of projection during central nervous system development e.g. cortical axon projection (Metin et al., 1997), thalamo-cortical axonal projection (Braisted et al., 2000). So far, four members (netrin-1/-4) of netrin family have been identified in vertebrates and of these, netrin-1 is the best-characterized member of the netrin family.

DCC (Deleted in colorectal cancer), a mammalian orthologue of Unc40, was identified as a netrin-1 receptor and mediates netrin-1-induced axon outgrowth and attraction (Keino-Masu, et al. 1996). DCC knockout mouse phenotype showed that it is required for ventral projection of spinal commissural axons toward the floor plate (Fazeli et al., 1997). Through Unc5, netrin-1 showed its repulsive function for trochlear motor axon (Colamarino and Tessier-lavigne, 1995). For short-range netrin-1-induced chemorepulsion requires Unc5 alone while long-range chemorepulsion is facilitated by the formation of receptor complex between DCC and Unc5 (Hong et al., 1999). Both short and long-range netrin-1 induced chemoattractive functions are mediated by its receptor DCC alone (Wen and Zheng, 2006). Down syndrome cell adhesion molecule (DSCAM) has been shown recently as another netrin receptor that collaborates with DCC to mediate netrin-1-induced spinal commissural axon path finding (Ly et al., 2008; Liu et al., 2009).

### **Slits and their receptors**

Slit is a large secreted protein, which is produced by midline glia, and this protein plays an important role in the development of commissural axon and its midline crossing (Rothberg et al., 1988; Rothberg et al., 1990). There are at least three *slit* genes in mammals: *slit1*, *slit2* and *slit3* and all of these are expressed by the midline cells (Brose

et al., 1999; Holmes et al., 1998; Itoh et al., 1998, Nakayama et al., 1998, Yuan et al., 1999a). Slit silences netrin-1 attraction to spinal cord commissural axons after crossing the midline (Stein and Tessier-lavigne, 2001). Slits also function as a chemorepulsive axon guidance cue for other axons including olfactory bulb, hippocampal and spinal motor axons (Brose and Tessier-Lavigne, 2000). Slit deficient mice showed striking defects in the formation of optic chiasm indicating its pivotal role in this developmental process (Plump et al., 2002). Slit functions through its receptor Robo (derived from 'roundabout'; drosophila mutation from which this cue was obtained) (Battye et al., 1999; Kidd et al., 1999; Brose et al., 1999; Li et al., 1999). In mammals, four members of Robo family have been identified. They are *Robo1*, *Robo2*, *Robo3 (Rig1)* and *Robo4* (also known as magic roundabout) (Kidd et al., 1998; Yuan et al., 1999b). Except *Robo4*, the other *Robos* are expressed in CNS neurons including commissural neurons.

### **Semaphorins and their receptors**

Semaphorins are large conserved family of axon guidance cues. Members of this family are either secreted or membrane bound and can repel and/or attract the growth cones of the axons. There are 8 classes of semaphorins. All semaphorins contain a ~500 amino acid conserved sema domain at their amino terminal end. Sema domain confers biological activity to the semaphorins (Raper, 2000). Among all the semaphorins vertebrate class III semaphorins were best characterized. These semaphorins directly bind to the neuropilins (1 and 2), which in turn binds to the plexins to transduce the signals. However, some membrane-associated semaphorins can bind to the plexins and can transduce the signal without forming receptor complexes with neuropilins (Raper, 2000).

Secreted semaphorins were identified as chemorepulsive guidance cues for several

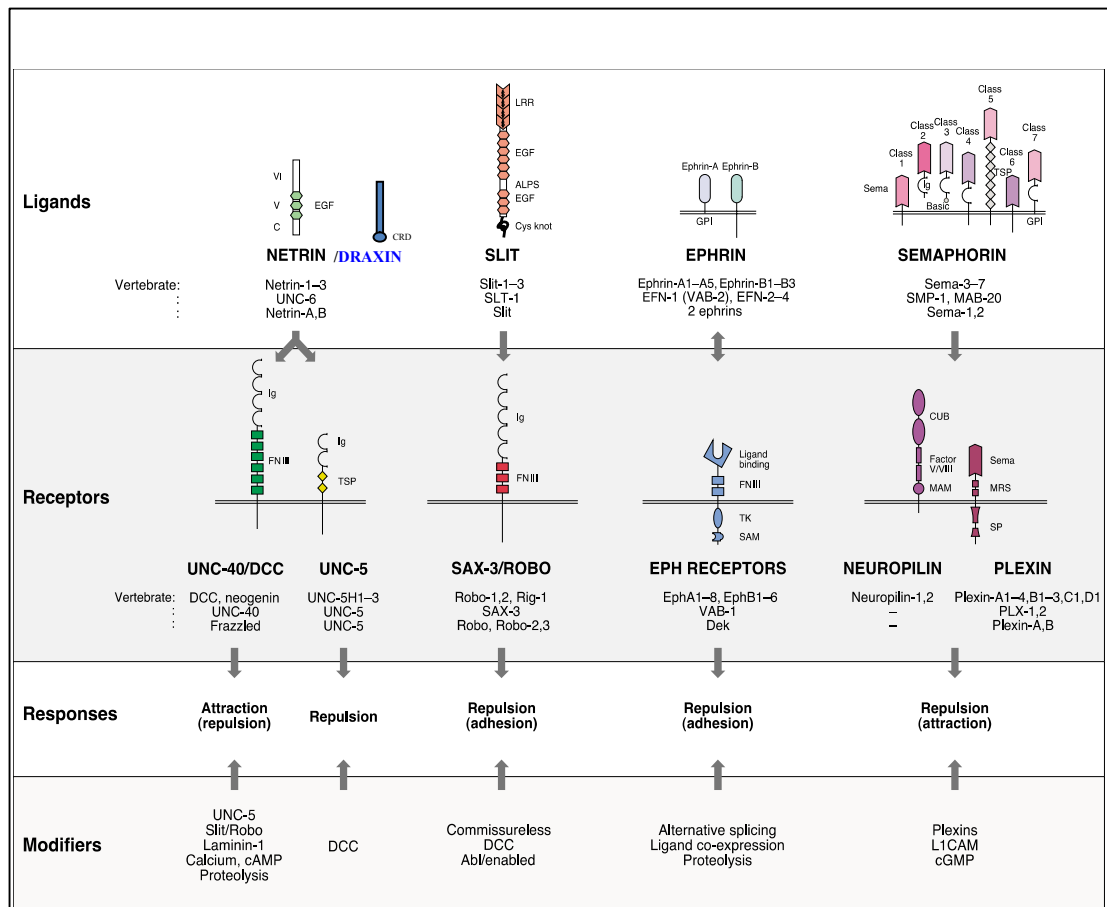


**Fig. 2.** Summary of the four conserved families of axon guidance cues and their respective receptor/s. CRD: cysteine rich domain; ALPS: agrin-laminin-perlecan slit domain; C: c terminus of netrin; CUB: C1/Uegf/BMP-1 domain; DCC: deleted in colorectal cancer; EGF: epidermal growth factor; FNIII: fibronectin type III domain; GPI: glycosylphosphatidyl-inositol anchor; Ig: immunoglobulin domain; LRR: leucine-rich repeat; MAM: meprin/A5 antigen motif; MRS: Met tyrosine kinase-related sequence; RK: arginine/lysine-rich basic domain; SAM: sterile alpha motif; SP: 'sex and plexins' domain; TK: tyrosine kinase domain; TSP: thrombospondin domain; VI and V: homology to laminin domains VI and V, respectively (Modified from Yu and Bargmann, 2001)

classes of axons in the forebrain including hippocampal, pontocerebellar and olfactory as well as sympathetic, sensory and motor neurons from peripheral nervous system. Some semaphorins (Sema3B and 3C) also induce axonal outgrowth from cortical and olfactory

bulb explant *in vitro* (Bagnard et al., 1998; De Castro et al., 1999). In addition, using genetic and culture models, Julien et al., 2005 provide evidence that both attraction and repulsion by Semaphorin 3B are critical for the positioning of a major brain commissural projection, the anterior commissure (AC). Semaphorin 7A, a membrane-anchored semaphorin, promotes axonal outgrowth from olfactory epithelium, olfactory bulb, cortical, and DRG explants (Pasterkamp et al., 2003). The importance of semaphorin function was pronounced by observing the several defects in the projection of sensory axons, cortical neurites orientation or distorted odor map in *sema3A* deficient mice (Behar et al., 1996; Taniguchi et al., 2003). Severe abnormality in peripheral nerve projection was also observed in *semaphoringIII/D* deficient mice (Kitsukawa et al., 1997). Semaphorin3F mutant mice also showed several defects in axonal projection in the hippocampus, midbrain, forebrain and in the PNS (Sahay et al., 2003).

### **Ephrins and their receptors**

Ephrins are the membrane bound ligand and are divided into two classes, ephrin A and ephrin B based on their membrane binding nature. Generally, ephrin As (A1-A5) classes ligand bind to Eph A (A1-A8) receptors and ephrin Bs (B1-B3) bind to EphB (B1-B6) receptors. Only exception is EphA4, which binds ligands from both type A and type B classes. Ephrins play crucial roles in topographic map formation of the retino-tectal projection system typically as repulsive guidance cues (O'Leary and Wilkinson, 1999; Wilkinson, 2001). In addition to topograph formation, ephrin-Eph has been implicated in various types of developmental events such as cell migration (Poliakov et al., 2004), angiogenesis (Wang et al., 1998), vascular remodeling (Adams et al., 1999) and neural tube closure (Holmberg et al., 2000). Ephrins have also been implicated to guide motor axons (O'Leary and Wilkinson, 1999; Luria et al., 2008; Gallarda et al.,

2008) and post crossing commissural axons (Imondi et al., 2000).

Apart from the above classical axon guidance cues and their receptors, another type of chemorepellent for chicken retinal axons named as repulsive guidance molecule (RGM) was identified (Monnier et al., 2002). Later, neogenin was reported to be a functional receptor for RGM (Rajagopalan et al., 2004).

### **Draxin and its receptors**

We have identified a molecule named draxin (dorsal repulsive axon guidance protein) from a cDNA library of enriched motoneurons, floor plate, and roof plate of chick embryos. Chick draxin mRNA was expressed transiently during development of the brain and spinal cord, especially in the roof plate and the dorsal lip of the dermomyotome (Islam, et al., 2009). We have recently reported DCC, as a functional receptor for draxin (Ahmed et. al., 2011). Draxin bind specifically to the IgG domain of the DCC and does not compete with netrin for binding to the receptor. There is a strong genetic interaction between draxin and DCC in formation of forebrain commissures (Ahmed et. al., 2011). By candidate approach we also found that Neogenin, Unc5 and DSCAM act as binding partner of draxin.

### **Morphogens act as axon guidance cues**

Morphogens such as bone morphogenic proteins (BMPs), sonic hedgehog (Shh) and Wnts are secreted signaling molecules and play critical roles in the axons guidance (Charron and and Tessier-Lavigne, 2005; Zou and Lyuksyutova, 2007). Morphogens usually have concentration gradient and exhibit their functions directly at a distance. During the development of vertebrate nervous system, members of the above morphogens play a critical role in the specification of diverse neural cell fates

and tissue patterning (Ingham and McMahon, 2001; Lee et al., 1998; Jessel, 2000; Muroyama et al., 2002).

### **Forebrain commissure and axon guidance cues**

The precise functioning of the mammalian central nervous system crucially depends on the proper wiring of neural circuits. Inter-hemispheric cross talk through the commissures is a critical event for proper development and function of the vertebrate forebrain (Chédotal, 2011; Cummings et al., 1997; Izzi and Charron, 2011; Pires-Neto and Lent, 1993; Unni et al., 2012). These long-distance connections in the mammalian forebrain are made by axons that traverse the telencephalic midline, principally in three commissural tracts, the corpus callosum, the hippocampal commissure and the anterior commissure.

In mice, formation of the CC axonal tract starts with the projection of pioneer axons of pyramidal neurons from the cingulate cortex. These axons first cross the midline at mouse embryonic stage of 15.5, paving the way for the later-arriving neocortical axons to follow and form a fascicle. En route to the midline, callosal axons encounter a specialized, wedge-shaped glial structure, called the glial wedge (GW), located at the medial aspect of the lateral ventricle (Shu and Richards, 2001) directly underlying the CC axonal decision point and the indusium griseum glia (IGG), an area of neurons and glia positioned dorsal to the CC (Donahoo and Richards, 2009) (Fig. 3A). Guidance cues, including members of the Slit, Semaphorin, Wnt and Ephrin families, as well as draxin, are expressed in the GW and the IG and have been implicated in regulating CC guidance. After crossing the midline, CC axons take a dorsal turn and grow into the contralateral hemisphere toward their designated target (Richards et al., 2004). Again, during forebrain development, the anterior and posterior parts of the anterior commissure (ACa

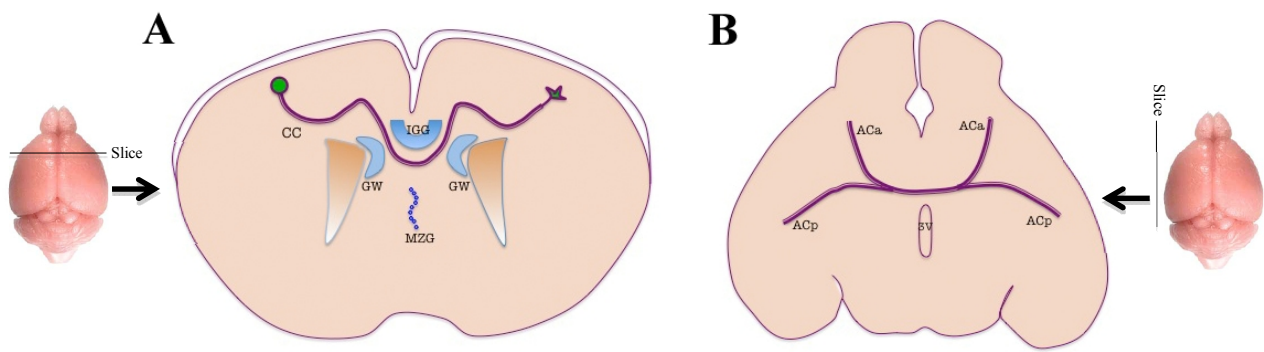


**Fig. 3.** Schematic presentation of mouse brain. A. coronaland B. horizontal depiction of a mouse brain, showing the location of the mammalian forebrain commissures: the corpus callosum (CC) in A, and the anterior commissure (AC) in B. CC: corpus callosum; IGG: indusium griseum glia;GW: glial wedge; MZG: midline zipper glia; ACa: anterior parts of AC; ACp: posterior parts of AC; 3V: 3<sup>rd</sup> ventricle

and ACp, respectively) progress in the same dorsoventral plane and approach a common fascicle for midline crossing (Fig. 3B). The synchronized combinatorial effects of selective attractive and repulsive guidance cues are required for the proper navigation and positioning of the ACa and ACp as evidenced by the phenotypes of mouse mutants lacking the cues of the *ephrin*, *netrin*, or *semaphorin* families or their receptors; these phenotypes range from axon defasciculation and aberrant dorsoventral trajectories to the absence of one or both limbs of the AC (Henkemeyer et al., 1996; Serafini et al., 1996; Fazeli et al., 1997; Chen et al., 2000; Giger et al., 2000; Kullander et al., 2001; Sahay et al., 2003; Julien et al., 2005; Suto et al., 2005).

Thus, the above studies established the fact that the classical axon guidance cues along with the morphogens play a significant role in proper development of nervous system.

## **1-1-2. Overview of proteomics approach**

Proteomics refers to the wide-ranging study of proteins, their structures, functions, and modifications, as well as their interactions with each other. This high throughput technology allows the screening of several hundreds or even thousands of proteins simultaneously. Generally, proteomic approaches can be used for proteome profiling; comparative expression analysis of two or more protein samples; localization and identification of posttranslational modifications; and for the study of protein–protein interactions (Chandramouli and Qian, 2009). Although, human genome comprise of 26000–31000 protein encoding genes; the total number of protein products has been estimated to near about one million including important posttranslational modifications and splicing variants (Baltimore, 2001; Wilkins et al., 1999; Godovac-Zimmermann and Brown, 2001). It is obvious that most of the functional information on the genes endure in the proteome that is the summation of multiple dynamic processes, which include protein phosphorylation, protein trafficking, localization, and protein-protein interactions (Alaoui-Jamali and Xu, 2006). Furthermore, mammalian cells proteomes are very complex and exhibit a broad range of proteins concentration; for instance, one cell can contain between one and more than 100000 copies of a single protein (Celis and Gromov, 1999). In spite of new techniques, analysis of complex biological samples, capability to quantify separated protein species, satisfactory sensitivity for low abundance proteins, quantification over an extensive dynamic range, ability to analyze protein complexes, and high throughput applications is yet challenging (Siitari and Koivistoinen, 2004). Moreover, processing and analysis of proteomics data is indeed a very complicated multistep process (Kearney and Thibault, 2003; Listgarten and Emili, 2005). Various proteomic approaches are available such as gel-based applications that include one-dimensional and two-dimensional polyacrylamide gel electrophoresis, and

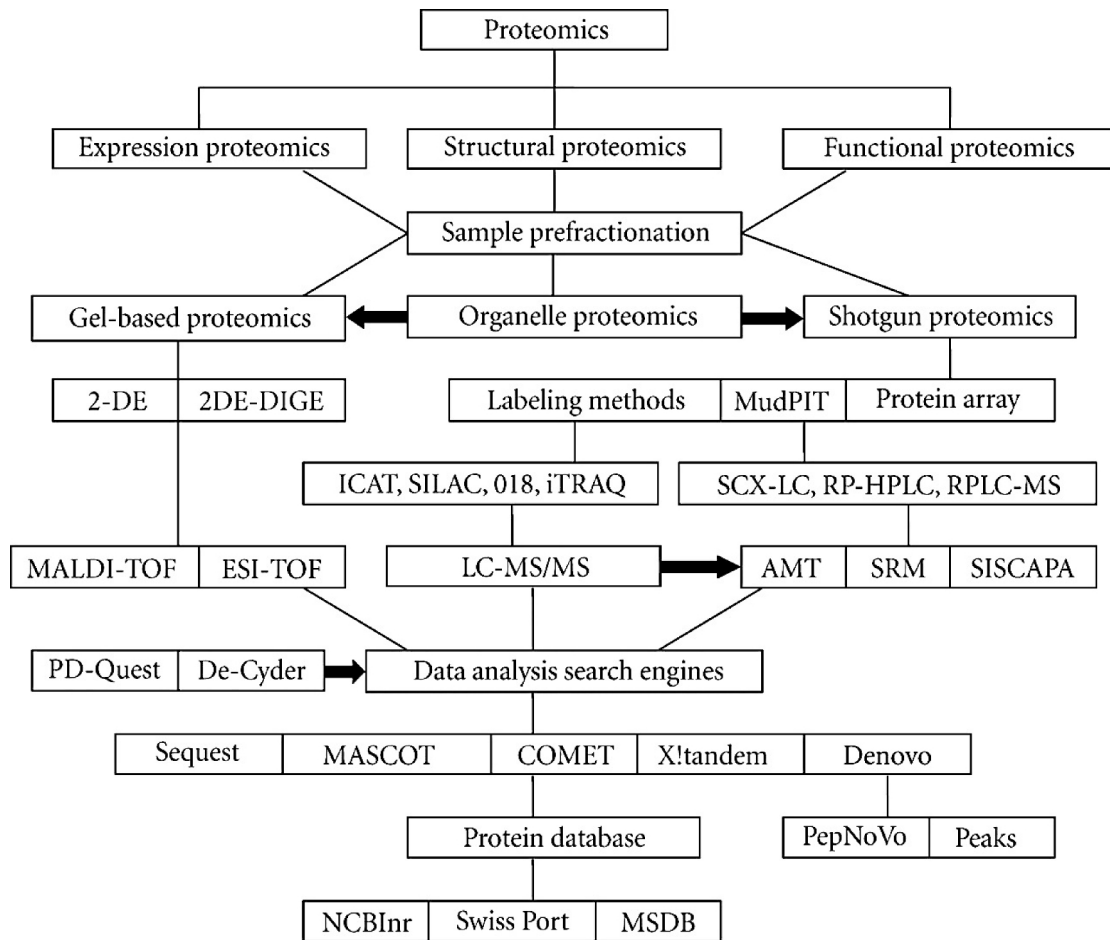


**Fig. 4.** An overview of proteomic strategies. 2DE: Two-dimensional gel electrophoresis; DIGE: Fluorescence 2D difference gel electrophoresis; MudPIT: Multidimensional protein identification technology; ICAT: Isotope-coded affinity tag; SILAC: Stable isotope labeling by amino acids in cell culture; O18: Stable isotope of oxygen; iTRAQ: Isobaric tags for relative and absolute quantitation; SCX-LC: Strong cation exchange- Liquid chromatography; RP-HPLC: Reverse-phase-high-performance liquid chromatography; RPLC-MS: Reverse-phase liquid chromatography- Mass spectrometry; MALDI- TOF: Matrix-assisted laser desorption/ionization-Time of flight, ESI: Electrospray ionization; AMT: Accurate Mass and Time; SRM: Selected reaction monitoring (Chandramouli and Qian; 2009)

| Technology        | Application  | Strengths  | Limitations   |
|-------------------|--|--|---|
| 2DE               | Protein separation<br>Quantitative expression profiling  | Relative quantitative<br>PTM information   | Poor separation of acidic, basic, hydrophobic and low abundant proteins   |
| DIGE              | Protein separation<br>Quantitative expression profiling  | Relative quantitative<br>PTM information<br>High sensitivity<br>Reduction of intergel variability      | Proteins without lysine cannot be labeled<br>Requires special equipment for visualization and fluorophores are very expensive   |
| ICAT              | Chemical isotope labeling for quantitative proteomics  | Sensitive and reproducible<br>Detect peptides with low expression levels                               | Proteins without cysteine residues and acidic proteins are not detected   |
| SILAC             | Direct isotope labeling of cells<br>Differential expression pattern  | Degree of labelling is very high<br>Quantitation is straightforward                                    | SILAC labeling of tissue samples is not possible  |
| iTRAQ             | Isobaric tagging of peptides   | Multiplex several samples<br>Relative quantification<br>High-throughput                                | Increases sample complexity<br>Require fractionation of peptides before MS  |
| MUDPIT            | Identification of protein-protein interactions<br>Deconvolve complex sets of proteins                      | High separation<br>Large protein complexes identification  | Not quantitative<br>Difficulty in analyzing the huge data set<br>Difficult to identify isoforms   |
| Protein array     | Quantitate specific proteins used in diagnostics (biomarkers or antibody detection) and discovery research | High-throughput<br>Highly sensitive<br>Low sample consumption  | Limited protein production<br>Poor expression methods<br>Availability of the antibodies<br>Accessing very large numbers of affinity reagents  |
| Mass spectrometry | Primary tool for protein identification and characterization   | High sensitivity and specificity<br>High-throughput<br>Qualitative and quantitative<br>PTM information | No individual method to identify all proteins. Not sensitive enough to identify minor or weak spots. MALDI and ESI do not favor identification of hydrophobic peptides and basic peptides |
| Bioinformatics    | Analysis of qualitative and quantitative proteomic data  | Functional analysis, data mining, and knowledge discovery from mass spectrometric data                 | No integrated pipeline for processing and analysis of complex data<br>Search engines do not yield identical results   |

**Tab. 1.** Common proteomic technologies, applications, and their limitations. 2DE: Two-dimensional gel electrophoresis; DIGE: Fluorescence 2D difference gel electrophoresis; ICAT: Isotope-coded affinity tag; SILAC: Stable isotope labeling by amino acids in cell culture; iTRAQ: Isobaric tags for relative and absolute quantitation; MudPIT: Multidimensional protein identification technology (Chandramouli and Qian; 2009).

gel-free high throughput screening technologies are equally available, including multidimensional protein identification technology (MudPIT); isotope-coded affinity tag (ICAT); Stable isotope labeling by amino acids in cell culture (SILAC); isobaric tagging for relative and absolute quantitation (iTRAQ) (Vercauteren et al., 2004; van den Bergh and Arckens, 2005; Florens and Washburn, 2006; Gygi et al., 1999; Ong et al., 2002;

Ross et al., 2004). Shotgun proteomics and 2DE DIGE as well as protein microarrays are also used to acquire outlines of protein expression in tissues, cells, and organelles (Washburn et al., 2001; Klose et al., 2002; Cutler, 2003; Melton, 2004). Figure 4 gives the general workflow in proteomics and Table 1 addresses their strengths and limitations. Large-scale western blot assays, multiple reaction monitoring assay (MRM), and label-free quantification of high mass resolution LC-MS data are being explored for high throughput analysis (Schulz et al., 2007; Stahl-Zeng et al., 2007; Mueller et al., 2007). Many different bioinformatics tools have been developed to assist research in proteomics; for instance, optimizing the storage and accessibility of proteomic data or statistically establishing the significance of protein identifications made from a particular peptide match (Smith et al., 2007). One of the most common uses of mass spectrometry-based proteomics is the identification of individual proteins from samples containing many proteins. This is especially useful for identifying members of purified protein complexes.

Hence, the above studies established the fact that despite some challenge, the power of proteomics is revolutionizing biological research including protein-protein interaction and thus proteomics has recently been expanded to include all manner of protein studies.

### **1-1-3. Overview of ischemic stroke and neuronal cell death**

Stroke is characterized by a blockage of blood flow to the brain. In humans, there are basically two types of stroke: that induced by a total loss of blood flow to the brain, such as during a cardiac arrest, or cerebral ischemia arising from a focal loss of blood flow to the brain due to an artery blockage (Hou and MacManus, 2002). Experimental models of stroke have been developed in animals in an attempt to mimic the events of human cerebral ischemia. Two ischemic models are commonly used: transient global ischemia, which reflects the clinical condition of cardiac arrest and focal cerebral ischemia that replicate the clinical condition of stroke (Tonchev, 2005).

In transient global ischemia, the bilateral common carotid artery is occluded that results entire blood supply to the brain is transiently interrupted; and in focal cerebral ischemia model, the middle cerebral artery is occluded either transiently or permanently and the consequence is the damage mainly to cerebral cortex and striatum of the same hemisphere (Ginsberg and Busto, 1989; Mhairi-Macrae, 1992; Crack et al., 2001; Hou and MacManus, 2002). In the transient global ischemia the blood flow is decreased uniformly throughout the brain since collateral blood flow is negligible. A unique phenomenon called delayed neuronal death occurs in this ischemic model. After brief global ischemia the pyramidal neurons in the CA1 region are lost 2-3 days after reperfusion, although no remarkable morphological change is observed at 1-2 days of post ischemia (Kirino, 1982).

The brain injuries induced by the focal ischemia are divided into two types:

1. Core of the injury or infarct (the focus of focal ischemia), which receives the relatively dense ischemia showing the strongest ischemic injury i.e., the cells in the core die rapidly (within minutes to a few hours) by necrosis.
2. Perifocal tissue (penumbra) which

receives less dense ischemia because of the blood supply by collateral arteries and the cells die more slowly over periods of days to weeks by apoptosis like delayed cell death in the global ischemia (Dirnagl et al., 1999; Mattson, 2001; Heiss et al., 2004). The ischemic injury in the penumbra is weaker than that in the core. In the transient focal ischemia there is a return of blood flow, and although this is correlated with recovery, there are damaging effects during this period (Crack and Taylor, 2005). Although the core of the ischemic injury is not recoverable, the penumbra remains a target for the development of therapeutic strategies.

### **Mechanism underlying neuronal cell death**

Brain tissue requires relatively high consumption of oxygen and glucose compare to the other tissues and most of the energy is required to maintain the membrane potential. The energy production in the brain tissue solely depends on oxidative phosphorylation. Focal or global impairments of cerebral blood flow cease the delivery of oxygen and glucose, and impair the energy supply to maintain ionic gradients through the plasma membranes (Martin et al., 1994). Due to the energy depletion, membrane potential is lost and thereby neurons and glial cells depolarize (Katsura et al., 1994). Consequently, somatodendritic and presynaptic voltage-dependent  $\text{Ca}^{2+}$  channels are activated and excitatory amino acid for instance glutamate is released to the extracellular space. The excitatory amino acids in turn activate the NMDA receptors that account for  $\text{Ca}^{2+}$  overload into cells (Fig. 5). The increased intracellular  $\text{Ca}^{2+}$  sequentially initiates cytoplasmic and nuclear events including activation of nitric oxide synthase (NOS), proteases, protein kinases, protein phosphatases, phospholipase  $\text{A}_2$  and  $\text{Ca}^{2+}/\text{Mg}^{2+}$ -activated endonuclease. Moreover,  $\text{Ca}^{2+}$ /calmodulin-dependent protein kinase II is inactivated following transient forebrain ischemia (Morioka et al., 1992).

After transient ischemia in the focal and global ischemia model, blood flow is restored by reperfusion. In combination with calcium overload, re-oxygenation by reperfusion provokes cytotoxicity through the generation of downstream reactive nitrogen and oxygen species that disrupt energy homeostasis through several modes of cellular damage. Excessive accumulation of calcium by mitochondria impairs oxidative phosphorylation and promotes production of reactive oxygen species such as superoxide

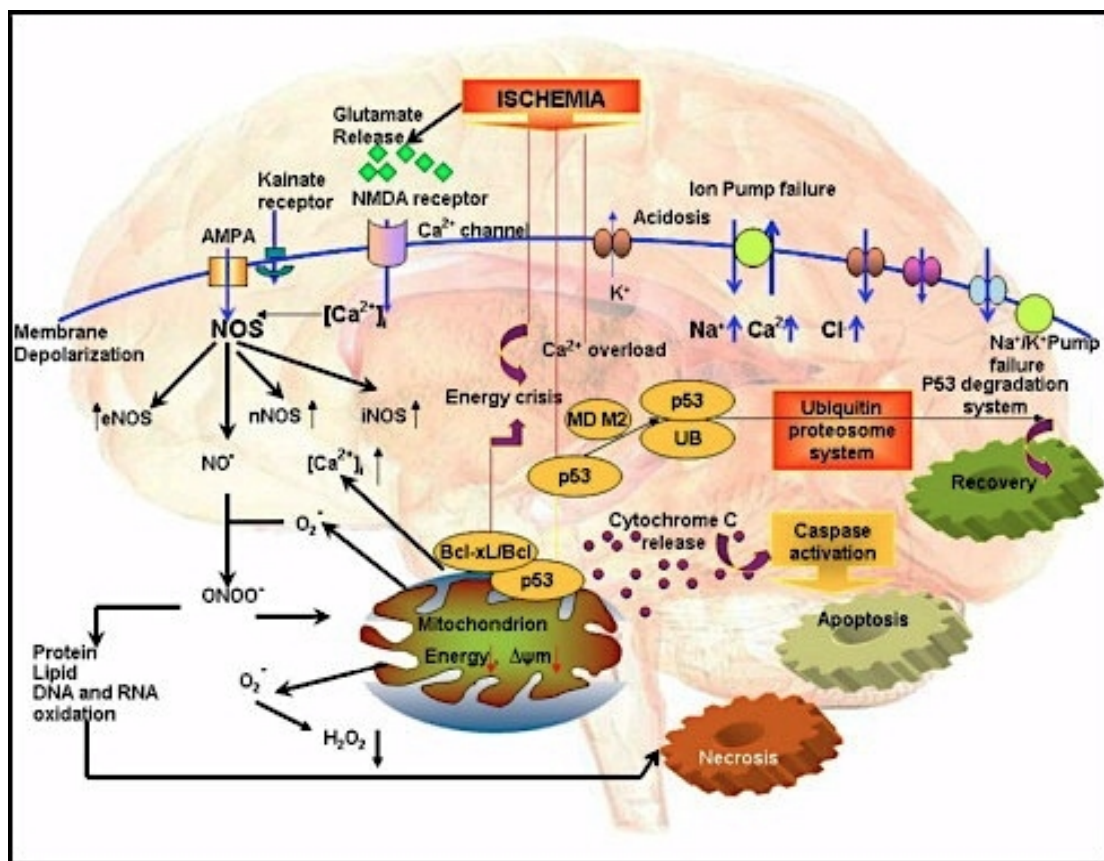


**Fig. 5.** Schematic diagram of intracellular pathways of ischemia induced neuronal death (Dohare et al., 2008).

( $O_2^-$ ) and hydrogen peroxide ( $H_2O_2$ ) via electron transport chain. High mitochondrial calcium accumulation also alters permeability of the mitochondrial membrane, which inhibits mitochondrial ATP production and promotes necrosis. In addition, selective

permeability of the outer membrane releases cytochrome c which activates caspases. Caspases, in turn cleave specific cytoplasmic and nuclear protein substrates to coordinate apoptosis. Hydrogen peroxide is formed from superoxide and it converts to the highly reactive hydroxyl radical via iron-catalyzed reactions.  $\text{Ca}^{2+}$  also activates NOS, a calmodulin-dependent enzyme to produce large amount of nitric oxide (NO). Superoxide and nitric oxide combine to form the much more reactive peroxynitrite anion ( $\text{ONOO}^-$ ). Peroxynitrite damages the cell membrane and leads to the oxidation and nitration of proteins containing aromatic amino acids such as tyrosine. DNA damage produced by either  $\text{Ca}^{2+}/\text{Mg}^{2+}$ -activated endonuclease,  $\text{ONOO}^-$ , or by hydroxyl radicals results in robust activation of poly-ADP-ribose polymerase (PARP) activation with subsequent depletion of NAD levels. Since NAD is required for ATP production, vice versa; excessive PARP activation depletes the cellular pool and that leads to the neuronal death.

### **Stroke induces neurogenesis**

Neurogenesis is the process by which neurons are generated from neural stem and progenitor cells. Neurogenesis is important in neurological repair and the fundamental function of the central nervous system (Ara et al., 2010; Vutskits et al., 2006). The sub granular zone (SGZ) of the hippocampal dentate gyrus (DG) and the sub ventricular zone (SVZ) are distinct regions of active neurogenesis in adult mammalian brains, and it is known to generate new neurons continuously throughout life (Eriksson et al., 1998; Schmetsdorf et al., 2005; Doetsch et al., 1997; Alvarez-Buylla and Garcia-Verdugo, 2002).

Neurogenesis in the brain is influenced by various environmental stimuli including aging and ischemic injury (Darsalia et al., 2005; Jin et al., 2004, Koketsu et al., 2006; Luo et al., 2006; Maslov et al., 2004; Tang et al., 2009; Hong et al., 2011; Rawson and

LaMantia, 2007). Neurogenesis decreases in intact brain including the DG (Heine et al., 2004; Kuhn et al., 1996; Hwang et al., 2008), and the subventricular zone of the lateral ventricle during the normal aging process (Luo et al., 2006; Maslov et al., 2004). On the other hand, following an ischemic damage enhances neurogenesis, and it could contribute to functional recovery through the generation of new neurons to replace those neurons lost by injury in the adult brain (Koketsu et al., 2006; Nygren et al., 2006; Matsumori et al., 2006; Planeet al., 2004; Salazar-Colocho et al., 2008). More specifically, usually global cerebral ischemia induces neurogenesis in DG/SGZ, whereas focal cerebral ischemia induces neurogenesis in the SVZ (Liu et al., 1998, Jin et al., 2003, Kee et al. 2001, Yagita et al. 2001, Yoshimura et al. 2001, Zhang et al. 2001, Arvidsson et al. 2002, Iwai et al. 2002, Parent et al. 2002, Schmidt and Reymann 2002, Iwai et al., 2003, Tonchev et al., 2003, Zhu et al., 2003, Tanaka et al., 2004, Zhang et al., 2004).

Furthermore, it was also observed that ischemia activates progenitor cells not only in DG, but also in the hippocampal CA1 region – the most vulnerable to global ischemic injury brain region (Lipton, 1999). Precursor cells residing in adjacent to CA1 periventricular region migrated toward cell-depleted pyramidal layer of CA1 where they differentiated into hippocampal pyramidal neurons (Nakatomi et al., 2002). Subsequent experiments in adult animals supported these observations, and suggested that the rodent brain possesses an endogenous ability to repair damaged hippocampal CA1 neurons (Schmidt and Reymann, 2002; Bendel et al., 2005).

Thus, the above studies depict the fact that ischemic stroke animal model is useful to mimic the clinical condition of cardiac arrest and/or stroke and thus can provide significant cue to understand the consequence of post ischemic milieu.

## 1-2. Background and Specific aims

### *Background*

Previously we reported the identification of a chemorepulsive axon guidance molecule, draxin that shares no sequence homology with other known guidance molecules (Islam, et al., 2009). *In vitro* draxin inhibited or repelled chicken spinal cord commissural, tectal, mouse cortical and olfactory bulb axonal outgrowth (Islam et al., 2009; Naser et al., 2009; Ahmed et al., 2010). Mice with mutations in *draxin* showed mild guidance defects in certain axons and a dramatic loss of all forebrain commissures (Islam et al., 2009). We also showed previously that the hippocampus size in *draxin* knockout mice is smaller than the wild type (Zhang et al., 2010). Additionally, we previously documented the discovery of the TSK protein, which belongs to the small leucine-rich proteoglycan family (SLRP) (Schaefer and Iozzo, 2008). We showed that TSK is an extracellular modulator of the TGF- $\beta$ , Notch, FGF and Wnt signaling cascades by binding to and inhibiting the activity of these signaling molecules during early embryonic development in the chick and frog (Ohta et al., 2004; Ohta et al., 2006; Kuriyama et al., 2006; Morris et al., 2007; Ohta et al., 2011). Genetic deletion of *TSK* causes malformation of the CC and agenesis of the AC (Ito et al., 2010) and affects hair cycle (Niimori et al., 2012).

We recently reported that draxin binds multiple netrin-1 receptors and that its high-affinity interaction with DCC is required for draxin's inhibitory effect on the cortical and olfactory bulb (OB) neurite outgrowth. The frequency of severity in corpus callosum (CC) malformation in *draxin/Dcc* double-hetero mice is more obvious than that in either of the single-hetero mice that implies DCC as a functional receptor or receptor component for draxin (Ahmed et al., 2011).

Earlier stroke was one of the major causes of mortality in both developing and developed countries. Recently, although the mortality of cerebrovascular disorder tends to decrease in the developed countries due to the developments of various management and the advances of preventive medicine, there are many people suffering from the post consequence of stroke. Endogenous neurogenesis might play important roles in post ischemic neurological healing. It was reported that axon guidance molecules and their receptors such as Sema4C, Sema3A and the receptor of Sema3A, NRP1 expression was increased in SVZ and DG in post ischemic situation and that play important roles for neurogenesis (Hou et al., 2008; Wu et al., 2009). Moreover, repulsive guidance molecule (RGM) a (RGMa), an axon guidance protein expression is up regulated after spinal cord injury and plays an important role in limiting axonal regeneration after injury (Hata et al., 2006).

### ***Specific Aims***

a) Since both *draxin* and *TSK* single mutant mice converge into common phenotypes—malformation of the CC and agenesis of the AC—I was interested in observing whether these two molecules interact genetically to form the CC and AC.

b) As draxin exerts its chemorepulsive function through netrin's chemoattractive receptor, DCC; there might be some other co-receptor(s) that also interact with DCC to perform the opposite signaling pathway of draxin. Therefore, my second aim was to identify the co-receptor by proteomics approach to elucidate draxin signaling pathway.

c) While other axon guidance molecules play important function of post ischemic adult neurogenesis as well as axonal regeneration/degeneration, I also tried to explore the new function of draxin after transient global ischemia and focal cerebral ischemia of adult mice.

## **2. Materials and Methods**

### **2-1. Mice**

Both *draxin* and *TSK* mutant mice were maintained in a mixed C57BL/6-CBA background (Islam et al., 2009; Ohta et al., 2011). Mice homozygous for *draxin* or *TSK* were crossed to obtain doubly heterozygous mutant mice. The procedure to generate both *draxin* and *TSK* knockout mice/ $\beta$ -galactosidase ( $\beta$ -gal) knockin and knockout mice was described previously (Islam et al., 2009; Ito et al., 2010). Stage-specific wild-type embryos were used for *in vitro* culture experiments. For *draxin* and *TSK* mRNA expression analysis, postnatal day 1 (P1) of *draxin-TSK* double heterozygous and single heterozygous of both mice were used. The day of the appearance of the vaginal plug was designated as embryonic day 0.5 (E0.5). All mice were handled according to guidelines approved by the Committee on Animal Research at the University of Kumamoto.

### **2-2. $\beta$ -gal staining and histological analyses**

To determine the mRNA expression patterns of *draxin* and *TSK* at E13.5, E18.5, P0, P1 and adult,  $\beta$ -gal staining was performed on 25~50 $\mu$ m horizontal or coronal cryostat sections and 50  $\mu$ m horizontal vibratome sections according to the standard protocol (Nagy et al., 2003). Section immunohistochemistry was performed following a protocol previously described in detail (Okafuji and Tanaka, 2005). The following primary antibodies were used for immunostaining: rat anti-L1, 1:5000 (Chemicon, USA) and rabbit anti- $\beta$ -gal, 1:10,000 (CAPEL, USA), chick anti- $\beta$ -gal, 1:1000 (Abcam, USA) and rabbit anti-GFAP, 1: 500 (Dako, Japan).

### **2-3. DiI labeling**

To trace the AC axonal tract, a 10% solution of 1,10-dioctadecyl-3,3,30,30-tetramethylindocarbocyanine perchlorate (DiI) (D3911, Molecular Probes) in

dimethylformamide (Sigma) was injected into the olfactory bulb at P6, and the pups were perfused at P8. The brains were fixed in 4% PFA over night, and horizontal sections of the brains (150  $\mu\text{m}$  thickness) were cut on a vibratome. The sections were counterstained with a 10 mg/ml solution of Hoechst 33342 (H21492, Molecular Probes).

#### **2-4. Hematoxylin and Kluver–Barrera (KB) staining**

For the axonal morphological analysis, adult brain sections were double stained with hematoxylin and Kluver–Barrera (KB), the sections were incubated with 0.1% Luxol fast blue at 56<sup>0</sup>C overnight and washed in 95% ethanol for 5 min at RT. After being washed with PBS, the sections were differentiated briefly in a 0.05% lithium carbonate solution, rinsed twice with 70% ethanol, and washed with PBS. After hematoxylin staining, the sections were dried at RT and cleared with xylene followed by entellan solution.

#### **2-5. Preparation of conditioned medium**

The cDNAs encoding chick draxin-AP, mouse TSK-Myc-His, mouse TSK-Flag, chick FGF1-Flag, DCC-ecto-Myc-His, DCC-Fc, chick TSK-Myc-AP and an empty AP tag vector (Islam et al., 2009) were transfected into 293T cells using Lipofectamine-2000 (Invitrogen), conditioned for 5 days and concentrated using an Amicon Ultra centrifugal device (Millipore). Protein production was assessed by western blot using an anti-draxin, anti-Myc, anti-Flag and anti-Fc antibody.

#### **2-6. Brain lysate preparation**

E 17.5 WT mouse brains were dissected and lysed in brain lysis solution (Tris-HCl 10mM, P<sup>H</sup> 8.0, PMSF (100mM) 10  $\mu\text{L}/\text{mL}$ , Leupeptin (10mM) 2  $\mu\text{L}/\text{mL}$ , Aprotinin 1  $\mu\text{g}/\text{mL}$ ). The mixtures were kept on ice for 30 minutes. Concentrated chick draxin-AP CM was mixed with freshly prepared brain lysate solution and rotate for 1 hour at 4<sup>0</sup>C

followed by adding detergent (Triton X 100, 1% conc.) to each tube & mix well by pipette. Further, rotate for 1 hr at 4<sup>0</sup>C and then ultracentrifuge at 111,111.11 xg (40,000 rpm) for 1 hr at 4<sup>0</sup>C and collect the supernatant.

## **2-7. Immunoprecipitation (IP) assay**

Different combinations of concentrated draxin-AP, TSK-Myc-His, TSK-Flag, DCC-Fc and DCC-ecto-Myc-His fusion protein CM, purified netrin-His (R & D Systems) were mixed together and incubated with anti-Myc (9E10) in IP buffer (150 mM NaCl, 20 mM Tris-HCl, pH 7.5, 1.5 mM CaCl<sub>2</sub>, 1.5 mM MgCl<sub>2</sub>, 0.1% Triton X-100, 0.1% CHAPS, 5% glycerol, and 0.1% BSA) at 4<sup>0</sup>C for 12 hours, and complexes were retained and washed extensively on either protein G-Sepharose beads (GE Healthcare) or Probond resin (Invitrogen). The immunoprecipitated/pull downed proteins was separated by 7.5% SDS-PAGE and detected by western blot using either a mouse monoclonal anti-chicken draxin antibody (Ahmed et al., 2011) or anti-Flag antibody (Sigma). As a negative control, draxin-AP or TSK-Flag was mixed with Sepharose beads; or TSK-Flag was mixed with Probond resins.

In proteomic approach for draxin co-receptor, collected brain lysate supernatant was pre-cleared by mixing with simple agarose A beads for 30 min at 4<sup>0</sup>C and centrifuge at 3000 rpm for 2 min. Pre-cleared sup was harvested to perform IP according to the standard protocol followed by Western Blot.

## **2-8. In situ hybridization**

Standard protocols were used for in situ hybridization with a digoxigenin-labeled antisense RNA probe, as previously described (Islam et al., 2009; Ohta et al., 2011). Embryos were dissected in diethyl pyrocarbonate (DEPC) treated phosphate buffered

saline (pH 7.0) and fixed in 4% paraformaldehyde in PBS at 4 °C overnight. For section in situ hybridization, fixed embryos were cryoprotected by immersion in 20% sucrose in PBS and embedded in OCT compound (Sakura Fine Technical Co. Ltd, Tokyo, Japan). Sixteen micrometer thick sections were cut on a cryostat and mounted on silanized glass slides (DAKO Cytomation). In situ hybridization was performed using our previous method with a little modification (Naser et al, 2009). Briefly, sections were treated with 10 µg/ml proteinase K and permeabilized with 1% Triton X-100 and then incubated with herring sperm DNA. Hybridization was performed overnight at 65 °C with 400 ng/ml probe in prehybridization solution. After hybridization, sections were washed in 0.2× SSC at the hybridization temperature followed by blocking reagent treatment (Roche). For immunochemical detection, alkaline phosphatase (AP)-conjugated anti-DIG Fab fragment (Roche) diluted 1:5000 in blocking reagent and incubated for 5 hours at room temperature. Samples were washed and signals were detected using 337.5µg/ml p-nitroblue tetrazolium (NBT) and 175µg/ml 5-bromo-4-chloro-3-indolylphosphate (BCIP) in AP buffer solution (0.1 M Tris-HCl (pH 9.5), 0.1 M NaCl, 50 mM MgCl<sub>2</sub>, 0.001% Triton-X 100, 50 mg/ml Polyvinyl alcohol) overnight at 4<sup>0</sup>C in the dark. Slides were washed and dried overnight, dehydrated in a graded series of ethanol and xylene, and then mounted.

## **2-9. Explant cultures**

Explants from E16.5 cortex were dissected as described previously (Shu and Richards, 2001) and cultured in collagen gels for 48 hours in the presence of either TSK conditioned medium (CM) or control CM (100nM) mixed with neurobasal medium (GIBCO) supplemented with B27 (GIBCO), glutamax-I and penicillin/streptomycin (GIBCO) at a 1:1 ratio. After 48 hours of culture, the TSK CM was removed, and fresh

neurobasal medium with supplements was added and cultured for 48 hours at 37<sup>0</sup>C in a 5% CO<sub>2</sub> incubator. At least, five independent experiments were performed where four to six explants were used in each experiment. Photographs were taken using an inverted microscope (Model Eclipse E600, Nikon).

For co-culture experiments, mouse draxin cDNA or control vector was transfected into COS7 cells using Lipofectamine 2000 (Gibco BRL). Forty-eight hours later, cell pellets containing 1000–2000 cells were generated by hanging drop cultures (Ohta et al., 1999). Explants from E16.5 mouse AON were dissected from wild type mice and were co-cultured with cell aggregates in rat-tail collagen and placed at a distance of 200–300 μm from each other and cultured in above-mentioned culture medium. Five independent experiments were performed where at least four explants were used in each experiment. Neurites were visualized by immunostaining with anti-neuron-specific β-tubulin (Tuj1) antibody (R&D systems, USA) and photographs were taken using Keyence (Bioevo) inverted microscope. Explants were subdivided into four equal quadrants. The quadrant nearest the aggregates was designated as the proximal side, and the opposite quadrant was labeled distal. The number of neurites in these two quadrants was measured and the Proximal/Distal ratio was determined.

## **2-10. Growth cone collapse and neurite outgrowth assays**

AON and cortical neurons from E16.5 mouse embryos were dissociated by trypsinization as described previously (Hata et al., 2006) and seeded at low density (30,000 cells/4-well dish) in 4-well dishes containing coverslips coated with poly-L-lysine (100 μg/ml).

For the neurite outgrowth assays, AON and cortical neurons were cultured in neurobasal medium (B27, glutamax-I, penicillin/streptomycin) with the desired concentration of draxin and TSK conditioned medium for 40 to 48 hours at 37<sup>0</sup>C in a 5% CO<sub>2</sub> incubator. Later, neurons were briefly fixed and stained with an anti-neuron-specific  $\beta$ -tubulin (Tuj1) antibody (R&D systems, USA). We quantified the length of the longest neurite from two individual neurons within a randomly selected field using the ImageJ software. Data were collected from five independent experiments and are expressed as means  $\pm$  SEM. In each independent experiment, at least 20 fields were counted per group.

For the growth cone collapse experiment, AON neurons were seeded at a low density in 4-well dishes containing coverslips coated with poly-L-lysine (100 mg/ml) and laminin (20 mg/ml) and cultured in neurobasal medium. Sixty hours after seeding, the neurons were incubated with TSK CM and control medium alone for 1 hour at 37<sup>0</sup>C in a 5% CO<sub>2</sub> incubator to induce collapse. The cultures were later fixed in 4% paraformaldehyde/10% sucrose for 1 hour. After the well was washed with PBS, the growth cones were stained with phalloidin-Alexa 568 (Invitrogen) diluted in PBS and 0.3% Triton X100, and images were acquired on a microscope (Model Eclipse E600, Nikon) to score the collapse. To calculate the percentage of the collapse, the number of collapsed growth cones was divided by the total number of growth cones. Data were collected from five independent experiments and are expressed as means  $\pm$  SEM. In each independent experiment, at least 50 neurons were counted per group.

## **2-11. AP binding assay**

AON and cortical explants were dissected at E16.5 as described above and cultured in poly-L-lysine and laminin coated 4-well dishes in the presence of supplemented

neurobasal medium for 48 hours at 37<sup>0</sup>C in a 5% CO<sub>2</sub> incubator. TSK-AP and control-AP binding to neurites was performed as previously described (Islam et al., 2009). Five independent experiments were performed using at least 4 to 5 explants in each experiment. Quantification of AP binding was measured using Keyence Bioevo BZ-9000 software. In brief, color images were converted into negative images. Then measure the darkness intensity of the axons in compared to the closest background intensity. Darkness intensity of the axon was divided by the closest background intensity to obtain AP binding ratio.

## **2-12. Mouse draxin monoclonal antibody productions**

At first mouse draxin (Fc fused) construct was created using P<sup>EF-Fc</sup> vector following restriction digestion, ligation, transformation and plasmid amplification and performed sequence PCR. COS7 cells were transfected using DEAE-dextran method and 4 hours later the DNA mixture was washed by 1x CMF media two times and added 25 mL of GIT:DMEM (1:1) serum free medium to each 15 cm dish. Following day, 50 µL of Gentamycin per 15 cm dish was added. After 4 days of transfection, the protein production was checked by WB using conditioned medium (CM). One week of post transfection CM was collected and stored at 4<sup>0</sup>C using preservative until the sufficient amount of CM harvested. Then for purification, CM was passed through the column contains Protein A beads for 2 times (20~24 hrs) followed by 2 times dialysis in PBS (12-14 hrs). Dialyzed purified mouse draxin-Fc protein was concentrated using 50 K centrifugal filter (Milipore) and the protein concentration was measured using BioRad protein assay kit. Protein purity was checked by SDS-PAGE followed by Silver Staining or coomassie blue staining.

In each trial at least 2 ICR female Draxin KO mice were immunized 2 times (100 µg/mouse in each trial at 14 days interval) through footpad and after 10 days of 2<sup>nd</sup> immunization checked the antibody titer by western blot using immunized mice serum compared with non immunized mouse serum. After 14 days of 2<sup>nd</sup> immunization, booster dose was performed through tail vein. Three days after booster dose, immunized mouse was sacrificed and spleen cell suspension was fused with 653 Myeloma cells using HAT medium supplemented with hybridoma cloning factor. Gradually, HAT medium was replaced by HT medium. Next, mouse draxin monoclonal antibody was screened and positive clones were further treated to make a single clone. Further single clone producing antibody was checked by immunocytochemistry and reconfirming positive single cloned antibody production was expanded and checked the subtype of the monoclonal antibody by dot blot assay.

### **2-13. Transient global cerebral ischemia**

Adult male mice were anesthetized with 1.5% fluothane (halothane) in a mixture of 30% O<sub>2</sub> and 70% N<sub>2</sub>O via a face mask with spontaneous breathing. A midline neck incision was made and the bilateral common carotid arteries (CCAs) were gently exposed without disturbing the vagus nerve. Both arteries were then occluded using aneurysm clips for 15 minutes. The clips were then removed to restore the cerebral blood flow. Rectal temperature was maintained at 37.0±0.5°C with a heating pad (Unique Medical, Japan) during the operation. After 15 minutes occlusion, the clips were removed to restore blood flow. After awakening from anesthesia, mice were returned to home cages and allowed to take food and water before experiments. Control animals were sham-operated and received the same experimental procedures except for occlusion of both CCAs. Mice were deeply anesthetized using mixture of selecter and ketalar on 3, 5, 7 or

10 days of post ischemia and the brains were perfused with PBS and then perfusion fixed with 4% paraformaldehyde in PBS. The brains were decapitated and postfixes in the same fixative overnight at 4°C. Each brain was then soaked overnight in 20% sucrose in PBS. Finally, sample was frozen in OCT compound. Coronal sections (50µm thick) were prepared using a cryostat machine.

#### **2-14. Focal cerebral ischemia (Middle cerebral artery occlusion)**

Adult male mice were anesthetized with 1.5% fluothane (halothane) in a mixture of 30% O<sub>2</sub> and 70% N<sub>2</sub>O via a face mask with spontaneous breathing. Following induction, anesthesia was maintained with 1.5% halothane in a 30% O<sub>2</sub>/70% N<sub>2</sub>O mixture by means of an open face mask. Pre-auditory skin incision was made, and the temporal muscle was reflected rostrally. A vinyl tube (inner diameter of 1.0 mm, outer diameter of 3.0 mm, 3.0 mm in length) was attached to the skull bilaterally by gentle pressure, 1 mm superior and posterior to the root of the zygomatic arch for measurement of cortical micro-perfusion by laser Doppler flowmetry (LDF; Advance Laser Flowmetry, model ALF-21, Advance Co., Ltd., Tokyo, Japan). Next rectal probe was inserted to maintain the body temperature at 37.0±0.5°C with a heating pad (Unique Medical, Japan). The fur on the ventral neck was shaved to expose the skin and disinfect the surgical site using 70% ethanol. A midline neck incision was made and the bilateral common carotid artery (CCA), external carotid artery (ECA), internal carotid artery (ICA) were carefully separated from the surrounding nerves and fascia. Dissect the ECA further distally and coagulate the ECA and its superior thyroid artery (STA) branch using a bipolar coagulator. Cut the ECA and STA at the coagulated segment. Then, loosely tie two 8-0 silk sutures around the ECA stump. Apply a vascular clamp (Fine Science Tools) at the bifurcation of the CCA into the ECA and ICA. Make a small incision at the end of ECA

stump with Vannas-style spring scissors (Fine Science Tools). Measure and record the length of a 5-0 monofilament suture rounded at the tip. Insert the suture into the incision and advance to the clamp. Tighten the two silk sutures around the lumen just enough to secure yet preserve mobility of the in-dwelling monofilament suture. Remove the clamp from the bifurcation and cut a bit in ECA and gently advance the silicon coated monofilament suture from the lumen of the ECA into the ICA for a distance of 9-10 mm beyond the bifurcation of CCA to occlude the origin of MCA. About 30-40 min later opens the clip of ECA and withdraws the suture gently and closes the incision area. Place the mouse in a 35°C nursing box to recover from anesthesia, and return it to the cage. It generally takes 5-10 min for the mice to recover from anesthesia. However, sometimes it takes a bit longer time. Twenty-four hours after the induction of MCAO anesthetize the mouse and decapitate the mouse and collect the brain. Slice the brain coronally into four 2-mm slices with a chopper. Incubate the brain slices in 1X PBS containing 2% 2,3,5-triphenyltetrazolium chloride (TTC) (Sigma-Aldrich) for 20 min at room temperature to determine the size and extent of the infarction.

### 3. Results

Results section has been divided into three sections: Part A Part B and Part C. Part A deals with the data, which suggest that draxin and Tsukushi genetically interact and their combined repulsive guidance activity is essential for forebrain commissure formation. In Part B, I have narrated our effort to identify the co-receptor of draxin. In Part C, I have shown the up-regulation of draxin in ischemic brain.

#### 3-1. Part A

##### 3-1-1. CC and AC formation in draxin/TSK doubly heterozygous mice is severely affected

*Draxin* or *TSK* single knockout mice show severe and common defects, i.e., the misprojection of the CC and AC (Islam et al., 2009, Ito et al., 2010). To determine whether there is a genetic interaction between these two molecules, we crossed *draxin* and *TSK* singly heterozygous mice and generated offspring with the following five genotypes: *draxin*<sup>+/+</sup>*TSK*<sup>+/+</sup> (WT); *draxin*<sup>+/-</sup>*TSK*<sup>+/+</sup>; *draxin*<sup>+/-</sup>*TSK*<sup>+/-</sup>; *draxin*<sup>+/+</sup>*TSK*<sup>+/-</sup> and *draxin*<sup>-/-</sup>*TSK*<sup>-/-</sup>. First, we compared all three forebrain commissure phenotypes in postnatal mice with the *draxin*<sup>+/-</sup>*TSK*<sup>+/+</sup>, *draxin*<sup>+/-</sup> *TSK*<sup>+/-</sup>, and *draxin*<sup>+/+</sup>*TSK*<sup>+/-</sup> genotypes. We performed L1 immunostaining and observed notable differences in the severity of CC and AC defects between singly and doubly heterozygous mice (Fig. 6). We classified the phenotypes into two categories depending on the severity of CC and AC defects. In the strong phenotype group of mice, the CC axons were not connected. Instead, they completely misprojected (Fig. 6C, arrow), and the ACp was completely missing at the midline (Fig. 6F, I). Mice in the weak group showed slightly disorganized bundles of axons in the CC (Fig. 6B, arrow) and a very thin ACp crossing the midline (Fig. 6E, H arrow). Although the frequencies of the strong AC phenotype in the *draxin*

and the *TSK* singly heterozygous mice were 8% and 0%, respectively, the strong CC phenotype was not observed in any of these singly heterozygous mice (Table 2). In contrast, compared with the singly heterozygous mice, *draxin/TSK* doubly heterozygous

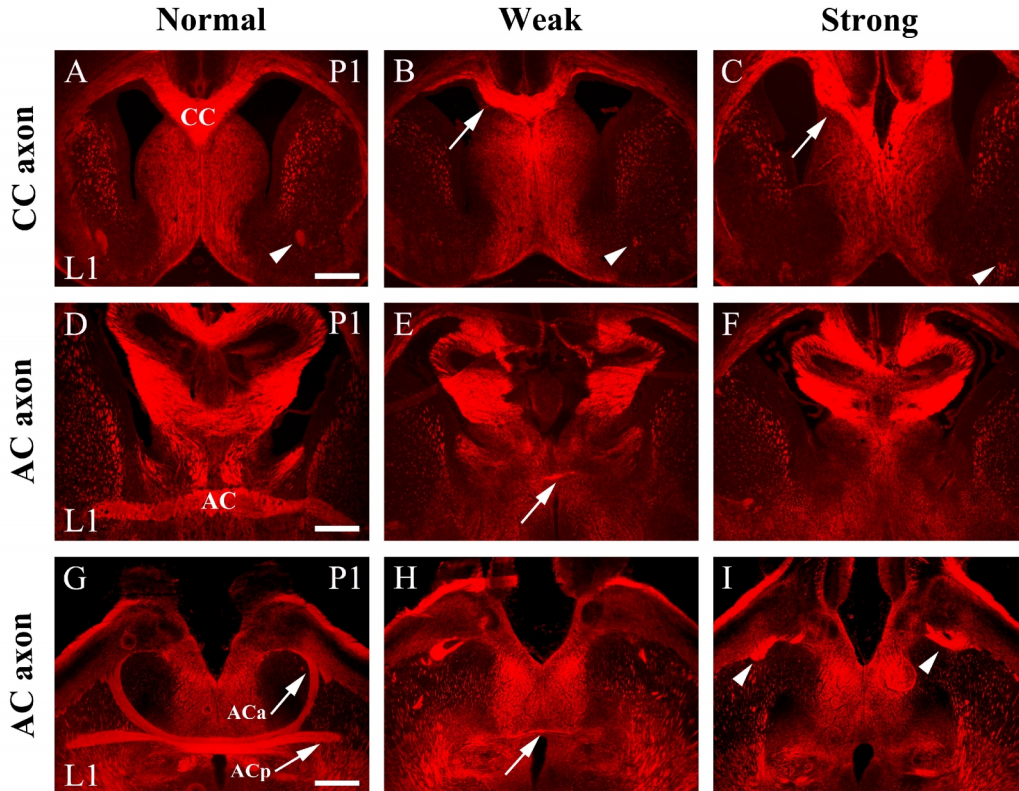


**Fig. 6.** CC and AC formation are severely affected in *draxin/TSK* doubly heterozygous mice. CCs and ACs immunostained with an antibody against L1 in coronal and horizontal sections of P1 mice (A–I). A, D and G are normal mice. B, E and H represent the weak CC and AC phenotypes, respectively. In the weak CC phenotype, the CC was well connected but slightly disorganized (arrow in B). In the weak AC phenotype, a very thin AC can be observed (arrowhead in B and arrow in E and H). C, F, and I show strong CC and AC phenotypes, respectively. For the CC, the strong phenotype was defined as being severely misprojected with no connection of the CC between the two hemispheres (arrow in C). The strong phenotype in the AC was defined as the absence of an AC in the midline (F, I). The arrowhead in C indicates defasciculation in the anterior parts of the AC (ACa). Misprojection or stopped of ACa was indicated by arrowheads (I). The scale bars indicate 500  $\mu$ m

| Genotype<br>(n)                          |    | Normal<br>n (%) | Weak<br>n (%) | Strong<br>n (%) |
|--|----|-----------------|---------------|-----------------|
| <i>draxin</i> +/- (13)                   | CC | 12 (92)         | 1 (8)         | 0 (0)           |
|  | AC | 11 (84)         | 1 (8)         | 1 (8)           |
| <i>TSK</i> +/- (13)                      | CC | 13 (100)        | 0 (0)         | 0 (0)           |
|  | AC | 13 (100)        | 0 (0)         | 0 (0)           |
| <i>draxin</i> +/-<br><i>TSK</i> +/- (26) | CC | 17 (65)         | 2 (8)         | 7 (27)          |
|  | AC | 3 (12)          | 7 (27)        | 16 (61)         |

**Tab. 2.** Frequencies of CC and AC phenotypes in singly and doubly heterozygous P1 mice.

mice showed a markedly higher (CC = 27% and AC = 61%) frequency of the strong phenotype (Table 2). The frequencies of the weak CC and AC phenotypes observed in *draxin* and *TSK* singly heterozygous mice were 8 and 0%, respectively, whereas doubly heterozygous *draxin/TSK* mice showed notably higher (CC = 8% and AC = 27%) frequencies (Table 2). We also observed thin and defasciculated ACa's (arrowhead in Fig. 6B, C). Furthermore, we observed ACp was also misguided in the doubly heterozygous *draxin/TSK* mice. Moreover, we investigated doubly homozygous mice (n=5) and found much higher frequency of AC defect compared with either singly homozygous *draxin* (n=5) or *TSK* mice (n=5). Whereas all doubly homozygous mice showed strong AC defect, only 60% and 20% of singly homozygous *draxin* and *TSK* mice, respectively displayed strong phenotype (Table 3).

| Genotype<br>(n)                                       |    | Normal<br>n (%) | Weak<br>n (%) | Strong<br>n (%) |
|---|----|-----------------|---------------|-----------------|
| <i>draxin</i> <i>-/-</i> (5)                          | CC | 1 (20)          | 2 (40)        | 2 (40)          |
|   | AC | 0 (0)           | 2 (40)        | 3 (60)          |
| <i>TSK</i> <i>-/-</i> (5)                             | CC | 5 (100)         | 0 (0)         | 0 (0)           |
|   | AC | 0 (0)           | 4 (80)        | 1 (20)          |
| <i>draxin</i> <i>-/-</i><br><i>TSK</i> <i>-/-</i> (5) | CC | 0 (0)           | 3 (60)        | 2 (40)          |
|   | AC | 0 (0)           | 0 (0)         | 5 (100)         |

**Tab. 3.** Frequencies of CC and AC phenotypes in singly and doubly homozygous P1 mice

Next, to assess the defects in the ACa clearly, we examined the DiI labeling (n=9) and observed remarkable differences in the AC axonal projection of the doubly heterozygous, but not the singly heterozygous mice. Depending on the misrouted pattern, we classified the phenotype into two categories. In the strongly affected case, the ACa axons were misprojected laterally from their beginning (Fig. 7C, arrow). In weakly affected cases, ACa axons were misrouted dorsally after nearly reaching the midline area (Fig. 7B, arrow). Fifty six percent of DiI labeled mice showed strong phenotype where as 33% mice showed weak phenotype. Our DiI labeling data illustrated that the AC axons grew normally out of the AON in both singly and doubly heterozygous mice; these axons later misprojected in the doubly heterozygous mice. These data indicated that the AONs were not affected in either the singly or the doubly heterozygous mice. It appeared that the absence of the AC in the midline area was caused by axon pathfinding errors rather than by the damage or death of neurons projecting toward the commissure. Overall, these data

indicated that the severe AC defects in doubly heterozygous mice might be due to the genetic interaction of the *draxin* and *TSK* genes.

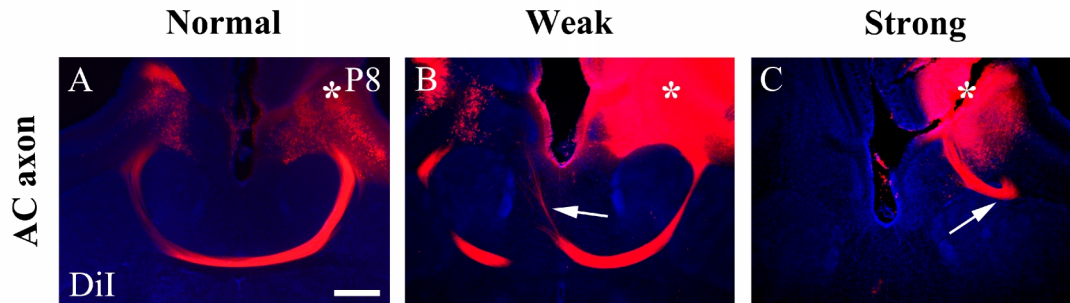


**Fig. 7.** AONs were not affected in the doubly heterozygous mice. DiI was injected into the P6 olfactory bulbs (\*) of singly and doubly heterozygous mice, and the labeled AC axons were observed horizontally at P8. In the normal case, the AC axons cross the midline (A), whereas in the weakly affected cases, the AC axons are misrouted dorsally after reaching the midline area (arrow) (B). In strongly affected cases (C), AC axons were misprojected laterally from the beginning (arrow). The scale bars indicate 500  $\mu\text{m}$ .

We also performed hematoxylin and Kluver–Barrera (KB) double staining to analyze the axonal morphogenesis in the mouse adult brain ( $n=5$ ). We observed significant new defects in the *draxin*/*TSK* doubly heterozygous adult mice compare to either *draxin* or *TSK* singly heterozygous adult mice which were not noticeable in the neonatal mice. We observed very thin CC (Fig. 8B, arrowhead), as well as expanded sub ventricular zone and lateral ventricle (Fig. 8D) in the *draxin*/*TSK* doubly heterozygous adult mice compare to either *draxin* or *TSK* singly heterozygous adult mice. Furthermore, we analyzed hippocampal size of the *draxin*/*TSK* doubly heterozygous adult mice brain. Interestingly, we observed smaller size of hippocampus in the *draxin*/*TSK* doubly heterozygous adult mice (Fig. 8F, arrow) compare to that of *draxin* or *TSK* singly heterozygous mice.

### **3-1-2. Draxin and TSK proteins do not interact biochemically**

Because we observed severe commissure defects in the *draxin/TSK* doubly heterozygous mice, we next investigated whether the draxin and TSK proteins interact directly. To address this issue, we performed immunoprecipitation (IP) assays using draxin-AP and TSK-Myc-His. We used Myc-tagged soluble DCC ectodomain as a positive control. Draxin-AP was specifically immunoprecipitated by the DCC ectodomain and not by TSK-Myc (Fig. 9). These data showed that there is no biochemical interaction between draxin and TSK. Next, we investigated whether TSK interacts with draxin receptor, DCC. To clarify this matter, we performed pull down assays using TSK-Flag and DCC-Fc; but we didn't observe any interaction between these two molecules (Fig. 10). As both netrin and draxin are the ligands of DCC, there is a possibility that TSK might interact with netrin. To address this issue, we performed pull down assay using TSK-Flag and netrin-His. Interestingly, we found that TSK was specifically pulled down by the netrin (Fig. 11). Taken together, these data indicate that TSK interacts neither draxin nor DCC but with netrin.

### **3-1-3. Expression of *draxin* and TSK mRNA is observed in the strategic region of AC and CC axons**

The key molecules and their receptors that regulate CC and AC formation are expressed in the neocortex, GW, IG, AON and/or piriform cortex (Lindwall et al., 2007). Because we observed malformation of the CC and agenesis of the AC in *draxin/TSK* doubly heterozygous mice, we investigated the expression of both *draxin* and *TSK* at specific developmental stages. We investigated the mRNA expression pattern of both *draxin* and *TSK* in singly heterozygous mice at different stages between E13.5 and P1. Between these stages, the AC and CC develop to form their complete trajectories. We examined

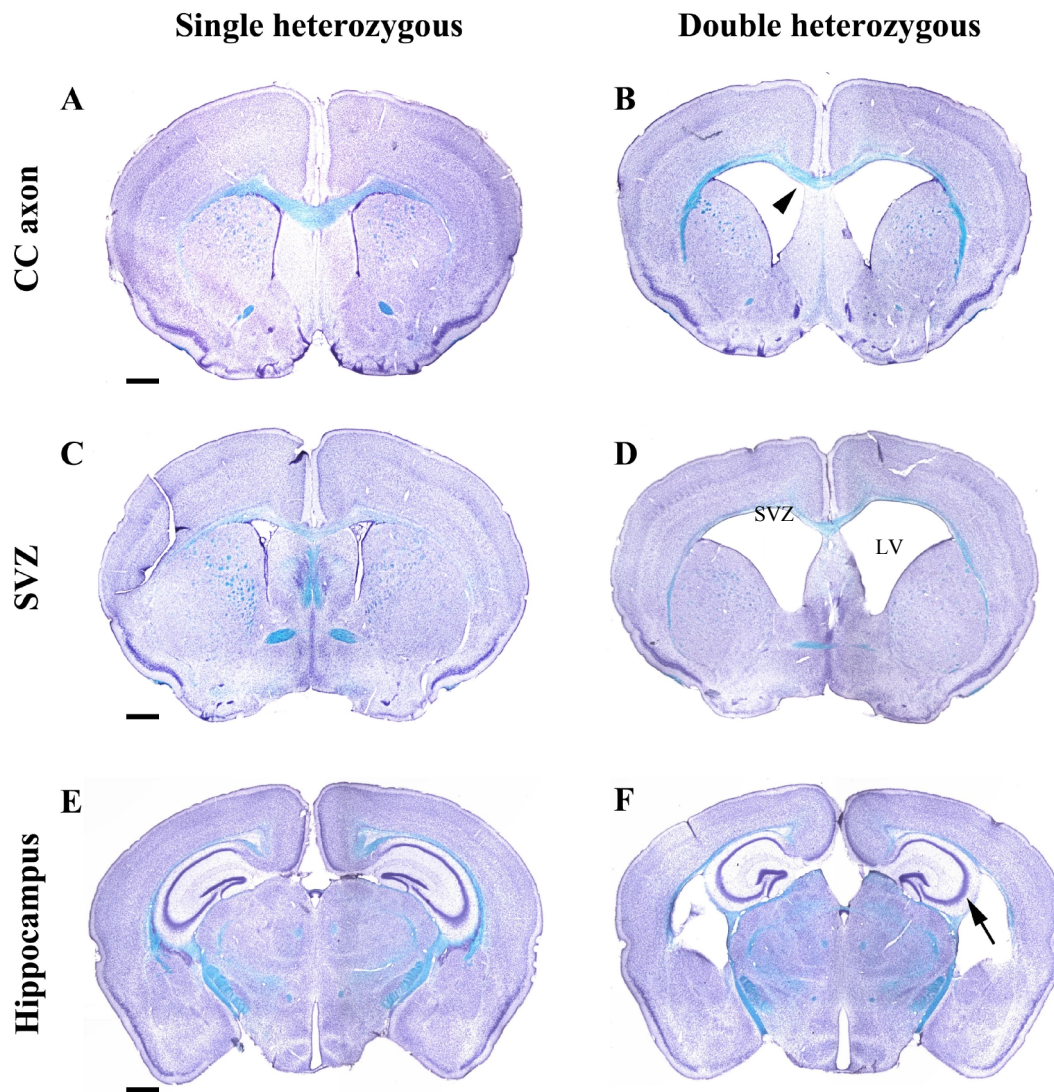


**Fig. 8.** CC, SVZ and hippocampus are malformed in *draxin/TSK* doubly heterozygous adult mice. CC, SVZ and hippocampus was double stained with Hematoxylin and Kluver–Barrera (KB) (A–F). A, C and E represent either *draxin* or *TSK* singly heterozygous adult mice. B, D and F represent *draxin/TSK* doubly heterozygous adult mice. In contrast to thinner CC (arrowhead in B), expanded SVZ and LV was observed in *draxin/TSK* doubly heterozygous adult mice. Smaller hippocampus was observed in *draxin/TSK* doubly heterozygous adult mice (F). The scale bars indicate 600  $\mu\text{m}$ .

the expression of *draxin* and *TSK* using  $\beta$ -galactosidase enzymatic reactions and immunostaining (Islam et al., 2009; Ito et al., 2010). We observed strong expression of both *draxin* and *TSK* in the olfactory bulb, AON, neocortex and piriform cortex at E13.5 (Fig. 12A-D). Moreover, both *draxin* and *TSK* are expressed in the GW (arrow in

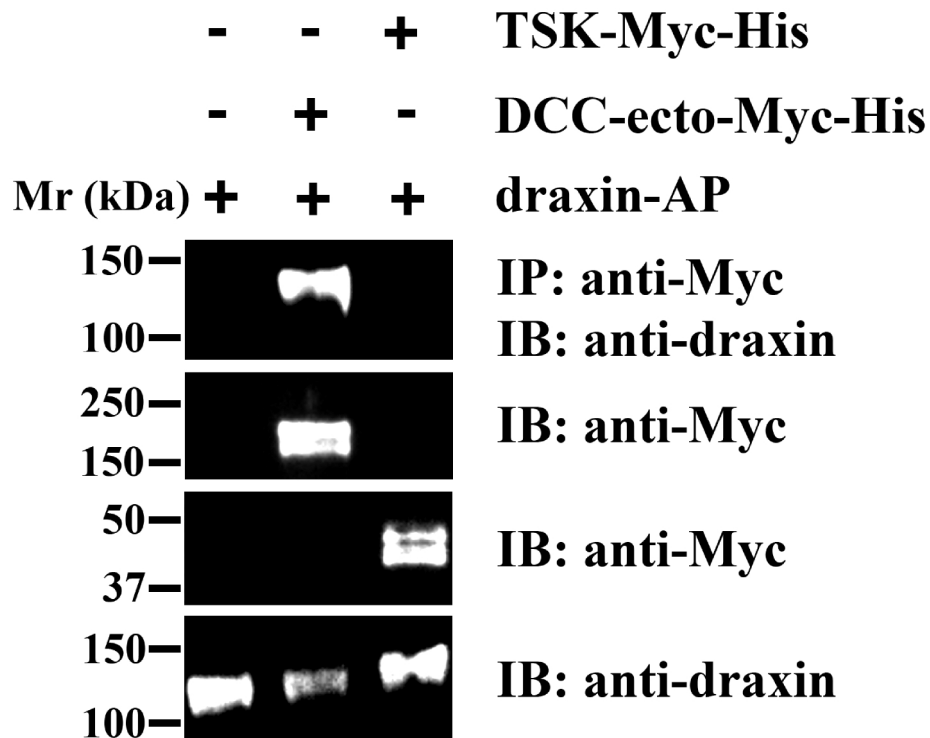


**Fig. 9.** TSK does not interact with draxin. Conditioned medium (CM) of draxin (alkaline phosphatase-tagged) was mixed either with TSK CM or with the extracellular domain of DCC CM (both tagged with Myc), and IP was performed using an anti-Myc antibody. Draxin was co-precipitated by DCC but not by TSK.

Fig. 13A, B; 3A', B'), Midline zipper glia (Fig. 13A, A'', B, B'') and IG (arrowhead in Fig. 13A, B; 13A''', B'''). Next, we sought to determine whether *TSK* and *draxin* expression are observed in the AC. Accordingly, we performed double immunostaining with antibodies against L1 and  $\beta$ -galactosidase on the horizontal sections of P1 singly heterozygous mice. We observed strong, spot-like expression of both *draxin* and *TSK*

mRNA in the AON, anterior and posterior piriform cortex, olfactory bulb (Fig. 14A, A'', B, B'') and area surrounding the AC (Fig. 14A, A', B, B') including midline of AC (arrow head in Fig. 14A, B; Fig. 15A-C), around the entorhinal cortex (\* in Fig. 14A, B) and the stria terminalis (\*\*Fig. 14A, B) but not on AC axons. Moreover, draxin and TSK expression pattern inferred from these  $\beta$ -galactosidase staining follows precisely the

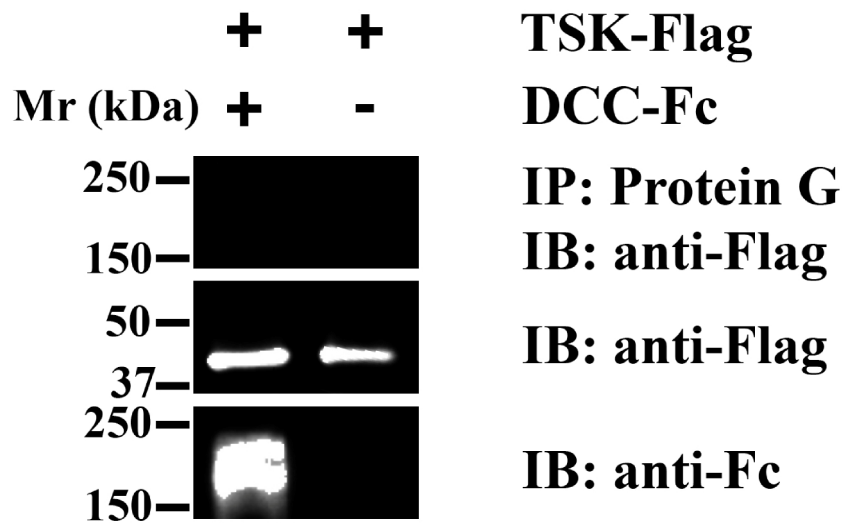


**Fig. 10.** TSK does not interact with DCC. Conditioned medium (CM) of TSK (Flag tagged) was mixed with DCC-Fc CM, and pull down assay was done using Protein G-Sepharose beads. No interaction was observed between TSK and DCC.

pattern of both transcripts detected by in situ hybridization (Zhang et al., 2010; Fig. 15).

Besides, we also investigated TSK and draxin expression in the midline of AC in the doubly heterozygous mice. We observed similar expression pattern of both TSK and draxin in the doubly heterozygous mice (Fig. 16B, E) compared with the singly heterozygous mice (Fig. 16A, D). These expression patterns of *draxin* and *TSK* in strategic regions of the AC and CC imply that these molecules may have a specific role in AC and CC formation.

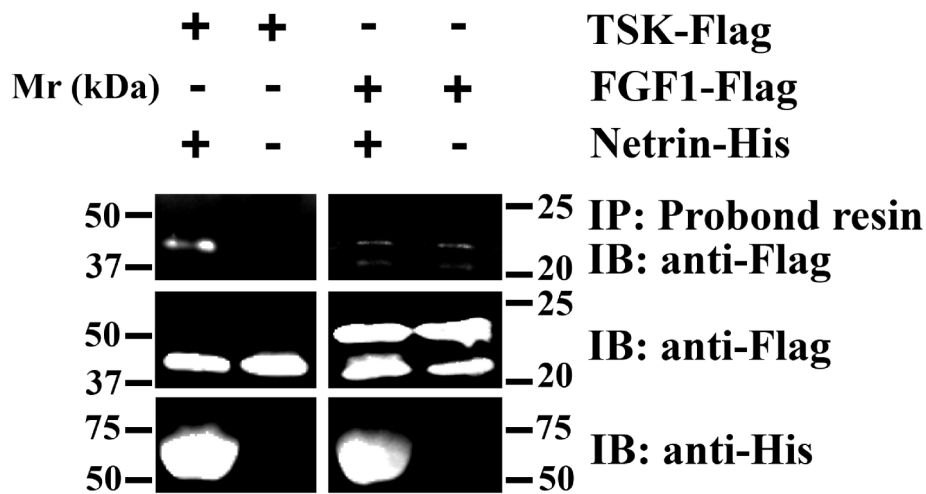


**Fig. 11.** TSK specifically binds with netrin. Conditioned medium (CM) of TSK- Flag was mixed with or without purified Netrin-His protein, and pull down assay was performed using Probond resins; specific interaction of TSK with netrin was clearly observed. As a negative control, an unrelated protein, FGF1-Flag CM was mixed with or without purified Netrin-His and no specific interaction was observed between FGF1 and netrin.

### 3-1-4. TSK inhibits neurite outgrowth

We previously reported that draxin is a chemorepulsive guidance protein. To address the guidance error that we observed in *draxin/TSK* doubly heterozygous mice, we examined whether TSK has guidance activity for commissural axons in the forebrain. We cultured cortical explants from wild-type E16.5 mouse embryos in collagen gel (Fig. 17A, B) in the presence of either control medium (Fig. 17A) or TSK-conditioned medium (TSK CM) (Fig. 17B). Neurite outgrowth from cortical explants was greatly inhibited in TSK CM (Fig. 17B), whereas there was robust neurite outgrowth in the control medium (Fig. 17A). When we replaced TSK CM with fresh culture medium, we observed robust neurite growth within 48 hours from the explant shown in Fig. 17B (Fig. 17C). Thus, the possibility that TSK may have caused cell death in this experiment

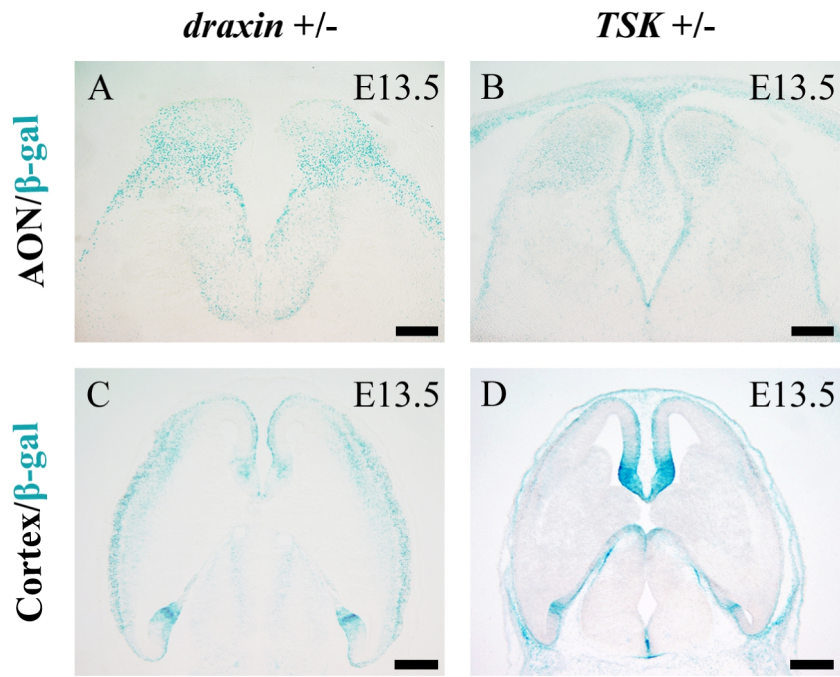


**Fig. 12.** Expression of *draxin* and *TSK*. *draxin* and *TSK* mRNA expression in horizontal sections of the AON region and cortex of *draxin* and *TSK* singly heterozygous E13.5 embryonic mouse brains (A–D). Scale bars = 300  $\mu$ m in A & B; 600  $\mu$ m in C & D.

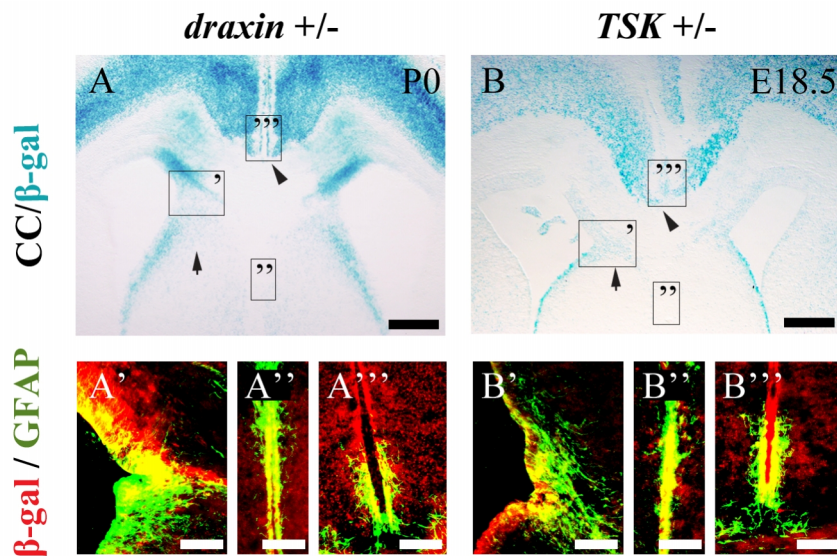


**Fig. 13.** Both *draxin* and *TSK* mRNA are expressed in the strategic region of the CC axons. Expression of *draxin* and *TSK* was observed in the glial wedge (arrows

in A, B; A', B'), Midline zipper glia (A, A'',B, B'') and indusium griseum (arrowheads in A, B; A''', B''') of coronal sections of *draxin* and *TSK* singly heterozygous mouse brains(A–B). Scale bars = 300  $\mu$ m in A, B; 100  $\mu$ m in A'–B''.

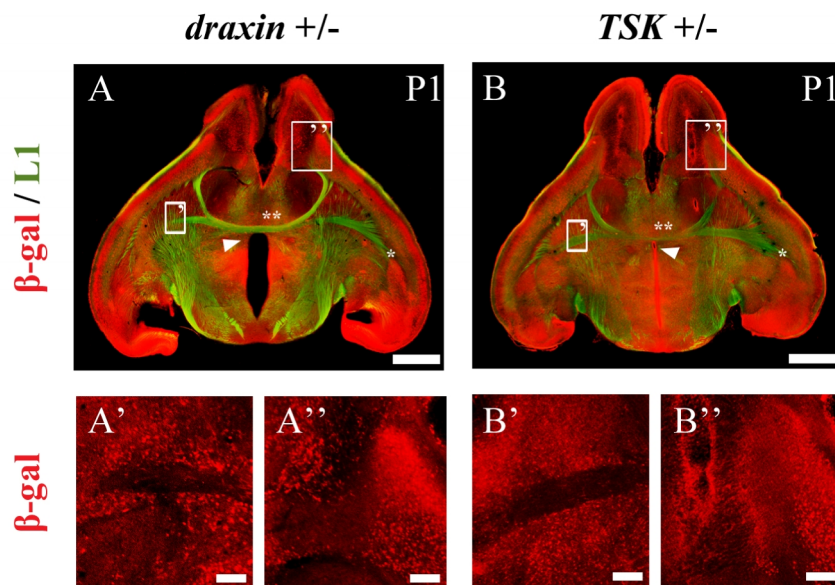


**Fig. 14.** *draxin* and *TSK* mRNA are expressed in the strategic region of the AC axons. Horizontal sections of P1 *draxin* and *TSK* singly heterozygous mouse brains were processed for double anti- $\beta$ -gal (red) and anti-L1 (green) immunohistochemistry (A–B). Both *draxin* and *TSK* mRNA were expressed in the AON region, and strong, punctate expression was observed in the area surrounding AC axons, but not on the axons. Higher magnification of the areas in white squares in A and B ('', ''') are represented in A', A'' and B', B'', respectively. Scale bars = 900  $\mu$ m in A–B, 150  $\mu$ m in A'–B''.

can be excluded, and the data confirm the notion that TSK does indeed function to inhibit neurite outgrowth. Moreover, AON explants from wild-type E16.5 mouse embryo were co-cultured with COS cell aggregates expressing mouse TSK in three dimensional collagen gels. After 48 h in culture, neurites extended radially from explants in control

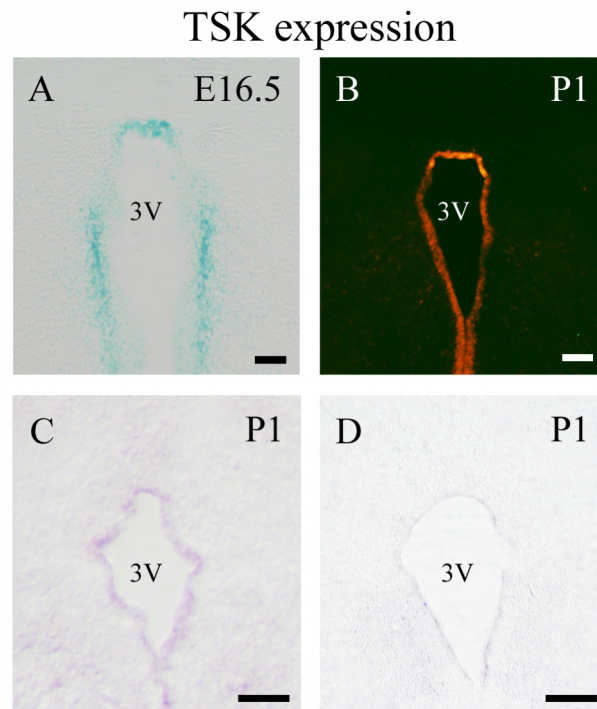


**Fig. 15.** TSK mRNA expressed in AC midline. TSK  $\beta$ -gal and in situ hybridization on neonatal and postnatal horizontal sections (A–D). Detection of TSK mRNA transcripts at E16.5 by  $\beta$ -gal enzymatic reaction (A). TSK was detected by anti- $\beta$ -gal immunostaining at P1 (B). In situ hybridization was performed to detect TSK mRNA transcripts at P1. TSK is not detected in sections from TSK knockout mice (D). Scale bars = 60  $\mu$ m in A, 150  $\mu$ m in B, 80  $\mu$ m in C, D. 3V= 3<sup>rd</sup> ventricle.

experiments (Fig. 18A, C). In contrast, the number of neurites was significantly reduced from the explants facing towards the COS cell aggregates expressing TSK (Fig. 18B, C). These differences were quantified in Fig. 18C. The P/D (proximal/distal) ratio was determined by dividing the number of neurites in the proximal site by that of distal site in relation to the COS cell aggregate (Fig. 18C).

Next, we examined the effects of TSK CM on dissociated neurons. We cultured AON and cortical dissociated neurons from E16.5 wild-type mouse embryos on poly-L-lysine coated dishes in the presence of either control medium (Fig. 19 A, C, E, F) or

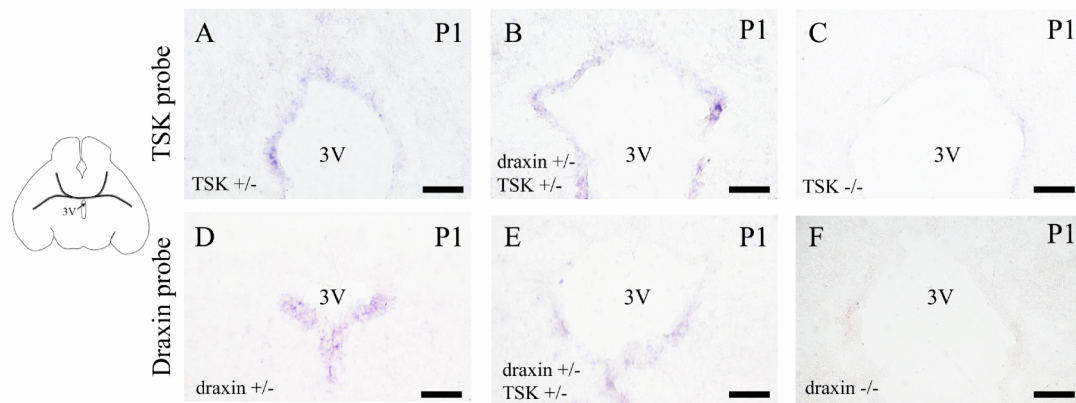


**Fig. 16.** TSK and draxin mRNA expressed in the single heterozygous and double heterozygous mice. TSK and draxin in situ hybridization on postnatal horizontal sections (A–F). Both TSK and draxin mRNA expressed in the midline of AC (A, D). Similar expression pattern was observed in the double heterozygous mice (B, E). TSK or draxin mRNA transcripts was not detected in sections from TSK or draxin knockout mice, respectively (C, F). Scale bars = 50  $\mu$ m. 3V= 3<sup>rd</sup> ventricle.

TSK CM (Fig. 19 B, D, E, F). Neurons were fixed and stained with an anti- $\beta$ -tubulin antibody. Then, we quantified the length of the longest neurite from two individual neurons within a randomly selected field using the ImageJ software and quantified the average maximal length. Representative figures show that TSK inhibited AON and cortical neurite outgrowth (Fig. 19 B, D, E, F) compared with the control (Fig. 19 A, C, E, F). Furthermore, we investigated the dose-dependency of the effects of TSK on neurite outgrowth. To obtain this information, we performed AON and cortical neurite outgrowth inhibition assays in different concentrations (10 nM, 30 nM, 60 nM, and 100 nM) of TSK CM. We found that TSK-mediated neurite outgrowth inhibition was enhanced with increasing concentrations of TSK protein. At 100 nM, TSK significantly inhibited both AON and cortical neurite outgrowth to 9% of control levels (Fig. 19E, F)

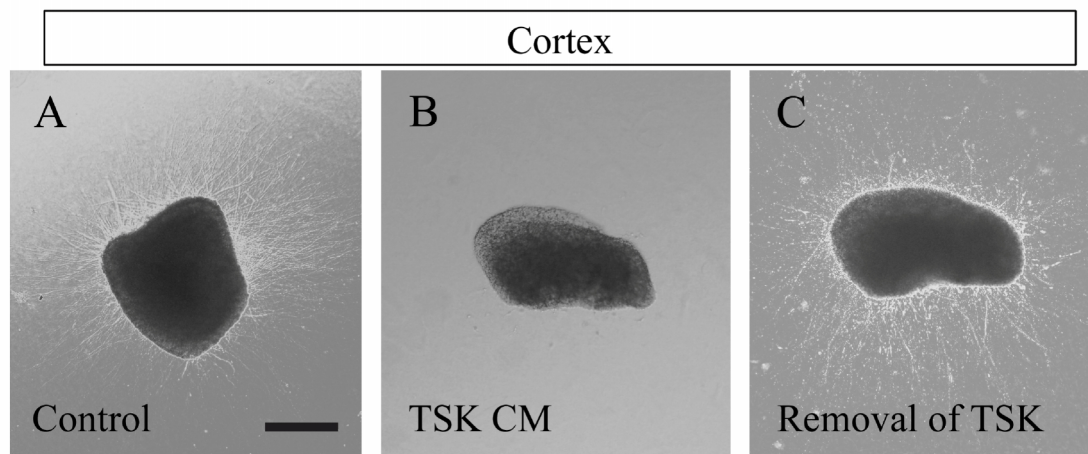


**Fig. 17.** TSK inhibits neurite outgrowth from cortical neurons. Cortical explants from wild-type E16.5 mouse embryos were cultured in collagen gel in the presence of either control medium (A) or TSK conditioned medium (TSK CM) (B). After 48 hours, the TSK CM was replaced by fresh culture medium. Robust outgrowth was observed within 48 hours (C). Scale bars = 300  $\mu$ m in A–C.

### 3-1-5. TSK protein directly binds to both AON and cortical axons

To test whether TSK inhibited axon outgrowth by directly binding to the neurites, AON and cortical explants from wild-type E16.5 mouse embryos were cultured in poly-L-lysine and laminin coated dishes and incubated with TSK-AP fusion protein, and AP protein alone was used as a negative control. We observed that TSK-AP bound to the AON and cortical neurites (Fig. 20C, D, E, F), whereas control AP protein did not bind to the AON or cortical neurites (Fig. 20A, B, E, F).

### 3-1-6. Growth cone collapse is induced by TSK protein

Because bath application of TSK inhibited neurite outgrowth, it is likely that the acute addition of TSK induces growth cone collapse. To test this possibility, we seeded AON dissociated neurons from E16.5 WT mouse embryos at a very low density in dishes coated with poly-L-lysine and laminin. Sixty hours after seeding, the neurons were

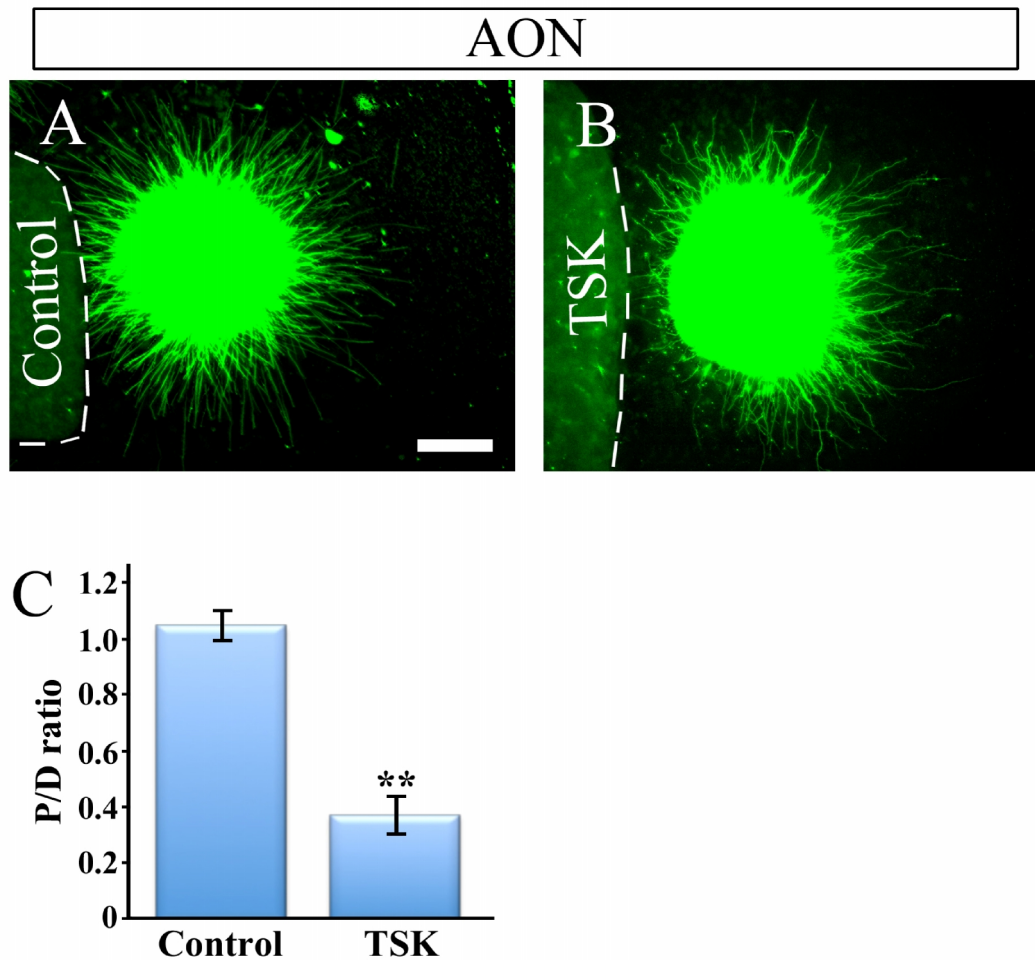


**Fig. 18.** TSK repulse AON neurite outgrowth from AON. AON explants from wild-type E16.5 mouse embryo were co-cultured with mock transfected COS cell aggregate and mouse TSK transfected COS cell aggregate (A, B). Axons grew radially when co-cultured with mock transfected COS cell aggregates (A), while co-cultured with TSK transfected cell aggregates, axons were inhibited (B). The number of axons in proximal, P and distal, D in relation to the COS cell aggregate was counted (n=10 for each group) and the total number of axons in P site was divided by that of D to get the P/D ratio (C). Significant repulsion was observed when explants were co-cultured with TSK compared with control cases. \*\*P < 0.0001. \*\*P < 0.0001 (P values were calculated by comparing with control). Scale bars = 200  $\mu$ m in A–B.

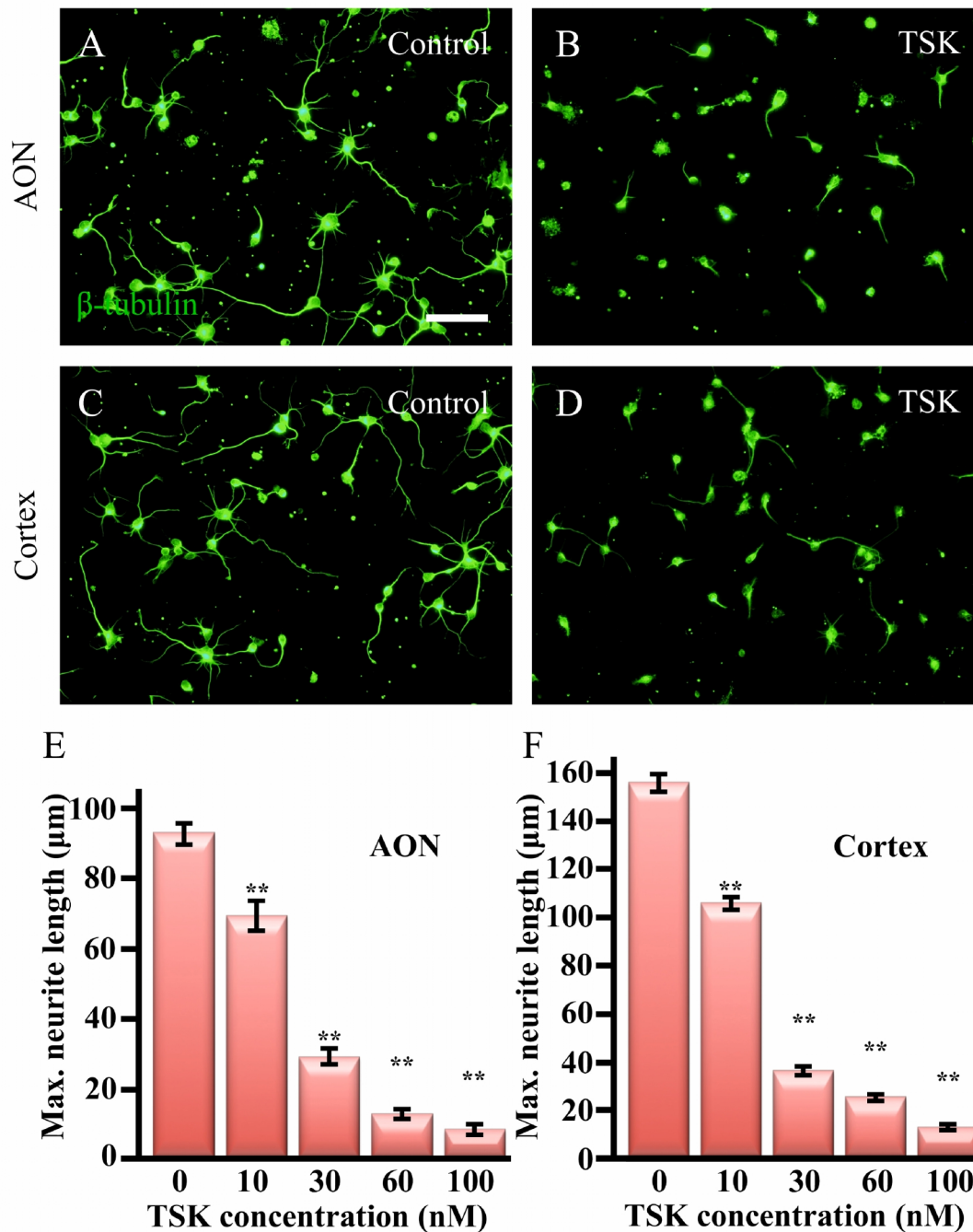


**Fig. 19.** TSK inhibits neurite outgrowth from AON and cortical dissociated neurons. AON and cortical dissociated neurons from E16.5 wild-type mouse embryos were cultured on poly-L-lysine coated dishes in the presence of either control medium (A, C) or TSK-conditioned medium (B, D) for 40 hours. Neurons were fixed and stained with anti- $\beta$ -tubulin antibody. The length of the longest neurite from two individual neurons within a randomly selected field ( $n=20$  for each experiment) was quantified using the ImageJ software, and the average maximal length was measured. Quantification of neurite outgrowth inhibition was conducted in 5 independent

experiments (mean  $\pm$  SEM) (E, F). Compared with the control (A, C, E, and F), TSK inhibited neurite outgrowth in a dose-dependent manner (B, D, E, and F). \*\* $P < 0.0001$  ( $P$  values were calculated by comparing with control). Scale bars = 60  $\mu\text{m}$  in A–D.

incubated with TSK CM (100 nM) or control medium alone for 1 hour at 37°C to induce collapse. The neurons were stained with phalloidin-A1 568 to visualize the growth cones. Representative pictures are shown in Fig. 21A and B. We found that the growth cones in this culture system had a high baseline level of collapse (~33%) that was further increased (to ~82%) after treatment with TSK (Fig. 21C). Taken together, these data indicated that TSK might function as a repulsive axon guidance molecule for subpopulations of neurons *in vivo*.

### **3-1-7. The effects of TSK and draxin on neurite outgrowth inhibition are additive**

Because we observed an inhibitory function of TSK on dissociated neurons, we next asked whether the inhibitory function of TSK is synchronized with the inhibitory function of draxin. To address this issue, we cultured AON dissociated neurons from E16.5 wild-type mouse embryos in the presence of either draxin-conditioned medium (30 nM) (Fig. 22B), TSK CM (30 nM) (Fig. 22C) or in a combination of draxin (30 nM) and TSK CM (30 nM) (Fig. 22D). The mean average maximal axonal length was  $95.3 \pm 3.7$   $\mu\text{m}$  in the control condition (Fig. 22A, E); this value was reduced to  $32.9 \pm 1.2$  or  $41.6 \pm 1.9$   $\mu\text{m}$  when AON neurons were cultured in the presence of either TSK (Fig. 22C, E) or draxin (Fig. 22B, E), respectively. Strikingly, we observed an additive effect of the combination of TSK and draxin-conditioned medium on neurite outgrowth inhibition (mean average maximal axonal length =  $10.3 \pm 0.7$   $\mu\text{m}$ ).

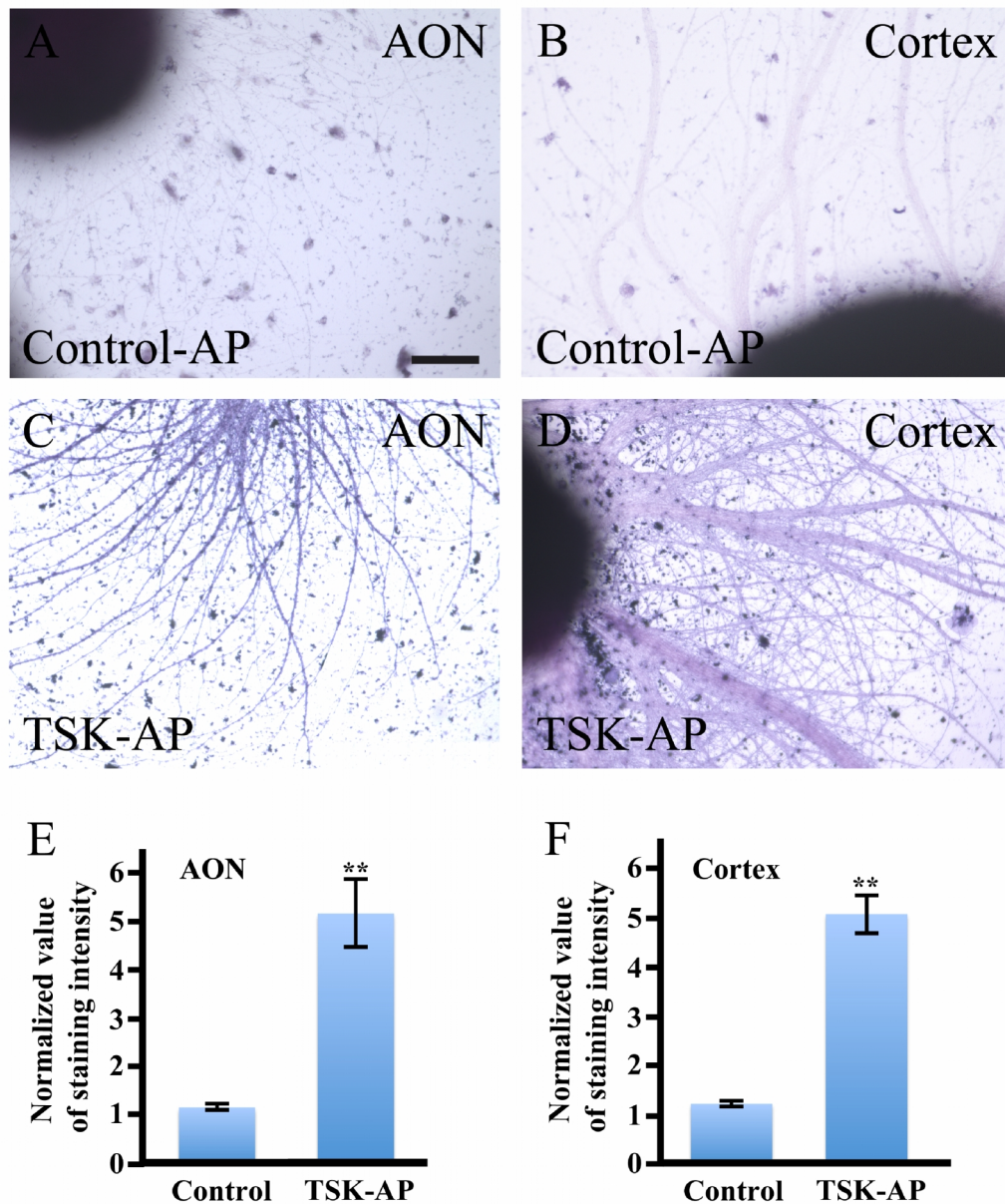


**Fig. 20.** TSK protein binds to both AON and cortical axons. AON and cortical explants from wild-type E16.5 mouse embryos were cultured in poly-L-lysine-laminin-coated dishes. Binding of TSK protein (TSK-AP) to AON and cortical neurites (A–D). Control-AP protein did not bind (A, B), whereas TSK-AP protein bound to the AON neurites (C, D). 5 independent experiments were carried out to quantify the TSK-AP binding intensity to the neurites (error bar indicates mean  $\pm$  SEM) (E, F). Strong binding was observed in case of TSK-AP (n=10) compared with the control (n=10). Scale bars = 120  $\mu$ m in A–D. \*\*P < 0.0001.

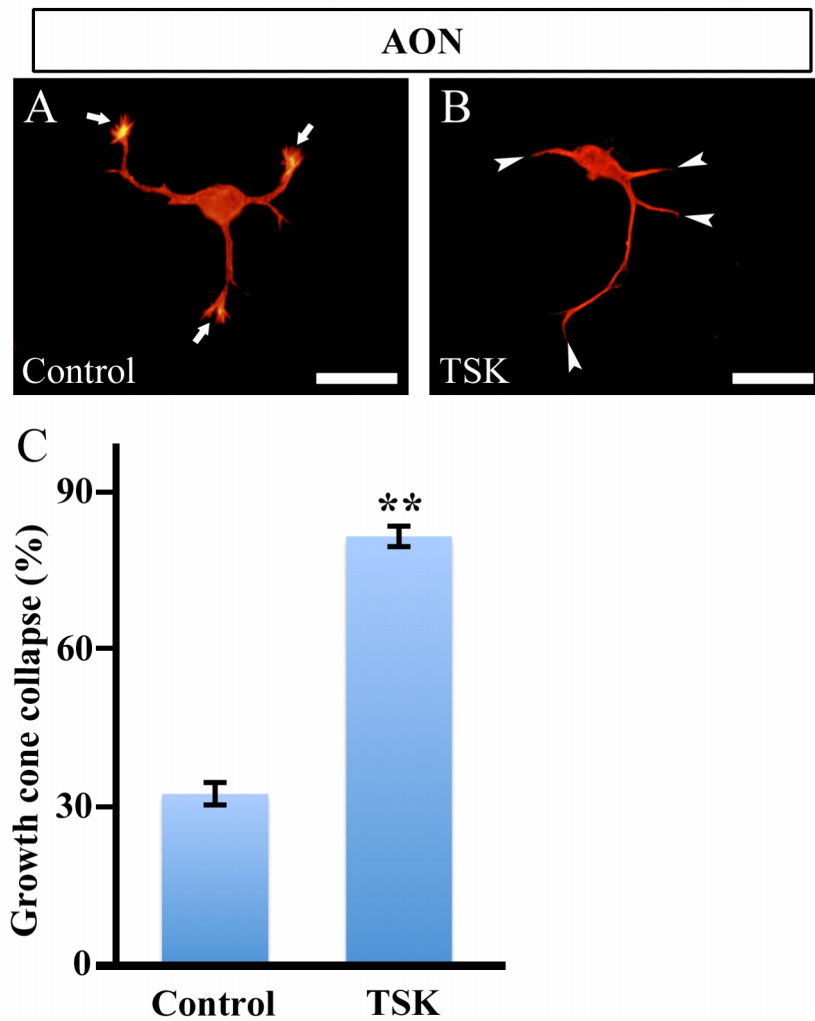


**Fig. 21.** TSK protein induces growth cone collapse. AON neurons from WT mice were treated with either control medium alone or 100 nM TSK for 1 hour at 37°C to induce collapses and stained with phalloidin-A1 568 to visualize the growth cones. Representative pictures are shown in A and B, and the quantified results are shown in C. The data were obtained from five independent experiments, and, on average, the growth cones of 50 neurons were counted in each group in each experiment. The arrows in A and the arrowheads in B indicate the intact and collapsed growth cones, respectively. The scale bars indicate 20  $\mu$ m. The error bars indicate means  $\pm$ SEM. \*\*P < 0.0001.

The combination of draxin and TSK exaggerated the inhibition of neurite outgrowth by 69% and 75% of TSK-induced and draxin-induced inhibition, respectively (Fig. 22D, E). These data indicated that the effects of TSK and draxin were additive.

## **3-2. Part B**

### **3-2-1. Mouse draxin monoclonal antibody productions**

Mouse draxin (Fc fused) construct was created and COS7 cells were transfected using DEAE-dextran method followed by the replacement of serum free medium. Four days of post transfection, the protein production was checked and one week after transfection CM was harvested. Later, CM was passed through the Protein A beads column followed by 2 times dialysis in PBS. Dialyzed concentrated purified mouse draxin-Fc protein was checked by SDS-PAGE followed by Silver Staining or coomassie blue staining.

In each trial at least 2 ICR female Draxin KO mice were immunized 2 times (100 µg/mouse in each trial at 14 days interval) and after 10 days of 2<sup>nd</sup> immunization the antibody titer was checked by western blot using immunized mice serum compared with non immunized mouse serum. After 14 days of 2<sup>nd</sup> immunization, booster dose was performed through tail vein. Three days after booster dose, immunized mouse was sacrificed and spleen cell suspension was fused with 653 Myeloma cells. Then after 2-3 weeks later (depending on the cell growth condition) we screened mouse draxin monoclonal antibody. Later, we treated the initially positive clones to make a single clone. Further, we checked whether the single clone can produce antibody by immunocytochemistry (Fig. 23). Later, we checked the sub-type of the monoclonal antibody by dot blot assay. In the first trial, we found two clones, IgG1 and IgM. Later, we succeeded for only IgM type (Fig. 24). In the 2<sup>nd</sup> attempt, we found 5 good

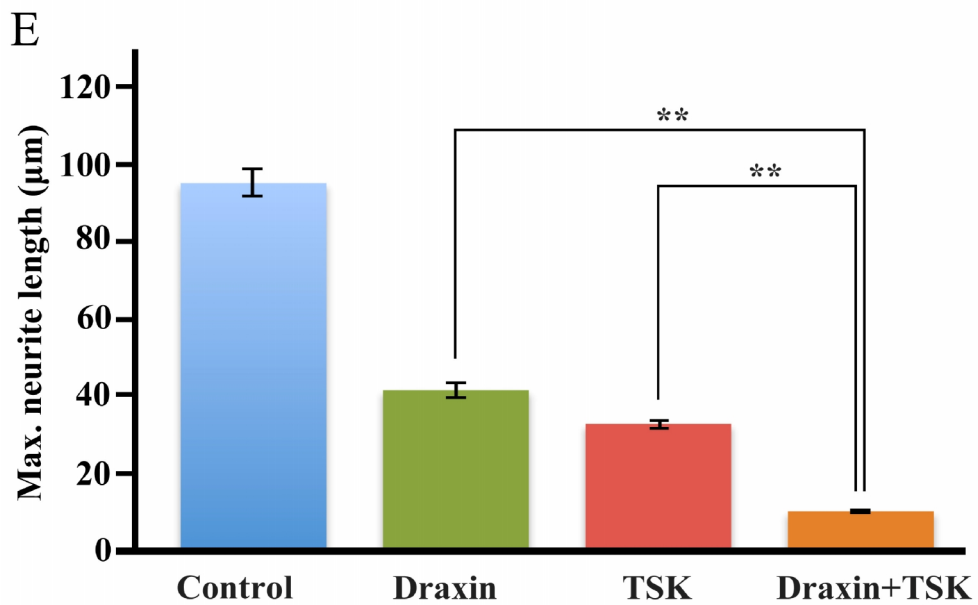
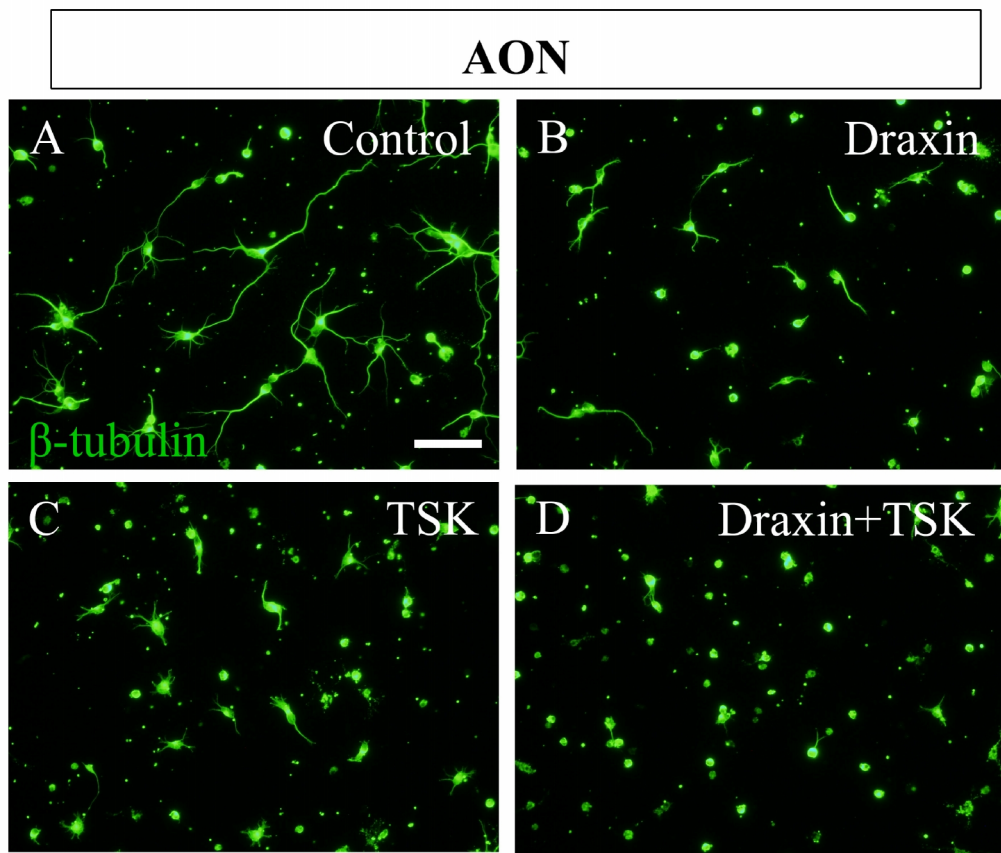


**Fig. 22.** TSK and draxin inhibit neurite outgrowth in an additive manner. AON dissociated neurons from E16.5 wild-type mouse embryos were cultured on poly-L-lysine-coated dishes in the presence of control medium (A), draxin-conditioned

medium (30 nM) (B), TSK-conditioned medium (30 nM) (C), or draxin (30 nM) and TSK (30 nM) conditioned medium (D) for 40 hours. The neurites were stained with an anti- $\beta$ -tubulin antibody, and the length of the longest neurite from two individual neurons within a randomly selected field (n=20 for each experiment) was quantified using the ImageJ software. The combination of TSK and draxin inhibited neurite outgrowth more strongly (D, E) than either TSK (C, E) or draxin alone (B, E). The quantification of neurite outgrowth inhibition was conducted in 5 independent experiments (mean  $\pm$  SEM, \*\*P <0.0001) (E).

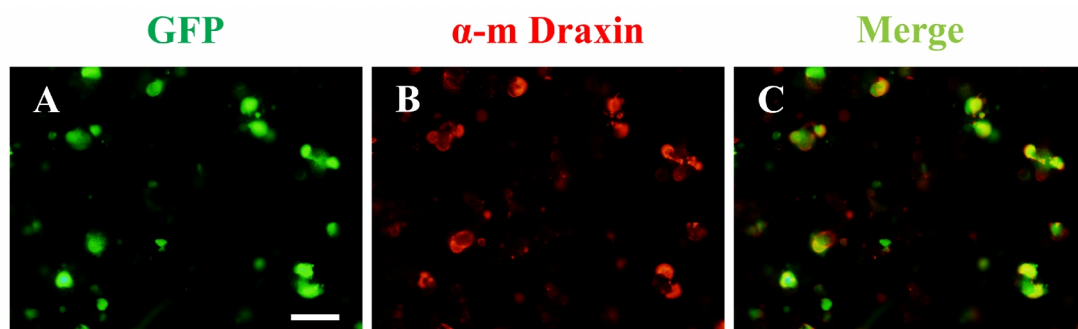


**Fig. 23.** Mouse draxin monoclonal antibody screening. A. 293 cells were transfected with mDra-Tm-IRES GFP and GFP expression of transfected cells; B. Anti-mouse Draxin monoclonal antibody staining; C. Co-localization of GFP expressing cells and anti-mouse Draxin monoclonal antibody stained cells. Scale bar= 60  $\mu$ m.

sub-clones (two IgG1, two igG2a and one igG2b) (Fig. 25). Unfortunately, we couldn't rescue all of them. In the 3<sup>rd</sup> challenge, initially we obtained 4 clones (one IgG1 and 3 IgG2a) but finally not succeeded. We also tried two more times but we couldn't get the desired end product.

### 3-2-2. Immunoprecipitation assay followed by mass spectrometry

In proteomic approach for draxin co-receptor, E 17.5 WT mouse brains lysate was prepared. Next, we added chick draxin (Alkaline phosphatase tagged) conditioned

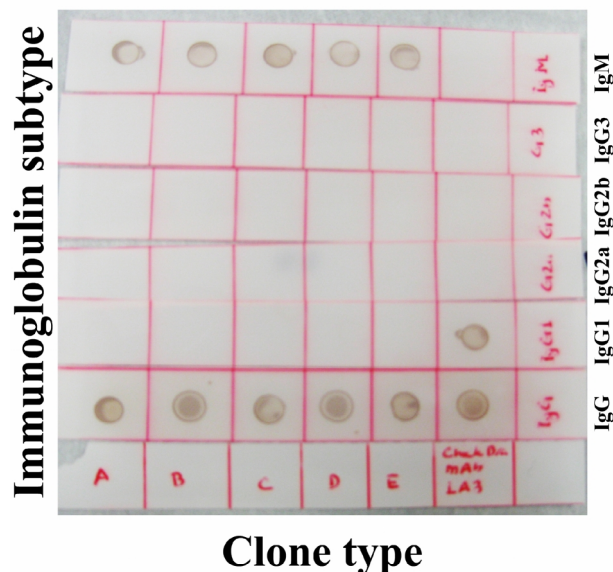


**Fig. 24.** Dot blot assay to identify mouse draxin monoclonal antibody subtype. Five clones show IgM positive whereas one clone shows IgG1 positive.

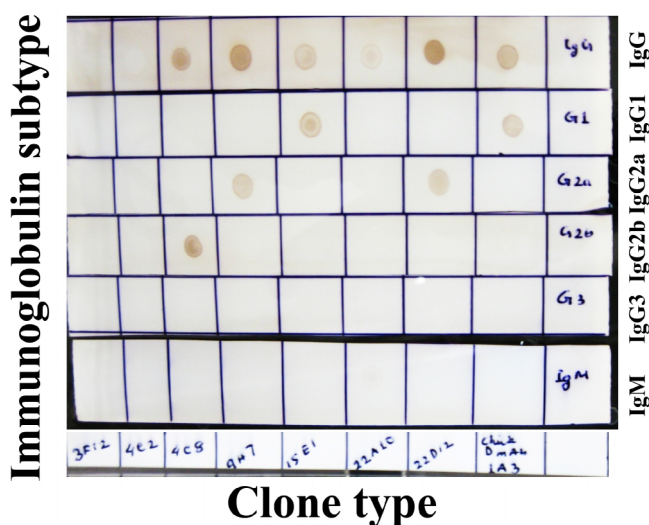


**Fig. 25.** Dot blot assay to identify mouse draxin monoclonal antibody subtype. Two clones showed IgG1 positive, two were IgG2a positive and one clone showed IgG2b.

medium in different concentration to these brain lysate and rotate for 1 hour at 4<sup>0</sup>C. After mixing the detergent followed by 1hour rotation at 4<sup>0</sup>C centrifuge at high speed. Later, brain lysate supernatant was pre-cleared by mixing with simple agarose A beads for 30

min at 4<sup>0</sup>C and harvested the supernatant. Meanwhile, Protein A sepharose beads was treated by binding buffer followed by antibody reaction either with anti-DCC pAb or anti-cDra MAb or anti-hIgG for each for 30 minutes. After triethanolamine treatment, cross linker was used to each tube and rotate for 1 hour. At this step, specific antibody tightly bound to the protein A beads. After washing by ethanolamine, we treated the beads with elution buffer to remove the unbound antibody with the crosslinker. At this step, we added the pre-cleared mouse brain lysate to this antibody bound protein A beads and rotate for O/N. Next day after treating the sample by lysis buffer, several times washed by washing buffer and transferred the beads to the low adhesive tubes.

We sent one part of the above treated samples to our collaborator for mass spectrometry analysis. We have checked the remaining part of the samples either by western blot and/or silver staining. After mass spectrometry analysis, we have found 126 hits (Tab. 4) among them 4 unique types of proteins i) ELKS/Rab6-interacting/CAST family member 1 (Gene name: Erc1), ii) Neogenin (Gene name: Neo1), iii) Potassium/sodium hyperpolarization-activated cyclic nucleotide-gated channel 4 (Gene name: Hcn4), Lethal(2) giant larvae protein homolog 1 (Gene name: Llg1) are promising.

### **3-3. Part C**

#### **3-3-1. Establishment of transient global ischemia**

To perform the transient global ischemia, adult male mice were anesthetized and a midline neck incision was made and the bilateral common carotid arteries (CCAs) were gently exposed without disturbing the vagus nerve. Both arteries were then occluded using aneurysm clips as shown in fig. 26 and the physiological temperature was

**Tab. 4.** Data obtained from mass spectrometry analysis

| <b>Serial number</b> | <b>DCC</b> | <b>Dra</b> | <b>IgG</b> | <b>Gene Name</b> | <b>Molecular Weight</b> |
|----------------------|------------|------------|------------|------------------|-------------------------|
| 1                    | 31         |            |            | Dcc              | 158 kDa                 |
| 2                    | 13         |            |            | Erc1             | 128 kDa                 |
| 3                    | 9          |            |            | Neol             | 163 kDa                 |
| 4                    | 7          |            |            | Hcn4             | 127 kDa                 |
| 5                    | 2          |            |            | Llgl1            | 113 kDa                 |
| 6                    | 36         | 40         | 34         | Hspa9            | 74 kDa                  |
| 7                    | 29         | 26         | 30         | Dhx9             | 149 kDa                 |
| 8                    | 29         | 28         | 27         | Hspa8            | 71 kDa                  |
| 9                    | 22         | 22         | 23         | Tubb3            | 50 kDa                  |
| 10                   | 20         | 20         | 20         | Tuba1a           | 50 kDa                  |
| 11                   | 22         | 23         | 19         | Hnrnpa2b1        | 37 kDa                  |
| 12                   | 16         | 14         | 19         | Actb             | 42 kDa                  |
| 13                   | 17         | 20         | 17         | Hnrnpk           | 51 kDa                  |
| 14                   | 16         | 15         | 17         | Hnrnpa3          | 40 kDa                  |
| 15                   | 15         | 15         | 16         | Hspa5            | 72 kDa                  |
| 16                   | 11         | 10         | 16         | Hnrnpu           | 88 kDa                  |
| 17                   | 15         | 18         | 14         | Hnrnph1          | 49 kDa                  |
| 18                   | 15         | 14         | 13         | Hnrnpa1          | 34 kDa                  |
| 19                   | 12         | 13         | 13         | Gapdh            | 36 kDa                  |
| 20                   | 12         | 13         | 13         | Tubb2b           | 50 kDa                  |
| 21                   | 14         | 13         | 12         | Hnrnpul1         | 96 kDa                  |
| 22                   | 8          | 10         | 12         | Ddx5             | 69 kDa                  |
| 23                   | 10         | 9          | 12         | Hnrnpm           | 78 kDa                  |
| 24                   | 11         | 11         | 10         | Hnrnpd           | 38 kDa                  |
| 25                   | 7          | 10         | 10         | Ddx3x            | 73 kDa                  |
| 26                   | 10         | 9          | 10         | Hnrnpf           | 46 kDa                  |
| 27                   | 8          | 9          | 10         | Camk2b           | 60 kDa                  |
| 28                   | 7          | 9          | 10         | Matr3            | 95 kDa                  |
| 29                   | 9          | 8          | 10         | Tardbp           | 45 kDa                  |
| 30                   | 10         | 11         | 9          | Hnrnpab          | 31 kDa                  |
| 31                   | 10         | 9          | 9          | Hnrpdl           | 34 kDa                  |
| 32                   | 5          | 9          | 9          | Eef1a1           | 50 kDa                  |
| 33                   | 6          | 8          | 9          | Hnrnpl           | 64 kDa                  |
| 34                   | 7          | 4          | 9          | Tnc              | 232 kDa                 |
| 35                   |            | 9          | 8          | Puf60            | 60 kDa                  |
| 36                   | 5          | 8          | 8          | Sec23a           | 86 kDa                  |
| 37                   | 5          | 7          | 8          | Hnrnpc           | 34 kDa                  |
| 38                   | 5          | 7          | 8          | Hnrnpul2         | 85 kDa                  |
| 39                   | 6          | 3          | 8          | Vim              | 54 kDa                  |
| 40                   | 8          | 10         | 7          | Fus              | 53 kDa                  |

**Tab. 4.** Data obtained from mass spectrometry analysis (Cont.)

| <b>Serial number</b> | <b>DCC</b> | <b>Dra</b> | <b>IgG</b> | <b>Gene Name</b> | <b>Molecular Weight</b> |
|----------------------|------------|------------|------------|------------------|-------------------------|
| 41                   | 10         | 8          | 7          | Akap8            | 76 kDa                  |
| 42                   | 5          | 7          | 7          | Khsrp            | 77 kDa                  |
| 43                   | 5          | 6          | 6          | Tubb4            | 50 kDa                  |
| 44                   | 6          | 3          | 6          | Map1b            | 270 kDa                 |
| 45                   | 4          | 3          | 6          | Tial1            | 43 kDa                  |
| 46                   | 1          | 3          | 6          | Hsp90ab1         | 83 kDa                  |
| 47                   | 5          | 8          | 5          | Ddx17            | 72 kDa                  |
| 48                   | 4          | 6          | 5          | Tubb5            | 50 kDa                  |
| 49                   | 4          | 6          | 5          | Elavl3           | 40 kDa                  |
| 50                   | 4          | 5          | 5          | Hnrnp2           | 49 kDa                  |
| 51                   |            | 5          | 5          | U2af2            | 54 kDa                  |
| 52                   | 3          | 3          | 5          | Atp5a1           | 60 kDa                  |
| 53                   | 2          | 2          | 5          | Eif2c2           | 97 kDa                  |
| 54                   | 2          | 2          | 5          | Dpysl3           | 62 kDa                  |
| 55                   | 3          | 1          | 5          | D10Wsu52e        | 55 kDa                  |
| 56                   | 0          |            | 5          | Cltc             | 192 kDa                 |
| 57                   | 2          | 11         | 4          | Krt6a            | 59 kDa                  |
| 58                   | 3          | 6          | 4          | Krt10            | 58 kDa                  |
| 59                   | 3          | 5          | 4          | Syncrip          | 70 kDa                  |
| 60                   | 4          | 4          | 4          | Tubb2c           | 50 kDa                  |
| 61                   | 4          | 4          | 4          | Hbb-b2           | 16 kDa                  |
| 62                   | 3          | 4          | 4          | Elavl1           | 36 kDa                  |
| 63                   |            | 4          | 4          | Srsf2            | 0 kDa                   |
| 64                   | 2          | 3          | 4          | Ilf3             | 96 kDa                  |
| 65                   |            | 3          | 4          | Rbm39            | 59 kDa                  |
| 66                   | 2          | 2          | 4          | Atp1a3           | 112 kDa                 |
| 67                   | 1          | 2          | 4          | Slc25a4          | 33 kDa                  |
| 68                   | 4          | 7          | 3          |                  | 12 kDa                  |
| 69                   | 2          | 5          | 3          |                  | 37 kDa                  |
| 70                   | 3          | 4          | 3          | Ybx1             | 36 kDa                  |
| 71                   | 3          | 4          | 3          | Khdrbs1          | 48 kDa                  |
| 72                   | 4          | 3          | 3          | Ewsr1            | 68 kDa                  |
| 73                   | 3          | 3          | 3          | Igh-3            | 44 kDa                  |
| 74                   | 3          | 3          | 3          | Znf326           | 65 kDa                  |
| 75                   | 3          | 3          | 3          | Myef2            | 63 kDa                  |
| 76                   | 3          | 3          | 3          | Krt1             | 66 kDa                  |
| 77                   | 3          | 3          | 3          | Tubb2a           | 50 kDa                  |
| 78                   | 2          | 2          | 3          | Sec13            | 36 kDa                  |
| 79                   | 1          | 2          | 3          | Dclk1            | 84 kDa                  |
| 80                   |            | 2          | 3          | Luc7l2           | 47 kDa                  |

**Tab. 4.** Data obtained from mass spectrometry analysis (Cont.)

| <b>Serial number</b> | <b>DCC</b> | <b>Dra</b> | <b>IgG</b> | <b>Gene Name</b> | <b>Molecular Weight</b> |
|----------------------|------------|------------|------------|------------------|-------------------------|
| 81                   | 4          | 1          | 3          | Ctnn             | 61 kDa                  |
| 82                   | 3          | 1          | 3          | Eef2             | 95 kDa                  |
| 83                   | 2          | 1          | 3          | Idh1             | 47 kDa                  |
| 84                   | 2          | 1          | 3          | Cspg5            | 60 kDa                  |
| 85                   |            | 1          | 3          | Hadha            | 83 kDa                  |
| 86                   | 1          | 0          | 3          | Elavl2           | 40 kDa                  |
| 87                   | 2          | 10         | 2          | Krt14            | 53 kDa                  |
| 88                   | 2          | 8          | 2          | Ighg1            | 43 kDa                  |
| 89                   | 3          | 6          | 2          |                  | 44 kDa                  |
| 90                   | 1          | 3          | 2          | Hspd1            | 61 kDa                  |
| 91                   | 1          | 3          | 2          | Krt17            | 48 kDa                  |
| 92                   | 0          | 3          | 2          | Krt73            | 59 kDa                  |
| 93                   |            | 3          | 2          | Dhx15            | 91 kDa                  |
| 94                   | 2          | 2          | 2          | Hba              | 15 kDa                  |
| 95                   | 1          | 2          | 2          | Gnao1            | 40 kDa                  |
| 96                   | 1          | 2          | 2          | Crbn             | 51 kDa                  |
| 97                   | 1          | 2          | 2          | Tubb6            | 50 kDa                  |
| 98                   | 1          | 2          | 2          | Actc1            | 42 kDa                  |
| 99                   | 0          | 2          | 2          | Ilf2             | 43 kDa                  |
| 100                  | 0          | 2          | 2          | Krt16            | 52 kDa                  |
| 101                  | 1          | 1          | 2          | Ddb1             | 127 kDa                 |
| 102                  | 1          | 1          | 2          | Prdx2            | 22 kDa                  |
| 103                  | 1          | 1          | 2          | Cct3             | 61 kDa                  |
| 104                  | 1          | 1          | 2          | Dnaja1           | 45 kDa                  |
| 105                  | 1          | 1          | 2          | Ncan             | 137 kDa                 |
| 106                  | 1          | 1          | 2          | Dcx              | 41 kDa                  |
| 107                  | 1          | 1          | 2          | Dpysl2           | 62 kDa                  |
| 108                  |            | 1          | 2          | Cct8             | 60 kDa                  |
| 109                  |            | 1          | 2          | Crmp1            | 62 kDa                  |
| 110                  |            | 1          | 2          | Raly             | 33 kDa                  |
| 111                  |            | 1          | 2          | Npepps           | 103 kDa                 |
| 112                  |            | 1          | 2          |                  | 28 kDa                  |
| 113                  |            | 1          | 2          | Ywhaq            | 28 kDa                  |
| 114                  | 0          | 0          | 2          | Ddx1             | 83 kDa                  |
| 115                  |            | 0          | 2          | Ywhaz            | 28 kDa                  |
| 116                  |            |            | 2          | Prdx1            | 22 kDa                  |
| 117                  |            |            | 2          | Dnaja2           | 46 kDa                  |
| 118                  | 0          | 4          | 1          | Krt5             | 62 kDa                  |
| 119                  |            | 4          | 1          |                  | 12 kDa                  |
| 120                  | 1          | 3          | 1          | Cirbp            | 19 kDa                  |

**Tab. 4.** Data obtained from mass spectrometry analysis (Cont.)

| Serial number | DCC | Dra | IgG | Gene Name | Molecular Weight |
|---------------|-----|-----|-----|-----------|------------------|
| 121           | 0   | 3   | 1   | Krt2      | 71 kDa           |
| 122           |     | 3   | 1   | Rsrc2     | 44 kDa           |
| 123           |     | 3   | 1   | Srsf3     | ?                |
| 124           | 1   | 2   | 1   |           | 13 kDa           |
| 125           |     | 2   | 1   | Mapt      | 76 kDa           |
| 126           |     | 4   | 0   |           | 13 kDa           |

maintained during the surgery. Control animals were sham-operated and received the same experimental procedures except for occlusion of both CCAs arteries. Mice were sacrificed on 3, 5, 7 or 10 days of post ischemia and the brains were fixed by paraformaldehyde followed by sucrose treatment. Coronal sections were prepared.

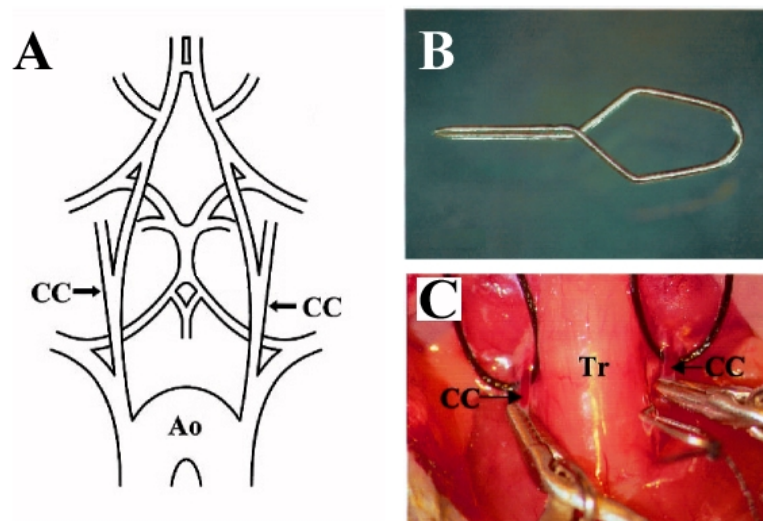


**Fig. 26.** Surgical technique for inducing global cerebral ischemia. A. Schematic illustration of arteries demonstrating the two points of clipping (arrows). B. Surgical view of two-vessel occlusion. C. A miniature clip for the CC artery was made of stainless steel with a diameter of 0.2 mm. CC: common carotid; Ao: aorta; Tr: trachea. (Modified from Yonekura et al., 2004)

CA1 cells in the hippocampus are vulnerable to ischemia and thus we have analyzed the CA1 cell death using Nissl staining. We found that all CA cells (CA1, CA2, CA3) were lost in the ischemic mouse hippocampus (Fig. 27) which suggest that transiently global ischemia method was successful.

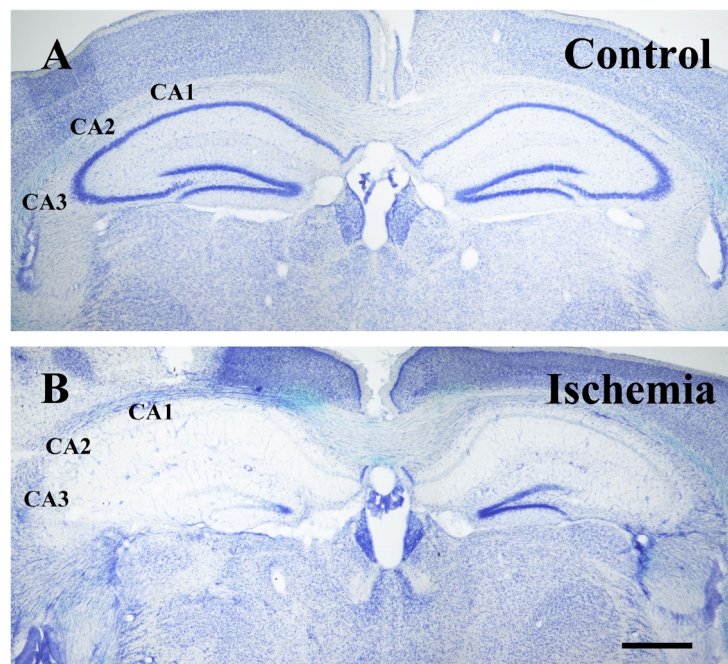


**Fig. 27.** Global cerebral ischemia induced CA cell death in the hippocampus. A. Nissl staining of non-ischemic CA region of wild type mouse hippocampus. B. CA region cell death of ischemic wild type mouse hippocampus. Scale bar=600  $\mu$ m

### **3-3-2. *draxin* expressions is up regulated after transient global ischemia**

Although draxin is established as a repulsive axon guidance molecule, there is a possibility that it might have different functions in addition to axon guidance. To explore this idea we performed transient global ischemia using draxin KO adult male mice (postnatal 97 days) to see whether draxin has any role during ischemia or post ischemic condition. Mice were sacrificed on 3, 5, 7 or 10 days of post ischemia and the brains were fixed followed by cryo-protection. Fifty-micrometer thicknesses of sequential

coronal sections were prepared and LacZ enzymatic reaction was performed. Interestingly, we observed that ischemia induced higher amount of draxin in the dentate gyrus of hippocampus, sub ventricular zone and olfactory bulb (n=8) (Fig. 28). We didn't notice any significant difference of draxin expression among the above-mentioned specified groups. Adult Draxin KO mice without ischemia were used as control (n=4). This data clearly indicate that draxin might have some function during ischemia or post ischemic situation.

### **3-3-3. Establishment of Focal cerebral ischemia**

Focal cerebral ischemia is one of the important tools for clinical trial because of its mimicry to regional stroke in humans. To understand whether draxin plays any role during stroke situation, we need to establish the middle cerebral artery occlusion (MCAO) model. Adult male mice were anesthetized with fluothane (halothane) via a facemask with spontaneous breathing. A midline neck incision was made and the bilateral common carotid artery (CCA), external carotid artery (ECA), internal carotid artery (ICA) were carefully separated from the surrounding nerves and fascia. Dissect the ECA further distally and coagulate the ECA and its superior thyroid artery branch using a bipolar coagulator. Cut the ECA and STA at the coagulated segment. Then, loosely tie two silk sutures around the ECA stump. Apply a vascular clamp (Fine Science Tools) at the bifurcation of the CCA into the ECA and ICA. Make a small incision at the end of ECA stump with Vannas-style spring scissors. Measure and record the length of a 5-0 monofilament suture rounded at the tip. Insert the silicon coated suture into the incision and advance to the clamp (Fig. 29A). Tighten the two silk sutures around the lumen just enough to secure yet preserve mobility of the in-dwelling monofilament suture. Remove the clamp from the bifurcation and cut a bit in ECA and gently advance the silicon coated

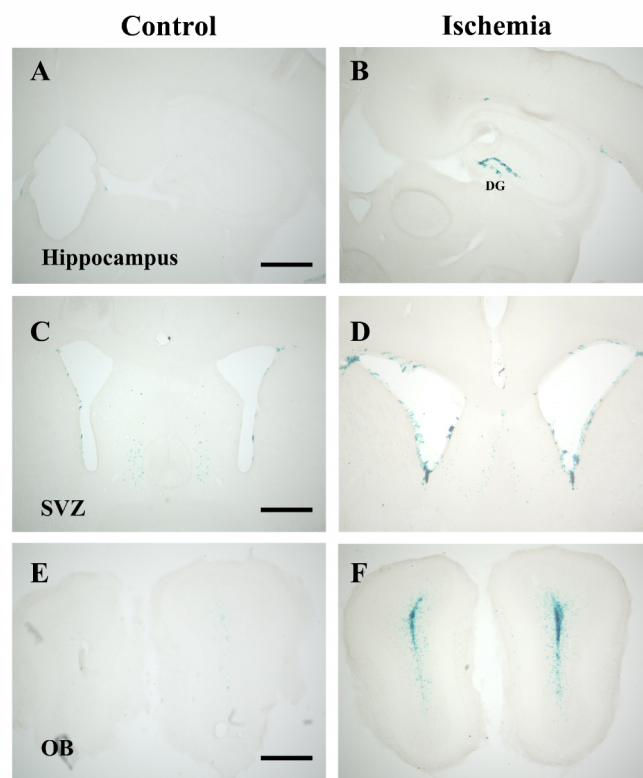


**Fig. 28.** *draxin* mRNA expression is up regulated in transient global cerebral ischemia. Post ischemic *draxin* up regulation was observed in DG of the hippocampus (B), SVZ (D) and OB (F) in the *draxin* KO mice compared to the non-ischemic *draxin* KO mice (A, C and E, respectively). DG: dentate gyrus; SVZ: sub ventricular zone; OB: olfactory bulb. Scale bar=600  $\mu$ m.

mono-filament suture from the lumen of the ECA into the ICA for a distance of 9-10 mm beyond the bifurcation of CCA to occlude the origin of MCA. About 30-40 min later open the clip of ECA and withdraw the suture gently and close the incision area. Place the mouse in a 35 °C nursing box to recover from anesthesia, and return it to the cage. We performed 2,3,5-triphenyltetrazolium chloride (TTC) treatment to the dissected brain sample 1 day after the induction of MCAO, to check whether the surgery is successful. We found that MCAO operated mice showed pink shading to half side of the brain

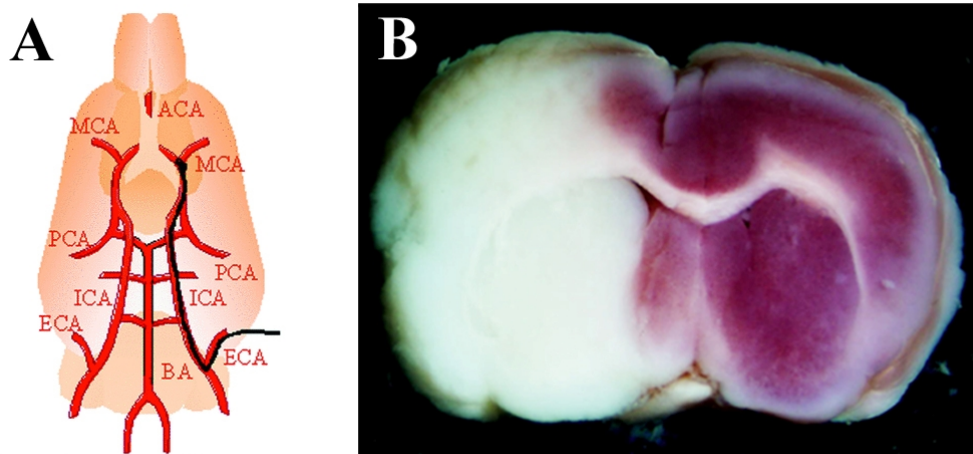


**Fig. 29.** TTC staining of MCAO model. A. MCAO in mouse was induced by introducing a silicon-coated suture into the external carotid artery and advancing it to block the origin of the artery. The pink shading in (B) represents the region of brain normally blood supplied by this artery. Following MCAO, cerebral blood flow to this region is severely reduced, resulting in cell death (pale white region in B). ECA: external carotid artery; ICA: internal carotid artery; MCA: middle cerebral artery (Ref. for fig. A: Macrae and Carswell, 2006)

section where as other half showed pale white color (Fig. 29B) after TTC treatment. This result indicates that the cells of one side of the brain were damaged due to lack of blood supply during MCAO and hence it shows pale white color.

## 4. Discussion

### 4-1. Part A

Our previous reports (Islam et al., 2009; Ito et al., 2010) show that both *draxin* and *TSK* single mutant mice have malformations of the AC and CC. The immunohistochemical analysis and DiI labeling of the present study showed that the frequency of severe malformation of both the AC and the CC were significantly higher in *draxin/TSK* doubly heterozygous mice compared with either singly heterozygous. While examining the reasons for the phenotypes observed in transheterozygotes, our study revealed a novel function for TSK as a repulsive axon guidance molecule for AC and CC axons. TSK inhibited the neurite outgrowth of dissociated AON and cortical neurons in a dose-dependent manner. Moreover, TSK and draxin showed an additive inhibitory effect on AON and cortical neurite outgrowth. Taken together, our data demonstrate that draxin and TSK function in concert to control the navigation of AC and CC axons.

The genetic analyses presented in this study provide strong support for the hypothesis that both TSK and draxin function in a similar pathway to regulate AC and CC formation. In general, reducing the gene dose by one copy reduces the protein production by 50%, which causes little or no phenotypic effects. However, when the doses of two genes with protein products that function together are simultaneously reduced, exacerbation of the impairment of their combined function may produce an increase in the incidence of strong phenotypes in the transheterozygotes. This effect may be one of the reasons why we observed higher frequencies of AC and CC malformation in the *draxin/TSK* double heterozygotes and homozygotes. The observation of such phenotypic severity in the double heterozygotes is reminiscent of earlier studies (Artavanis-Tsakonas, et al., 1995; Winberg, et al., 1998; Kidd, et al., 1999; Strickland, et al., 2006;

Ahmed et al., 2011). This genetic interaction provides strong evidence that draxin and TSK function together to form the AC and CC.

Both *draxin* and *TSK* mRNA are highly expressed in the GW, IG, anterior and posterior piriform cortex, olfactory bulb, AON and areas surrounding the AC and CC. Guidance proteins for which the knockout mice show agenesis of the forebrain commissures are expressed in these regions (Lindwall et al., 2007). We previously hypothesized that TSK might be involved in the navigation of AC axons independently or might interact with the known guidance molecules and/or their receptors and modulate their activity in guiding the AC axons (Ito et al., 2010). In this study, we explored these possibilities and found that TSK inhibits neurite outgrowth from dissociated AON and cortical neurons in a dose-dependent manner (Fig. 19). Although, TSK binds BMP and inhibits its activity (Ohta et al., 2004), we found that TSK does not interact directly with draxin rather it interacts with netrin. Therefore, it is unlikely that these proteins modulate each other's function directly. Furthermore, the inhibition was additive when draxin and TSK were present together compared with the presence of either draxin or TSK protein alone. There is a possibility that both the common and the independent functions of these two proteins are essential for guiding AC and CC axons, and due to the reduction of protein product, doubly heterozygous and homozygous mice exhibited higher frequencies of malformations of the AC and CC axonal tracts.

The combinatorial chemoattractive and chemorepulsive activities of guidance molecules contribute to the proper navigation of the commissural axons. In situ hybridization of neonates has revealed Sema3B expression in the SVZ and at the ventral levels. Both *in vivo* analysis and functional assays suggest that ACa axons are attracted

by a dorsal source of *Sema3B* that emanates from the SVZ (Julien et al., 2005). *Netrin-1* mRNA distributions have also been observed in the SVZ, along the paths of the commissural axons and at the points where they cross the midline (Serafini et al., 1996). *Wnt5a* (Keeble et al, 2006) and *TSK* mRNA expression has also been detected in the SVZ. Thus, ACa axons might be guided by the combined activity of a dorsal source of chemoattractive *Sema 3B*, chemorepulsive *TSK*, and *Netrin-1* (through either chemoattraction or chemorepulsion).

The functional activities of the guidance molecules and certain factors (e.g., cell adhesion molecules) in the ventral forebrain are essential for steering of the ACp. Repulsive cues, such as *Sema 3B* and *Sema3F* are expressed in the ventral forebrain during the formation of the anterior commissure (Sahay et al., 2003; Julien et al., 2005). Both *draxin* and *TSK* were also expressed in the ventral forebrain, suggesting that ACp axons might also be guided by *draxin* and *TSK*. Moreover, the expression of *draxin* and *TSK* along the forebrain commissural axons suggests a role for these molecules in the proper guidance of these axons.

The decussation of the commissural axons at the midline is one of the critical events for the proper channeling of the forebrain commissure. Although in neuron-specific *Sema 3F* conditional KO mice the decussation of the AC is largely disorganized, a minuscule fraction of AC axons still cross the midline, indicating that other guidance cues must be functional in this region (Sahay et al., 2003). Indeed, anterior commissure defects have been observed in *netrin-1*, *Sema 3F*, *Sema 3B*, *Nrp2*, *plexin-A4*, *Rac1* (conditional), *draxin* and *TSK* mutant mice (Serafini et al., 1996; Chen et al., 2000; Sahay et al., 2003; Julien et al., 2005; Suto et al., 2005; Kassai et al., 2008; Islam et al.,

2009, Ito et al., 2010). The AC midline crossing occurs in close association with the ependymal layer of the third ventricle, and the AC is surrounded by a tunnel of extracellular matrix molecules, glial cells, netrin, draxin and TSK that may provide cell contact guidance for AC fibers (Pires-Neto and Lent, 1993; Henkemeyer et al., 1996; Serafini et al., 1996; Cummings et al., 1997; Lent et al., 2005; Islam et al., 2009, Ito et al., 2010, present work). Taken together, attractive and repulsive double signaling may be needed to achieve fine control of axonal trajectories and may guide the progressive lateromedial turning of AC fibers that directs the tract toward the midline. A simplified schematic diagram showing the different axon guidance molecules that are responsible for formation of the AC is shown in Fig. 30B.

Although *netrin-1* and *DCC* mutant mice lack a CC and midline cortical tissues and callosal axons express netrin-1 and DCC, respectively, no direct evidence currently exists to support a role for netrin-1/DCC signaling in the attraction of callosal axons toward the midline (Serafini et al., 1996; Fazeli et al., 1997; Molyneaux et al., 2009; Izzi and Charron, 2011; Chédotal, 2011). However, Sema 3C has been recently reported to be a midline attractant for callosal axons (Niquille et al., 2009; shown in Fig. 30A). The GW assists the guidance of callosal axons across the midline by preventing their ventral growth into the septum, and the IG is thought to act as a dorsal repulsive barrier for callosal axons. These boundaries were thought to be due to anatomical position and their expression of the repulsive guidance molecules Slit2, Ephrins and draxin (Bagri et al., 2002; Shu et al., 2003; Mendes et al., 2006; Islam et al., 2009). Interestingly, TSK is also expressed in a zone similar to that of the above-mentioned repulsive guidance molecules around the GW and IG (Fig. 3F, Fig. 8A); that is, the strategic area of CC axon formation. This observation suggests that TSK also has a guiding effect on CC

development. Because netrin-1, Sema3C, Slit, draxin and TSK are secreted molecules, one could question whether and how they are maintained close to their sources to establish a gradient strong enough to be perceived by the growing commissural axons. One possibility is that adjacent cellular or molecular barriers limit their diffusion away from the midline. Similarly, the question of what makes the callosal and commissural axons remain within their tracts may be answered by the existence of organizing, growth-inhibiting structures at the borders of these tracts that may not only maintain diffusible molecules within the tracts but also inhibit axonal deviation from the main path of growth. Glial cells and their extra cellular matrix (ECM) are good candidates for this function because they form tunnels, lanes, or simply borders around the AC (Pires-Neto et al., 1998; Lent et al., 2005) and the CC (Shu and Richards, 2001; Lent et al., 2005), through which the efferent fibers grow. Both draxin and TSK are expressed in glial cells. Furthermore, our previous studies have shown that draxin has a high affinity for basement membranes (Islam et al., 2009), which are part of the ECM. Moreover, the SLRP family (of which TSK is a member) participates in the organization of the ECM and has important effects on cells (McEwan et al., 2006). Taken together, the functions of both draxin and TSK are required to form the commissural axons.

It is not yet clear why switching off a single ligand/receptor complex is sufficient to fully prevent the crossing of the commissural axons, given the redundancy of chemorepulsive molecules and their receptors. One possibility is that these repellents and their receptors might share some common downstream signaling. For instance, neucrin (an alternative name for draxin) and TSK bind to Wnt receptor LDL receptor-related protein 6 (LRP 6) and Fzd4, respectively, and both inhibit the Wnt signaling pathway (Miyake et al., 2009; Ohta et al., 2011). Moreover, TSK binds to netrin and both draxin

and netrin share the common receptor, DCC. Thus, draxin and TSK might exert their functions through a common downstream signaling pathway. Alternatively, multiple signaling pathways might be involved in commissural axon formation, and draxin and TSK could follow independent pathways. Although DCC is one of the functional receptors for draxin that partially regulates the formation of the CC, other receptors must be involved in mediating draxin's function in the formation of the AC and CC. Further research is necessary to identify the functional receptors of both draxin and TSK that are required for the formation of forebrain commissures and to elucidate the downstream signaling components of draxin and TSK.

#### **4-2. Part B**

Netrin exerted its chemoattractive function through interacting with DCC, whereas draxin shows its chemorepulsive activity via binding to the same receptor (Ahmed et al., 2011). As different ligands interacted with the same receptor, DCC; and shows opposite functions of axon guidance, there might be some other molecule(s) that also interact with DCC to perform the opposite signaling pathway. To identify the receptor-associated molecules through proteomics approach we need a good antibody against draxin to perform immunoprecipitation (IP). So far there was no good antibody commercially available against mouse draxin to fulfill our requirement. Thus, we went for the production of mouse draxin monoclonal antibody. We were successful after several trials to raise the antibody against mouse draxin using draxin knockout mice as a host. Later, we confirmed that the produced antibody is mouse draxin IgM monoclonal antibody which could be used for immunocytochemistry (Fig. 23) but not for IP experiments.

As an alternative way, we mixed draxin-conditioned medium to the wild type mouse

E17.5 brain lysate and perform IP using anti-DCC and anti-chick Draxin antibody. Excessive draxin might boost up the interaction with higher numbers of DCC and thus other interacting molecules to the DCC will make complex. Therefore, IP by anti-DCC antibody precipitated DCC as well as the interacting molecules to DCC. As, draxin CM was mixed with brain lysate; it will interact with DCC, and anti-CDra MAb could pull down the chick draxin as well as DCC with its interacting molecule(s). As a negative control anti-human IgG antibody was used. Later, our collaborator performed mass spectrometry analysis. We found 4 unique prominent candidates. We carefully need to screen these candidate molecules to identify the real interacting partner protein.

#### **4-3. Part C**

Draxin is a chemorepulsive axon guidance molecule required for development of all forebrain commissures: the corpus callosum, hippocampal commissure and anterior commissure (Islam et al., 2009). Hippocampus is one of the best-analyzed parts of the brain due to its involvement in the higher functions of learning and memory and in various mental diseases. Hippocampus is particularly vulnerable to ischemia, which selectively affects CA1 pyramidal neurons and destroys hippocampal circuitry by inducing cell death. Draxin is expressed from differentiating neurons, astroglia and radial glia in the developing hippocampus (Zhang et al., 2010). Draxin might have different functions other than axon guidance in the brain. As hippocampus is a very important part of the brain, in the present study we tried to elucidate the effects of global cerebral ischemia and also middle cerebral artery occlusion (MCAO) on draxin gene expression as well as neurogenesis in the adult mouse brain hippocampus. Global cerebral ischemia was confirmed by CA1 cell death analysis by Nissl staining where as MCAO was confirmed by TTC staining.

Draxin gene is replaced by LacZ gene in the Draxin KO mice. Lac Z (draxin) expression is almost disappeared in 3-4 months old mice. Thus, ischemic experiment was performed on 3-4 months adult draxin KO mice and we found that draxin is either up regulated or reappeared in dentate gyrus of hippocampus as well as SVZ and olfactory bulb after 3 days of ischemia. This data provided us a very important clue about draxin that might have other significant function besides the axon guidance activity. In the present study, we have experienced higher mortality rate of ischemic mice like other researchers (Ueda, 2009). One reason might be the hypothermia during the surgery or in the post surgery environment. Another reason might be the severe disturbance of vagus nerve while performing the operation. Furthermore, it seemed that draxin KO mice are weaker than that of wild type mice.

Draxin is expressed from differentiating neurons, astroglia and radial glia in the developing hippocampus (Zhang et al., 2010). We need to perform immunohistochemistry to check which cells express draxin using neuronal and glial cell marker in ischemic dentate gyrus. As it is certain that draxin is re-expressed or up regulated after ischemia; at this stage one burning question is that, what is the function this newly formed draxin? More simply we can find out the answer of the following question; does draxin has a role in the adult neurogenesis? Several researchers established the fact that ischemia induces neurogenesis in the DG and SVZ (Liu et al., 1998, Jin et al., 2001, Kee et al. 2001, Yagita et al. 2001, Yoshimura et al. 2001, Zhang et al. 2001, Arvidsson et al. 2002, Iwai et al. 2002, Parent et al. 2002, Schmidt and Reymann 2002, Iwai et al. 2003, Tonchev et al. 2003, Zhu et al. 2003, Tanaka et al. 2004, Zhang et al., 2004). As draxin is up regulated in the DG as well as SVZ following ischemia and ischemia induced neurogenesis in these regions; there is a high possibility that draxin might play an important role in neurogenesis.

## 5. Conclusion

- Tsukushi (TSK) is a novel repulsive axon guidance molecule for cortical and AON axons; and the combinatorial guidance activity of draxin and TSK is essential for forebrain commissure formation.
- Four unique types of protein (i) ELKS/Rab6-interacting/CAST family member 1 (Gene name: Erc1), ii) Neogenin (Gene name: Neo1), iii) Potassium/sodium hyperpolarization-activated cyclic nucleotide-gated channel 4 (Gene name: Hcn4), Lethal(2) giant larvae protein homolog 1 (Gene name: Llg1) are identified by proteomics approach which are promising candidates as co-receptor(s) of draxin.
- Both MCAO and global cerebral ischemia methods are established and most importantly draxin mRNA expression is up regulated or re-expressed after ischemia which might have role in adult neurogenesis.

## **6. Future perspectives**

### **6-1. Part A**

Our next challenge is to elucidate the common signaling mechanism of draxin and TSK. Although, TSK does not bind to DCC, there is a possibility that it could bind with other receptors of draxin - Neogenin, Unc5 and Dscam. Moreover, we also need to check whether draxin binds with TSK receptor frizzled 4. After attainment of any positive interaction, we could further proceed to explore the common signaling mechanism.

### **6-2. Part B**

Further careful investigation is obligatory to screen these candidate molecules. In brief, COS-7 cell will be seeded and will be transfected by individual candidate clone. Two days later of transfection, cells will be stained by Draxin-AP. If signal is observed any of individual clones, we could proceed for cell surface binding analysis. Cell surface Binding analysis experiment will be done to check whether the screened clone is true receptor for Draxin or not. COS-7 cells will be transfected with an expression vector encoding Draxin receptor candidates. After 48 hrs of transfection COS-7 cell will be used for binding assay for Draxin protein according to the standard protocol. Later, we need to analyze the mRNA expression pattern of these candidate receptor proteins by in situ hybridization in different region of chick and mouse embryo, especially where Draxin sensitive neurons exist. Further, to compare the receptor mRNA pattern with that of protein expression, immunohistochemistry need to be performed. Besides, functional analysis of the Draxin receptor candidate could be performed. The aim of this experiment is to confirm whether the Draxin receptor candidate is truly receptor for Draxin. Functional analysis could possible by i) siRNA approach: siRNA-IRES-GFP construct against Draxin receptor candidate mRNA would be made and then would be

electroporated in the dorsal spinal cord. Explant from the siRNA-GFP electroporated site would be cut and cultured in the collagen gel either in presence of Draxin and Netrin protein or in presence of Draxin only. If GFP positive neurite growth is not inhibited in presence of Draxin, it means the candidate mRNA must be the receptor for draxin; ii) Functional antibody approach: After getting the receptor's sequence, receptor protein would be purified and would be used to immunize the rabbit several times. Then, explant from dorsal spinal cord will be made and cultured in collagen gel both in presence of Draxin with its immunized serum and Draxin with non-immunized serum. If neurite growth inhibition by Draxin is not occurred in presence of immunized serum, it indicates that the antibody is function blocking which in turn indicates that the immunized protein is receptor protein.

### **6-3. Part C**

As, there is a high possibility that draxin might play an important role in neurogenesis, it would be interesting to check the cell proliferation. To check the cell proliferation/neurogenesis in hippocampus in adult mice, after 9 days of post ischemia, BrdU (thymidine analog) need to be administered intra-peritoneally for consecutive 3 days (twice daily) and analyzed on 15<sup>th</sup> day of post ischemia. By comparing the number of BrdU positive cells of post-ischemic WT and draxin KO mice, it would be possible to determine whether draxin has any role in the cell proliferation. If the BrdU positive cell number is higher in WT than KO mice, it will be clear that draxin has a role in neurogenesis.

## 7. References

- Adams, R., Wilkinson, G., Weiss, C., Diellia, F., Gale, N.W., Deutsch, U., Risau, W., Klein, R., 1999. Roles of ephrinB ligands and EphB receptors in cardiovascular development: demarcation of arterial/venous domains, vascular morphogenesis, and sprouting angiogenesis. *Genes and Dev.* 13, 295-306.
- Ahmed, G., Shinmyo, Y., Naser, I.B., Hossain, M., Song, X., Tanaka, H., 2010. Olfactory bulb axonal outgrowth is inhibited by draxin. *Biochem. Biophys. Res. Commun.* 398, 730–734.
- Ahmed, G., Shinmyo, Y., Ohta, K., Islam, S.M., Hossain, M., Naser, I.B., Riyadh, M.A., Su, Y., Zhang, S., Tessier-Lavigne, M., Tanaka, H., 2011. Draxin inhibits axonal outgrowth through the netrin receptor DCC. *J. Neurosci.* 31, 14018-14023.
- Alaoui-Jamali, M.A., Xu, Y.J., 2006. Proteomic technology for biomarker profiling in cancer: an update. *Journal of Zhejiang University Science B* 7, 411–420.
- Alvarez-Buylla, A., Garcia-Verdugo, J.M., 2002. Neurogenesis in adult subventricular zone. *J Neurosci* 22, 629-34.
- Ara, J., Fekete, S., Zhu, A., Frank, M., 2010. Characterization of neural stem/progenitor cells expressing VEGF and its receptors in the sub ventricular zone of newborn piglet brain. *Neurochem Res* 35,1455–1470.
- Artavanis-Tsakonas, S., Matsuno, K., Fortini, M.E., 1995. Notch signaling. *Science* 268, 225–232.
- Arvidsson, A., Collin, T., Kirik, D., Kokaia, Z., Lindvall, O., 2002. Neuronal replacement from endogenous precursors in the adult brain after stroke. *Nat. Med.* 8, 963-970.
- Bagnard, D., Lohrum, M., Uziel, D., Puschel, A.W., Bolz, J., 1998. Semaphorins act as attractive and repulsive guidance signal during the development of cortical projections. *Development* 125, 5043-5053.
- Bagri, A., Marin, O., Plump, A.S., Mak, J., Pleasure, S.J., Rubenstein, J.L., Tessier-Lavigne,

M., 2002. Slit proteins prevent midline crossing and determine the dorsoventral position of major axonal pathways in the mammalian forebrain. *Neuron* 33, 233–248.

Baltimore, D., 2001. Our genome unveiled. *Nature* 409, 814–816.

Battye, R., Stevens, A., Jacobs, J.R., 1999. Axon repulsion from the midline of the *Drosophila* CNS requires slit function. *Development* 126, 2475-81.

Behar, O., Golden, J.A., Mashimo, H., Schoen, F.J., Fishman, M.C., 1996. Semaphorin III is needed for normal patterning and growth of nerves, bones and heart. *Nature* 383, 525-528.

Bendel, O., Bueters, T., von Euler, M., Ove Ogren, S., Sandin, J., von Euler, G., 2005. Reappearance of hippocampal CA1 neurons after ischemia is associated with recovery of learning and memory. *J Cereb Blood Flow Metab* 25, 1586-1595.

Braisted, J. E., Catalano, S. M., Stimac, R., Kennedy, T. E., Tessier-Lavigne, M., Shatz, C. J., O'Leary, D. D. M., 2000. Netrin-1 Promotes Thalamic Axon Growth and Is Required for Proper Development of the Thalamocortical Projection. *J. Neurosci.* 20, 5792-5801.

Brose, K., Bland, K.S., Wang, K.H., Arnott, D., Henzel, W., Goodman, C.S., Tessier-Lavigne, M., Kidd, T., 1999. Slit proteins bind Robo receptors and have an evolutionarily conserved role in repulsive axon guidance. *Cell* 96, 795-806.

Brose, K., Tessier-Lavigne, M., 2000. Slit proteins: key regulators of axon guidance, axonal branching, and cell migration. *Curr. Opin. Neurobiol.* 10, 95-102.

Celis, J.E., Gromov, P., 2D protein electrophoresis: can it be perfected? 1999. *Current Opinion in Biotechnology* 10, 16–21.

Chandramouli, K., Qian P.Y., 2009. *Genomics Proteomics* 1, 239204.

Charron, F., Stein, E., Jeong, J., McMahon, A.P., Tessier-Lavigne, M., 2003. The morphogen sonic hedgehog is an axonal chemoattractant that collaborates with netrin-1 in midline axon guidance. *Cell* 113, 11-23.

Charron, F., Tessier-Lavigne, M., 2005. Novel brain wiring functions for classical

morphogens: a role as graded positional cues in axon guidance. *Development* 132, 2251-2262.

Chédotal, A., 2011. Further tales of the midline. *Curr. Opin. Neurobiol.* 21, 68–75.

Chen, H., Bagri, A., Zupicich, J.A., Zou, Y., Stoeckli, E., Pleasure, S.J., Lowenstein, D.H., Skarnes, W.C., Chedotal, A., Tessier-Lavigne, M., 2000. Neuropilin-2 regulates the development of selective cranial and sensory nerves and hippocampal mossy fiber projections. *Neuron* 25, 43–56.

Colamarino, S.A., Tessier-Lavigne, M., 1995. The axonal chemoattractant netrin-1 is also a chemorepellent for trochlear motor axons. *Cell* 81, 621-629.

Crack, P. J., Taylor, J. M., Flentjar, N. J., de Haan, J., Hertzog, P., Iannello, R. C., Kola, I., 2001. Increased infarct size and exacerbated apoptosis in the glutathione peroxidase-1 (Gpx-1) knockout mouse brain in response to ischemia/reperfusion injury. *J. Neurochem.* 78, 1389–1399.

Crack, P.J., Taylor, J.M., 2005. Reactive oxygen species and the modulation of stroke. *Free Radic Biol Med.* 38, 1433-44.

Cutler, P., 2003. Protein arrays: the current state-of-the-art. *Proteomics* 3, 3–18.

Cummings, D.M., Malun, D., Brunjes, P.C., 1997. Development of the anterior commissure in the opossum: midline extracellular space and glia coincide with early axon decussation. *J. Neurobiol.* 32, 403–414.

Darsalia, V., Heldmann, U., Lindvall, O., Kokaia, Z., 2005. Stroke-induced neurogenesis in aged brain. *Stroke* 36, 1790–1795.

De Castro, F., Hu, L., Drabkin, H., Sotelo, C., Chedotal, A., 1999. Chemoattraction and chemorepulsion of olfactory bulb axons by different secreted Semaphorins, *J. Neurosci.* 19, 4428–4436.

Dickson, B. J., 2002. Molecular mechanisms of axon guidance. *Science* 298, 1959-1964.

Dirnagl, U., Iadecola, C., Moskowitz, M.A., 1999. Pathobiology of ischaemic stroke: an

integrated view. *Trends Neurosci* 22, 391-397.

Doetsch, F., Garcia-Verdugo, J.M., Alvarez-Buylla, A., 1997. Cellular composition and three-dimensional organization of the subventricular germinal zone in the adult mammalian brain, *J. Neurosci.* 17, 5046–5061.

Dohare, P., Varma, S., Ray, M., 2008. Curcuma oil modulates the nitric oxide system response to cerebral ischemia/reperfusion injury. *Nitric Oxide* 19,1–11.

Donahoo, A.L., Richards, L.J., 2009. Understanding the mechanisms of callosal development through the use of transgenic mouse models. *Semin. Pediatr. Neurol.* 16, 127–142.

Eriksson, P.S., Perfilieva, E., Björk-Eriksson, T., Alborn, A.M., Nordborg, C., Peterson, D.A., Gage, F.H., 1998. Neurogenesis in the adult human hippocampus. *Nat. Med.* 4, 1313–1317.

Fazeli, A., Dickinson, S.L., Hermiston, M.L., Tighe, R.V., Steen, R.G., Small, C.G., Stoeckli, E.T., Keino-Masu, K., Masu, M., Rayburn, H., 1997. Phenotype of mice lacking functional Deleted in colorectal cancer (*Dcc*) gene. *Nature* 388, 796–804.

Florens, L., Washburn, M.P., 2006. Proteomic analysis by multidimensional protein identification technology. *Methods in Molecular Biology* 328, 159–175.

Gallarda, B. W., Bonanomi, D., Müller, D., Brown, A., Alaynick, W. A., Andrews, S. E., Lemke, G., Pfaff, S. L., Marquardt, T., 2008. Segregation of Axial Motor and Sensory Pathways via Heterotypic Trans-Axonal Signaling. *Science* 320, 233-236.

Giger, R.J., Cloutier, J.F., Sahay, A., Prinjha, R.K., Levenson, D.V., Moore, S.E., Pickering, S., Simmons, D., Rastan, S., Walsh, F.S., 2000. Neuropilin-2 is required in vivo for selective axon guidance responses to secreted semaphorins. *Neuron* 25, 29–41.

Ginsberg, M.D., Busto, R., 1989. Rodent models of cerebral ischemia. *Stroke* 20, 1627-1742.

Godovac-Zimmermann, J., Brown, L.R., 2001. Perspectives for mass spectrometry and functional proteomics. *MassSpectrometry Reviews* 20, 1–57.

Gygi, S.P., Rist, B., Gerber, S.A., Turecek, F., Gelb, M.H., Aebersold, R., 1999. Quantitative

analysis of complex protein mixtures using isotope-coded affinity tags. *Nature Biotechnology* 17, 994–999.

Hata, K., Fujitani, M., Yasuda, Y., Doya, H., Saito, T., Yamagishi, S., Mueller, B.K., Yamashita, T., 2006. RGMA inhibition promotes axonal growth and recovery after spinal cord injury. *J. Cell Biol.* 173, 47–58.

Henkemeyer, M., Orioli, D., Henderson, J.T., Saxton, T.M., Roder, J., Pawson, T., Klein, R., 1996. Nuk controls pathfinding of commissural axons in the mammalian central nervous system. *Cell* 86, 35–46.

Heine, V.M., Maslam, S., Joe's, M., Lucassen, P.J., 2004. Prominent decline of newborn cell proliferation, differentiation, and apoptosis in the aging dentate gyrus, in absence of an age-related hypothalamus pituitary-adrenal axis activation. *Neurobiol Aging* 25, 361–375.

Heiss, W. D., Sobesky, J., Hesselmann, V., 2004. Identifying thresholds for penumbra and irreversible tissue damage. *Stroke* 35, 2671–2674.

Holmberg, J., Clarke, D.L., Frisen, J., 2000. Regulation of repulsion versus adhesion by different splice forms of an Eph receptor. *Nature* 408, 203-206.

Holmes, G.P., Negus, K., Burridge, L., Raman, S., Algar, E., Yamada, T., Little, M.H., 1998. Distinct but overlapping expression patterns of two vertebrate slit homologs implies functional roles in CNS development and organogenesis. *Mech Dev.* 79, 57-72.

Hong, K., Hinck, L., Nishiyama, M., Poo, M. M., Tessier-Lavigne, M., Stein E., 1999. A ligand-gated association between cytoplasmic domains of UNC5 and DCC family receptors converts netrin-induced growth cone attraction to repulsion. *Cell* 97, 927-941.

Hong, X.P., Peng, C.X., Wei, W., Tian, Q., Liu, Y.H., Cao, F.Y., Wang, Q., Wang, J.Z., 2011. Relationship of adult neurogenesis with tau phosphorylation and GSK-3beta activity in subventricular zone. *Neurochem Res* 36, 288–296.

Huber, A. B., Kolodkin, A.L., Ginty, D. D., Cloutier J. F., 2003. Signaling at the growth cone: l-receptor complexes and the control of axon growth and guidance. *Annu. Rev. Neurosci.* 26, 509-63.

Hou, S. T., MacManus, J. P., 2002. Molecular mechanisms of cerebral ischemia-induced neuronal death. *Int. Rev. Cytol.* 221, 93–148.

Hou, S.T., Keklikian, A., Slinn, J., O'Hare, M., Jiang, S.X., Aylsworth, A., 2008. Sustained up-regulation of Semaphorin 3A, Neuropilin1, and Doublecortin expression in ischemic mouse brain during long-term recovery. *Biochemical and Biophysical Research Communications* 367, 109–115.

Hwang, I.K., Yoo, K.Y., Yi, S.S., Kwon, Y.G., Ahn, Y.K., Seong, J.K., Lee, I.S., Yoon, Y.S., Won, M.H., 2008. Age-related differentiation in newly generated DCX immunoreactive neurons in the subgranular zone of the gerbil dentate gyrus. *Neurochem Res* 33, 867–872.

Ingham, P. W., McMahon, A. P., 2001. Hedgehog signaling in animal development: paradigms and principles. *Genes Dev.* 15, 3059-3087.

Imondi, R., Wideman, C., and Kaprielian, Z., 2000. Complementary expression of transmembrane ephrins and their receptors in the mouse spinal cord: a possible role in constraining the orientation of longitudinally projecting axons. *Development* 127, 1397-1410.

Islam, S.M., Shinmyo, Y., Okafuji, T., Su, Y., Naser, I.B., Ahmed, G., Zhang, S., Chen, S., Ohta, K., Kiyonari, H., Abe, T., Tanaka, S., Nishinakamura, R., Terashima, T., Kitamura, T., Tanaka, H., 2009. Draxin, a repulsive guidance protein for spinal cord and forebrain commissures. *Science* 323, 388–393.

Ito, A., Shinmyo, Y., Abe, T., Oshima, N., Tanaka, H., Ohta, K., 2010. Tsukushi is required for anterior commissure formation in mouse brain. *Biochem. Biophys. Res. Commun.* 402, 813–818.

Itoh, A., Miyabayashi, T., Ohno, M., Sakano, S., 1998. Cloning and expressions of three mammalian homologues of *Drosophila* slit suggest possible roles for Slit in the formation and maintenance of the nervous system. *Brain Res. Mol. Brain Res.* 62, 175-86.

Iwai, M., Sato, K., Omori, N., Nagano, I., Manabe, Y., Shoji, M., Abe, K., 2002. Three steps

of neural stem cells development in gerbil dentate gyrus after transient ischemia. *J Cereb Blood Flow Metab* 22, 411-9.

Iwai, M., Sato, K., Kamada, H., Omori, N., Nagano, I., Shoji, M., Abe, K., 2003. Temporal profile of stem cell division, migration, and differentiation from subventricular zone to olfactory bulb after transient forebrain ischemia in gerbils. *J Cereb Blood Flow Metab* 23, 331-41.

Izzi, L., Charron, F., 2011. Midline axon guidance and human genetic disorders. *Clin. Genet.*80, 226–234.

Jessell, T. M., 2000. Neuronal specification in the spinal cord: inductive signals and transcriptional codes. *Nat. Rev. Genet.*1, 20-29.

Jin, K., Minami, M., Xie, L., Sun, Y., Mao, X.O., Wang, Y., Simon, R.P., Greenberg, D.A., 2004. Ischemia-induced neurogenesis is preserved but reduced in the aged rodent brain. *Aging Cell* 3, 373–377.

Jin, K., Sun, Y., Xie, L., Peel, A., Mao, X.O., Bateur, S., Greenberg, D.A., 2003. Directed migration of neuronal precursors into the ischemic cerebral cortex and striatum. *Mol Cell Neurosci* 24,171-89.

Julien, F., Bechara, A., Fiore, R., Nawabi, H., Zhou, H., Hoyo-Becerra, C., Bozon, M., Rougon, G., Grumet, M., Püschel, A.W., Sanes, J.R., Castellani, V., 2005. Dual functional activity of semaphorin 3B is required for positioning the anterior commissure. *Neuron* 48, 63–75.

Kassai, H., Terashima, T., Fukaya, M., Nakao, K., Sakahara, M., Watanabe, M., Aiba, A., 2008. *Rac1* in cortical projection neurons is selectively required for midline crossing of commissural axonal formation. *Eur. J. Neurosci.* 28, 257–267.

Katsura, K., Kristián, T., Siesjö, B.K., 1994. Energy metabolism, ion homeostasis, and cell damage in the brain. *Biochem Soc Trans.* 22, 991-6.

Kearney, P., Thibault, P., 2003. Bioinformatics meets proteomics—bridging the gap between mass spectrometry data analysis and cell biology. *The Journal of Bioinformatics and*

Computational Biology 1, 183–200.

Kee, N.J., Preston, E., Wojtowicz, J.M., 2001. Enhanced neurogenesis after transient global ischemia in the dentate gyrus of the rat. *Exp Brain Res* 136, 313-20.

Keeble, T.R., Halford, M.M., Seaman, C., Kee, N., Macheda, M., Anderson, R.B., Stacker, S.A., Cooper, H.M., 2006. The Wnt receptor Ryk is required for Wnt5a-mediated axon guidance on the contralateral side of the corpus callosum. *J Neurosci.* 26, 5840-5848.

Keino-Masu, K., Masu, M., Hinck, L., Leonardo, E. D., Chan, S.S-Y., Culotti, J. G., Tessier-Lavigne, M., 1996. *Deleted in colorectal cancer (DCC)* encodes a netrin receptor. *Cell* 87, 175-185.

Kennedy, T. E., Serafini, T., de la Torre, J., Tessier-Lavigne, M., 1994. Netrins are chemotropic factors for C axons in the embryonic spinal cord. *Cell* 78, 425–435.

Kidd, T., Brose, K., Mitchell, K.J., Fetter, R.D., Tessier-Lavigne, M., Goodman, C.S., Tear, G., 1998. Roundabout controls axon crossing of the CNS midline and defines a novel subfamily of evolutionarily conserved guidance receptors. *Cell* 92, 205-215.

Kidd, T., Bland, K.S., Goodman, C.S., 1999. Slit is the midline repellent for the robo receptor in *Drosophila*. *Cell* 96, 785–794.

Kirino, T., 1982. Delayed neuronal death in the gerbil hippocampus following ischemia. *Brain Res* 239, 57-69.

Kitsukawa, T., Shimizu, M., Sanbo, M., Hirata, T., Taniguchi, M., Bekku, Y., Yagi, T., Fujisawa, H., 1997. Neuropilin-semaphorin III/D-mediated chemorepulsive signals play a crucial role in peripheral nerve projection in mice. *Neuron* 19, 995-1005.

Klose, J., Nock, C., Herrmann, M., Stühler, K., Marcus, K., Blüggel, M., Krause, E., Schalkwyk, L.C., Rastan, S., Brown, S.D., Büssow, K., Himmelbauer, H., Lehrach, H., 2002. Genetic analysis of the mouse brain proteome. *Nature Genetics* 30, 385–393.

Koketsu, D., Furuichi, Y., Maeda, M., Matsuoka, N., Miyamoto, Y., Hisatsune, T., 2006. Increased number of new neurons in the olfactory bulb and hippocampus of adult non-human

primates after focal ischemia. *Exp Neurol* 199, 92–102.

Kuhn, H.G., Dickinson-Anson, H., Gage, F.H., 1996. Neurogenesis in the dentate gyrus of the adult rat: age-related decrease of neuronal progenitor proliferation. *J Neurosci* 16, 2027–2033.

Kullander, K., Croll, S.D., Zimmer, M., Pan, L., McClain, J., Hughes, V., Zabski, S., DeChiara, T.M., Klein, R., Yancopoulos, G.D., Gale, N.W., 2001. Ephrin-B3 is the midline barrier that prevents corticospinal tract axons from recrossing, allowing for unilateral motor control. *Genes Dev.* 15, 877–888.

Kuriyama, S., Lupo, G., Ohta, K., Ohnuma, S., Harris, W.A., Tanaka, H., 2006. Tsukushi controls ectodermal patterning and neural crest specification in *Xenopus* by direct regulation of BMP4 and X-delta-1 activity. *Development* 133, 75–88.

Lee, K. J., Mendelsohn, M., Jessell, T. M., 1998. Neuronal patterning by BMPs: a requirement for GDF7 in the generation of a discrete class of commissural interneurons in the mouse spinal cord. *Genes Dev.* 12, 3394-3407.

Lent, R., Uziel, D., Baudrimont, M., Fallet, C., 2005. Cellular and molecular tunnels surrounding the forebrain commissures of human fetuses. *J. Comp. Neurol.* 483, 375–382.

Li, H.S., Chen, J.H., Wu, W., Fagaly, T., Zhou, L., Yuan, W., Dupuis, S., Jiang, Z.H., Nash, W., Gick, C., Ornitz, D.M., Wu, J.Y., Rao, Y., 1999. Vertebrate slit, a secreted ligand for the transmembrane protein roundabout, is a repellent for olfactory bulb axons. *Cell* 96, 807-818.

Lindwall, C., Fothergill, T., Richards, L.J., 2007. Commissure formation in the mammalian forebrain. *Curr. Opin. Neurobiol.* 17, 3–14.

Lipton, P., 1999. Ischemic cell death in brain neurons. *Physiol Rev* 79, 1431-1568.

Listgarten, J., Emili, A., 2005. Statistical and computational methods for comparative proteomic profiling using liquid chromatography-tandem mass spectrometry. *Molecular and Cellular Proteomics* 4, 419–434.

Liu, G., Li, W., Wang, L., Kar, A., Guan, K.L., Rao, Y., Wu, J.Y., 2009. DSCAM functions

as a netrin receptor in commissural axon pathfinding. *Proc. Natl. Acad. Sci. U S A.* 106, 2951-2956.

Liu, J., Sohway, K., Messing, R.O., Sharp, F.R., 1998. Increased neurogenesis in the dentate gyrus after transient global ischemia in gerbils. *J Neurosci* 18, 7768-78.

Luo, J., Daniels, S.B., Lenington, J.B., Notti, R.Q, Conover, J.C., 2006. The aging neurogenic subventricular zone. *Aging Cell* 5,139–152.

Luria, V., Krawchuk, D., Jessell, T. M., Laufer, E., Kania, A., 2008. Specification of Motor Axon Trajectory by Ephrin-B:EphB Signaling: Symmetrical Control of Axonal Patterning in the Developing Limb. *Neuron* 60, 1039-1053.

Ly, A., Nikolav, A., Suresh, G., Zheng, Y., Tessier-Lavigne M., and Stein E., 2008. DSCAM is a netrin receptor that collaborates with DCC in mediating turning response to netrin-1. *Cell* 133:1241-1254.

Macrae, I.M., Carswell, H.V., 2006. Oestrogen and stroke: the potential for harm as well as benefit. *Biochemical Society Transactions.* 34,1362–1365.

Martin, R.L, Lloyd, H.G., Cowan, A.I., 1994. The early events of oxygen and glucose deprivation: setting the scene for neuronal death? *Trends Neurosci.* 17, 251-7.

Maslov, A.Y., Barone, T.A., Plunkett, R.J., Pruitt, S.C., 2004. Neural stem cell detection, characterization, and age-related changes in the subventricular zone of mice. *J Neurosci* 24, 1726–1733.

Mattson, M. P., 2001. Pathogenesis of neurodegenerative disorders. Totowa, NJ: Humana Press.

Matsumori, Y., Hong, S.M., Fan, Y., Kayama, T., Hsu, C.Y., Weinstein, P.R., Liu, J., 2006. Enriched environment and spatial learning enhance hippocampal neurogenesis and salvages ischemic penumbra after focal cerebral ischemia. *Neurobiol Dis* 22,187–19.

McEwan, P.A., Scott, P.G., Bishop, P.N., Bella, J., 2006. Structural correlations in the family of smallleucine-rich repeat proteins and proteoglycans. *J. Struct. Biol.* 155, 294–305.

Melton, L., 2004. Proteomics in multiplex. *Nature* 429, 101–107.

Mendes, S.W., Henkemeyer, M., Liebl, D.J., 2006. Multiple Eph receptors and B-class ephrins regulate midline crossing of corpus callosum fibers in the developing mouse forebrain. *J. Neurosci.* 26, 882–892.

Métin, C., Deléglise, D., Serafini, T., Kennedy, T. E., Tessier-Lavigne, M., 1997. A role for netrin-1 in the guidance of cortical efferents. *Development* 124, 5063-5074.

Mhairi-Macrae, I., 1992. New models of focal cerebral ischaemia. *Br J Clinical Pharmacol* 34, 302-308.

Miyake, A., Takahashi, Y., Miwa, H., Shimada, A., Konishi, M., Itoh, N., 2009. Neucrin is a novel neural-specific secreted antagonist to canonical Wnt signaling. *Biochem. Biophys. Res. Commun.* 390, 1051–1055.

Molyneaux, B.J., Arlotta, P., Fame, R.M., MacDonald, J.L., Mac-Quarrie, K.L., Macklis, J.D., 2009. Novel subtype-specific genes identify distinct subpopulations of callosal projection neurons. *J. Neurosci.* 29, 12343–12354.

Monnier, P. P., Sierra, A., Macchi, P., Deitinghoff, L., Andersen, J. S., Mann, M., Flad, M., Hornberger, M.R., Stahl, B., Bonhoeffer, F., Mueller, B.K., 2002. RGM is a repulsive guidance molecule for retinal axons. *Nature* 419, 392-395.

Morioka, M., Fukunaga, K., Yasugawa, S., Nagahiro, S., Ushio, Y., Miyamoto, E., 1992. Regional and temporal alterations in Ca<sup>2+</sup>/calmodulin-dependent protein kinase II and calcineurin in the hippocampus of rat brain after transient forebrain ischemia. *J Neurochem.* 58, 1798-809.

Morris, S.A., Almeida, A.D., Tanaka, H., Ohta, K., Ohnuma, S., 2007. Tsukushi modulates Xnr2, FGF and BMP signaling: regulation of *Xenopus* germ layer formation. *PLoS One.* 2, e1004.

Mueller, L. N., Rinner, O., Schmidt, A., Letarte, S., Bodenmiller, B., Brusniak, M.Y., Vitek, O., Aebersold, R., Müller, M., 2007. SuperHirn—a novel tool for high resolution LC-MS-based peptide/protein profiling, *Proteomics* 7, 3470–3480.

- Muroyama, Y., Fujihara, M., Ikeya, M., Kondoh, H., Takada, S., 2002. Wnt signaling plays an essential role in neuronal specification of the dorsal spinal cord. *Genes Dev.* 16, 548-553.
- Nagy, A., Gertsenstein, M., Vinterstenand, K., Behringer, R., 2003. *Manipulating the Mouse Embryo: A Laboratory manual*, Cold Spring Harbor Laboratory Press, Cold Spring Harbor, New York.
- Nakatomi, H., Kuriu, T., Okabe, S., Yamamoto, S., Hatano, O., Kawahara, N., Tamura, A., Kirino, T., Nakafuku, M., 2002. Regeneration of hippocampal pyramidal neurons after ischemic brain injury by recruitment of endogenous neural progenitors. *Cell* 110, 429-441.
- Nakayama, M., Nakajima, D., Nagase, T., Nomura, N., Seki, N., Ohara, O., 1998. Identification of high-molecular-weight proteins with multiple EGF-like motifs by motif-trap screening. *Genomics* 51, 27-34.
- Naser, I.B., Su, Y., Islam, S.M., Shinmyo, Y., Zhang, S., Ahmed, G., Chen, S., Tanaka, H., 2009. Analysis of a repulsive axon guidance molecule, draxin, on ventrally directed axon projection in chick early embryonic midbrain. *Dev. Biol.* 332, 351–359.
- Niimori D., Kawano R., Felemban A., Niimori-Kita K., Tanaka H., Ihn H., Ohta K., 2012. Tsukushi controls the hair cycle by regulating TGF- $\beta$ 1 signaling. *Dev. Biol.* 372, 81-87.
- Niquille, M., Garel, S., Mann, F., Hornung, J.P., Otsmane, B., Chevalley, S., Parras, C., Guillemot, F., Gaspar, P., Yanagawa, Y., Lebrand, C., 2009. Transient neuronal populations are required to guide callosal axons: a role for semaphorin3C. *PLoS Biol.* 7, e1000230.
- Nygren, J., Wieloch, T., Pesic, J., Brundin, P., Deierborg, T., 2006. Enriched environment attenuates cell genesis in subventricular zone after focal ischemia in mice and decreases migration of newborn cells to the striatum. *Stroke* 37, 2824–2829.
- Ohta, K., Tannahill, D., Yoshida, K., Johnson, A.R., Cook, G.M., Keynes, R.J., 1999. Embryonic lens repels retinal ganglion cell axons. *Dev Biol.* 211, 124-32.
- Ohta, K., Lupo, G., Kuriyama, S., Keynes, R., Holt, C.E., Harris, W.A., Tanaka, H., Ohnuma, S., 2004. Tsukushi functions as an organizer inducer by inhibition of BMP activity in cooperation with chordin. *Dev. Cell* 7, 347–358.

Ohta, K., Kuriyama, S., Okafuji, T., Gejima, R., Ohnuma, S., Tanaka, H., 2006. Tsukushi cooperates with VG1 to induce primitive streak and Hensen's node formation in the chick embryo. *Development* 133, 3777–3786.

Ohta, K., Ito, A., Kuriyama, S., Lupo, G., Kosaka, M., Ohnuma, S., Nakagawa, S., Tanaka, H., 2011. Tsukushi functions as a Wnt signaling inhibitor by competing with Wnt2b for binding to transmembrane protein Frizzled4. *Proc. Natl. Acad. Sci. U S A.*108, 14962–14967.

Okafuji, T., Tanaka, H., 2005. Expression pattern of LINGO-1 in the developing nervous system of the chick embryo. *Gene Expr. Patterns.*6, 57–62.

O'Leary, D. D. M., Wilkinson, D. G., 1999. Eph receptors and ephrins in neural development. *Current Opinion in Neurobiology* 9, 65-73.

Ong, S.E., Blagoev, B., Kratchmarova, I., 2002. Stable isotope labeling by amino acids in cell culture, SILAC, as a simple and accurate approach to expression proteomics. *Molecular and Cellular Proteomics* 1, 376–386.

Parent, J.M., Vexler, Z.S., Gong, C., Derugin, N., Ferriero, D.M., 2002. Rat forebrain neurogenesis and striatal neuron replacement after focal stroke. *Ann Neurol* 52, 802-813.

Pasterkamp, R.J., Peschon, J.J., Spriggs, M.K., Kolodkin, A.L., 2003. Semaphorin 7A promotes axon outgrowth through integrins and MAPKs. *Nature* 424, 398-404.

Pires-Neto, M.A., Lent, R., 1993. The prenatal development of the anterior commissure in hamsters: pioneer fibers lead the way. *Brain Res. Dev. BrainRes.*72, 59–66.

Pires-Neto, M.A., Braga-de-Souza, S., Lent, R., 1998. Molecular tunnels and boundaries for growing axons in the anterior commissure of hamster embryos. *J. Comp. Neurol.* 399, 176–188.

Plane, J.M., Liu, R., Wang, T.W., Silverstein, F.S., Parent, J.M., 2004. Neonatal hypoxic ischemic injury increases forebrain subventricular zone neurogenesis in the mouse. *Neurobiol Dis* 16, 585–595.

Poliakov, A., Cotrina, M., Wilkinson, D.G., 2004. Diverse roles of eph receptors and ephrins in the regulation of cell migration and tissue assembly. *Dev. Cell* 7, 465-480.

Plump, A. S., Erskine, L., Sabatier, C., Brose, K., Epstein, C. J., Goodman, C.S., Mason, C.A., Tessier-Lavigne, M., 2002. Slit1 and slit2 cooperate to prevent premature midline crossing of retinal axons in the mouse visual system. *Neuron* 33, 219-232.

Rajagopalan, S., Deitinghoff, L., Davis, D., Conrad, S., Skutella, T., Chedota, A., Mueller, B. K., Strittmatter, S. M., 2004. Neogenin mediates the action of repulsive guidance molecule. *Nature Cell Biology* 6, 756-762.

Raper, J.A., 2000. Semaphorins and their receptors in vertebrates and invertebrates. *Curr. Opin. Neurobiol.* 10, 88-94.

Rawson, N.E., LaMantia, A.S., 2007. A speculative essay on retinoic acid regulation of neural stem cells in the developing and aging olfactory system. *Exp Gerontol* 42, 46–53.

Richards, L.J., Plachez, C., Ren, T., 2004. Mechanisms regulating the development of the corpus callosum and its agenesis in mouse and human. *Clin. Genet* 66, 276–289.

Rothberg, J.M., Hartley, D.A., Walther, Z., Artavanis-Tsakonas, S., 1988. *Slit*: an EGF-homologous locus of *D. melanogaster* involved in the development of the embryonic central nervous system. *Cell* 55, 1047-1059.

Ross, P.L., Huang, Y.N., Marchese, J.N., 2004. Multiplexed protein quantitation in *Saccharomyces cerevisiae* using amine-reactive isobaric tagging reagents. *Molecular and Cellular Proteomics* 3, 1154–1169.

Rothberg, J.M., Jacobs, J.R., Goodman, C.S., Artavanis-Tsakonas, S., 1990. *Slit*: an extracellular protein necessary for development of midline glia and commissural axon pathways contains both EGF and LRR domains. *Genes Dev.* 4, 2169-2187.

Sahay, A., Molliver, M.E., Ginty, D.D., Kolodkin, A.L., 2003. Semaphorin 3F is critical for development of limbic system circuitry and is required in neurons for selective CNS axon guidance events. *J. Neurosci.* 23, 6671–6680.

Salazar-Colocho, P., Lanciego, J.L., Del Rio, J., Frechilla, D., 2008. Ischemia induces cell proliferation and neurogenesis in the gerbil hippocampus in response to neuronal death. *Neurosci Res* 61, 27–37.

- Schaefer, L., Iozzo, R.V., 2008. Biological functions of the small leucine-rich proteoglycans: from genetics to signal transduction. *J. Biol. Chem.* 283, 21305-21309.
- Schmetsdorf, S., Gärtner, U., Arendt, T., 2005. Expression of cell cycle-related proteins in developing and adult mouse hippocampus. *Int J Dev Neurosci* 23,101–112.
- Schmidt, W., Reymann, K.G., 2002. Proliferating cells differentiate into neurons in the hippocampal CA1 region of gerbils after global cerebral ischemia. *Neurosci Lett.* 334,153-156.
- Schulz, T. C., Swistowska, A. M., Liu, Y., Swistowski, A., Palmarini, G., Brimble, S.N., Sherrer, E., Robins, A.J., Rao, M.S., Zeng, X., 2007. A large-scale proteomic analysis of human embryonic stem cells. *BMC Genomics* 8, 478.
- Serafini, T., Kennedy, T. E., Galko, M. J., Mirzayan, C. M., Jessell, T. M., Tessier-Lavigne, M., 1994. The netrins define a family of axon outgrowth-promoting proteins homologous to *C. elegans* UNC-6. *Cell* 78, 409-424.
- Serafini, T., Colamarino, S.A., Leonardo, E.D., Wang, H., Beddington, R., Skarnes, W.C., Tessier-Lavigne, M., 1996. Netrin-1 is required for commissural axon guidance in the developing vertebrate nervous system. *Cell* 13, 1001–1014.
- Shu, T., Richards, L.J., 2001. Cortical axon guidance by the glial wedge during the development of the corpus callosum. *J. Neurosci.* 21, 2749–2758.
- Shu, T., Sundaresan, V., McCarthy, M.M., Richards, L.J., 2003. Slit2 guides both precrossing and postcrossing callosal axons at the midline in vivo. *J. Neurosci.* 23, 8176–8184.
- Siitari, H., Koivistoinen, H., 2004. Proteomics—challenges and possibilities in Finland. National Technology Agency. *Technology Review* 157, 1–36.
- Smith, J. C., Lambert, J.P., Elisma, F., Figeys, 2007. Proteomics in 2005/2006: developments, applications and challenges,” *Analytical Chemistry* 79, 4325– 4343.
- Stahl-Zeng, J., Lange, V., Ossola, R., Eckhardt, K., Krek, W., Aebersold, R., Domon, B.,

2007. High sensitivity detection of plasma proteins by multiple reaction monitoring of N-glycosites. *Molecular and Cellular Proteomics* 6, 1809–1817.
- Stein, E., Tessier-Lavigne, M., 2001. Hierarchical organization of guidance receptors: silencing of netrin attraction by slit through a Robo/DCC complex. *Science* 291, 1928-1938.
- Strickland, P., Shin, G.C., Plump, A., Tessier-Lavigne, M., Hinck, L., 2006. Slit2 and netrin 1 act synergistically as adhesive cues to generate tubular bi-layers during ductal morphogenesis. *Development* 133, 823–832.
- Suto, F., Ito, K., Uemura, M., Shimizu, M., Shinkawa, Y., Sanbo, M., Shinoda, T., Tsuboi, M., Takashima, S., Yagi, T., Fujisawa, H., 2005. Plexin-a4 mediates axon-repulsive activities of both secreted and transmembrane semaphorins and plays roles in nerve fiber guidance. *J. Neurosci.* 25, 3628–3637.
- Tang, H., Wang, Y., Xie, L., Mao, X., Won, S.J., Galvan, V., Jin, K., 2009. Effect of neural precursor proliferation level on neurogenesis in rat brain during aging and after focal ischemia. *Neurobiol Aging* 30, 299–308.
- Tanaka, R., Yamashiro, K., Mochizuki, H., Cho, N., Onodera, M., Mizuno, Y., Urabe, T., 2004. Neurogenesis after transient global ischemia in the adult hippocampus visualized by improved retroviral vector. *Stroke* 35, 1454-9.
- Taniguchi, M., Nagao, H., Takahashi, Y.K., Yamaguchi, M., Mitsui, S., Yagi, T., Mori, K., Shimizu, T., 2003. Distorted odor maps in the olfactory bulb of semaphorin 3A-deficient mice. *J Neurosci.* 23, 1390-1397.
- Tessier-Lavigne, M., Goodman, C. S., 1996. The molecular biology of axon guidance. *Science* 274, 1123-1133.
- Tonchev, A.B., Yamasima, T., Zhao, L., Okano, H.J., Okano, H., 2003. Proliferation of neural and neuronal progenitors after global brain ischemia in young adult macaque monkeys. *Mol Cell Neurosci* 23, 292-301.

Tonchev, A.B., 2005. Neurogenesis in adult mammalian hippocampus after ischemia: rodent *versus* primate models. *Biomedical Reviews* 16, 1-11.

Ueda, H., 2009. Prothymosin  $\alpha$  and cell death mode switch, a novel target for the prevention of cerebral ischemia-induced damage. *Pharmacology & Therapeutics* 123, 323–333.

Unni, D.K., Piper, M., Moldrich, R.X., Gobius, I., Liu, S., Fothergill, T., Donahoo, A.L., Baisden, J.M., Cooper, H.M., Richards, L.J., 2012. Multiple Slits regulate the development of midline glial populations and the corpus callosum. *Dev. Biol.* 365, 36–49.

Van den Bergh, G., Arckens, L., 2005. Recent advances in 2D electrophoresis: an array of possibilities. *Expert Review of Proteomics* 2, 243–252.

Vercauteren, F. G. G., Bergeron, J. J. M., Vandesande, F., Arckens, L., Quirion, R., 2004. Proteomic approaches in brain research and neuropharmacology. *European Journal of Pharmacology* 500, 385–398.

Vutskits, L., Gascon, E., Zraggen, E., Kiss, J.Z., 2006. The polysialylated neural cell adhesion molecule promotes neurogenesis in vitro. *Neurochem Res* 31, 215–225.

Wang, H.U., Chen, Z.-F., Anderson, D.J., 1998. Molecular distinction and angiogenic interaction between embryonic arteries and veins revealed by ephrin-B2 and its receptor Eph-B4. *Cell* 93, 741-753.

Washburn, M.P., Wolters, D., Yates III, J.R., 2001. An automated multidimensional protein identification technology for shotgun proteomics. *Analytical Chemistry* 73, 5683–5690.

Wen, Z., Zheng, J.Q., 2006. Directional guidance of nerve growth cones. *Curr. Opin. Neurobiol.* 16, 52-58.

Wilkins, M.R., Gasteiger, E., Gooley, A.A., Herbert, B.R., Molloy, M.P., Binz, P.A., Ou, K., Sanchez, J.C., Bairoch, A., Williams, K.L., Hochstrasser, D.F., 1999. High throughput mass spectrometric discovery of protein posttranslational modifications. *Journal of Molecular Biology* 289, 645–657.

Wilkinson, D. G., 2001. Multiple roles of eph receptors and ephrins in neural development. *Nature Review Neuroscience* 2, 155-164.

Winberg, M.L., Noordermeer, J.N., Tamagnone, L., Comoglio, P.M., Spriggs, M.K., Tessier-Lavigne, M., Goodman, C.S., 1998. Plexin A is a neuronal semaphorin receptor that controls axon guidance. *Cell* 95, 903–916.

Wu, H., Fan, J., Zhu, L., Liu, S., Wu, Y., Zhao, T., Wu, Y., Ding, X., Fan, W., Fan, M., 2009. Sema4c expression in neural stem/progenitor cells and in adult neurogenesis induced by cerebral ischemia. *J Mol Neurosci.* 39, 27–39.

Yagita, Y., Kitagawa, K., Ohtsuki, T., Takasawa, K., Miyata, T., Okano, H., Hori, M., Matsumoto, M., 2001. Neurogenesis by progenitor cells in the ischemic adult rat hippocampus. *Stroke* 32, 1890-6.

Yonekura, I., Kawahara, N., Nakatomi, H., Furuya, K., Kirino, T., 2004. A Model of Global Cerebral Ischemia in C57 BL/6 Mice. *J. Cereb. Blood Flow Metab.* 24, 151–158.

Yoshimura, S., Takagi, Y., Harada, J., Teramoto, T., Thomas, S.S., Waever, C., Bakowska, J.C., Breakefield, X.O., Moskowitz, M.A., 2001. FGF-2 regulation of neurogenesis in adult hippocampus after brain injury. *Proc. Natl. Acad. Sci. USA* 98, 5874-9.

Yu, T.W., Bargmann, C.I., 2001. Dynamic regulation of axon guidance. *Nat. Neurosci.* 4, 1169-1176.

Yuan, S.S., Cox, L.A., Dasika, G.K., Lee, E.Y., 1999. Cloning and functional studies of a novel gene aberrantly expressed in RB-deficient embryos. *Dev. Biol.* 207, 62–75.

Yuan, W., Zhou, L., Chen, J.H., Wu, J.Y., Rao, Y., Ornitz D.M. 1999. The mouse SLIT family: secreted ligands for ROBO expressed in patterns that suggest a role in morphogenesis and axon guidance. *Dev. Biol.* 212, 290-306.

Zhang, R.L., Zhang, Z.G., Zhang, L., Chopp, M., 2001. Proliferation and differentiation of progenitor cells in the cortex and the sub ventricular zone in the adult rat after focal cerebral

ischemia. *Neuroscience* 105, 33-41.

Zhang, R., Zhang, Z., Wang, L., Wang, Y., Gousev, A., Zhang, L., Ho, K.L., Morshead, C., Chopp, M., 2004. Activated neural stem cells contribute to stroke-induced neurogenesis and neuroblast migration toward the infarct boundary in adult rats. *J Cereb Blood Flow Metab* 24, 441-8.

Zhang, S., Su, Y., Shinmyo, Y., Islam, S.M., Naser, I.B., Ahmed, G., Tamamaki, N., Tanaka, H., 2010. Draxin, a repulsive axon guidance protein, is involved in hippocampal development, *Neurosci. Res.* 66, 53–61.

Zhu, D.Y., Liu, S.H., Sun, H.S., Lu, Y.M., 2003. Expression of inducible nitric oxide synthase after focal cerebral ischemia stimulates neurogenesis in the adult rodent dentate gyrus. *J Neurosci* 23, 223-9.

Zou, Y., Lyuksyutova, A. I., 2007. Morphogens as conserved axon guidance cues. *Current Opinion in Neurobiology* 17, 22-28.